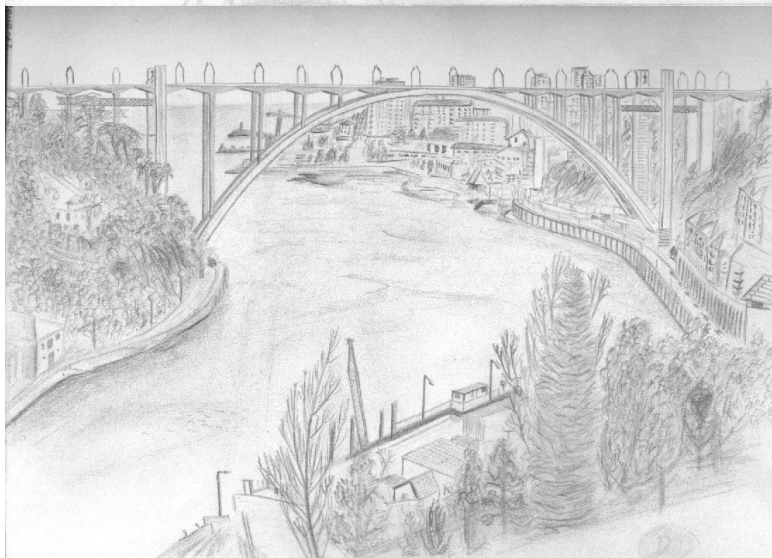
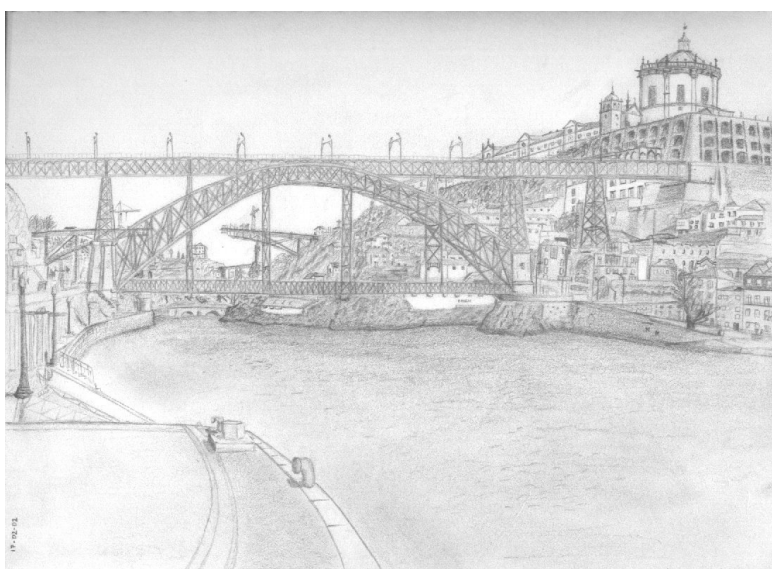
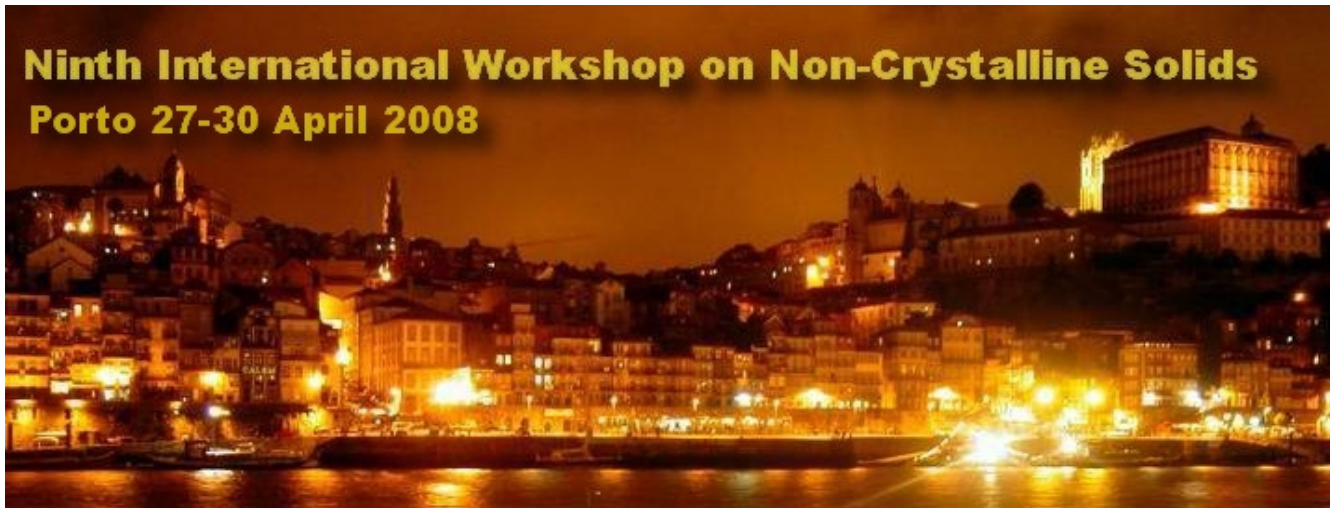


**Ninth International Workshop on Non-Crystalline Solids
Porto 27-30 April 2008**



Welcome to IWNCs 2008, Porto

WORKSHOP ORGANIZATION**INTERNATIONAL COMITTEE**

R. Balda, Bilbao, Spain
J.M. Barandiarán, Bilbao, Spain
F.J. Bermejo, Bilbao, Spain
J. Colmenero, San Sebastián, Spain
G. Cuello, Grenoble, France
H.A. Davies, Sheffield, UK
J.M. González, Madrid, Spain
A.B. Granovsky, Moscow, Russia
R. Hasegawa, New Jersey, USA
A. Hernando, Madrid, Spain
G. Herzer, Hanau, Germany
A. Lindsay Greer, Cambridge, UK
V. Madurga, UPN, Pamplona, Spain
M.T. Mora, Barcelona, Spain
E. Riande, Madrid, Spain
J. Rivas, Santiago de Compostela, Spain
R. Sato Turtelli, Vienna, Austria
R. Valenzuela, Mexico DF, Mexico
M. Vázquez, Madrid, Spain
J. S. Garitaonandia, Bilbao, Spain
P. Gorria, Oviedo, Spain

LOCAL ORGANIZING COMMITTEE

D. S. Schmool, Chair, Porto
J. B. Sousa, Porto
V. Amaral, Aveiro
J. P. Araújo, Porto
J. Ventura, Porto
I. Alves, Secretary-Porto

Mailing address

International Workshop on Non-Crystalline Solids

IFIMUP

Rua do Campo Alegre, 687

4169-007 Porto – Portugal

Tel: +351-22 60 82 662

E-mail: iwncs@fc.up.pt

<http://www2.fc.up.pt/iwncs/index.php>

SPONSORS

The workshop is organized and supported by the Department of Physics, Science Faculty of Porto University. The meeting also received the financial support of the:

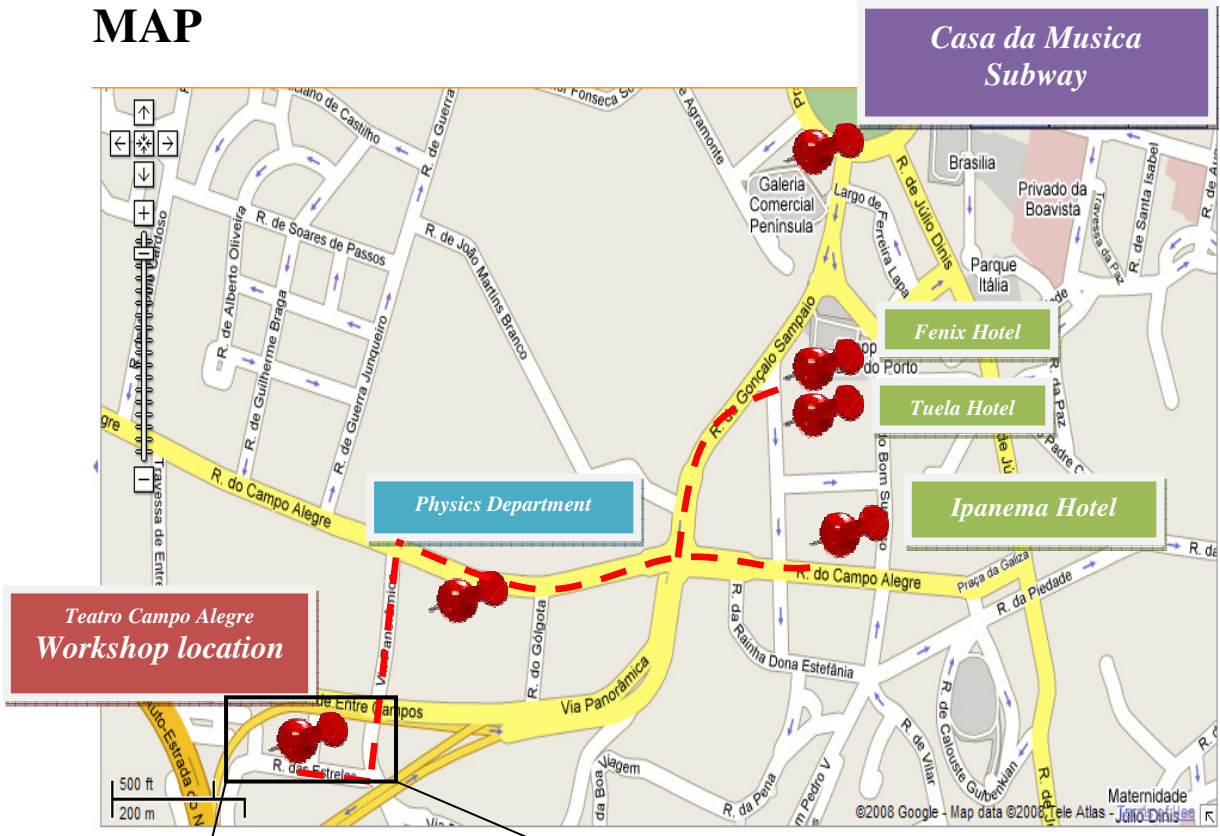
The logo for IFIMUP, consisting of the letters I, F, I, M, U, P in a blue serif font, each letter contained within a separate blue rectangular box.The logo for the Institute of Nanotechnologies (IN), featuring the text "INSTITUTE OF NANOTECHNOLOGIES (IN)" in white serif font, centered within a blue rectangular box.

FCT Fundação para a Ciência e a Tecnologia
MINISTÉRIO DA CIÊNCIA, TECNOLOGIA E ENSINO SUPERIOR Portugal

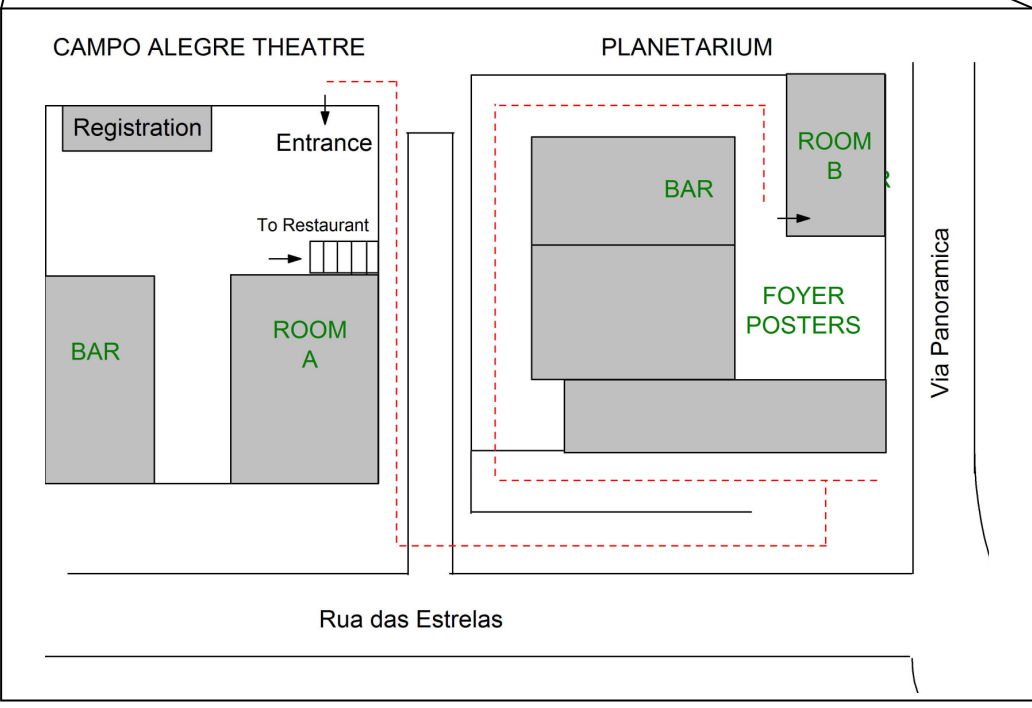
FC FACULDADE DE CIÊNCIAS
UNIVERSIDADE DO PORTO

The logo for U. PORTO, with the letter "U." in white serif font on a black rectangular background, followed by the word "PORTO" in black serif font on a white rectangular background.The logo for m.t. brandão, lda, featuring the lowercase letters "mt" in a grey serif font and "b" in a red serif font, with a grey arrow pointing upwards from the top of the "t". Below the letters, the text "m. t. brandão, lda" is written in a small, grey, sans-serif font.

MAP



--- walking route



GENERAL INFORMATION

The Department of Physics of the University of Porto will host the Ninth International Workshop on Non-Crystalline Solids, which will take place from the 27th to the 30th of April 2008. As in previous years, the workshop will focus on recent advances and emerging technologies in non-crystalline and nanostructured materials.

SCOPE

The meeting, organized by the Department of Physics, (University of Porto), focuses on the recent advances on non-crystalline and nanostructured materials from fundamental studies to applications.

The Workshop will be a forum where participants can present and discuss their recent works. The attendance of young researchers and students has been encouraged by the Organising Committee.

SCIENTIFIC PROGRAM

The program will consist of invited lectures (25 min. plus 5 min of discussion), oral presentations (12 min. plus 3 min of discussion), and contributions in poster sessions. Invited lectures will review recent work and progress in the field of amorphous and nanocrystalline materials.

Posters must present well-prepared visual material on a 1.0×1.2 m² poster board. Authors must be available during the whole poster session assigned to answer questions and discuss about the presented work.

POSTER SESSIONS AND ORAL PRESENTATIONS

Posters must be of 0.75 m×1.2 m about. Two poster sessions will take place: Monday and Tuesday from 17:00 to 19:00 hrs.

Authors must set up their posters the same day of the corresponding poster session during the morning. During the whole poster session at least one of the presenting authors should be available for discussion at the poster.

A number of oral presentations are also programmed as shown in the Workshop Timetable (12 min. plus 3 min of discussion).

AUDIO-VISUAL EQUIPMENT

The plenary room will be equipped with digital projection equipment. A PC will be also available (not MAC!).

Speakers should come prepared with their presentations in Microsoft Power Point format recorded on a CD or on USB memory stick. The lecturers should contact to the plenary room attendant, the day before or before the beginning of the morning session (09:00 hrs), and give their presentations.

PUBLICATION AND PAPER STATUS

The contributions of participants will be published as a special issue of the Journal of Non-Crystalline Solids (JNCS). The volume will contain the lectures of the invited lecturers and the contributed papers. Only one paper by participant registered in the Workshop will be published.

Authors will be able to check the status of their manuscripts in a board that will be located close to the room of the Workshop Secretariat. Authors are encouraged to

send back the corrected manuscripts as soon as possible to help the promptness in the publication.

WORKSHOP REGISTRATION

Registration of participants will take place at the Teatro Campo Alegre on Sunday April 27, starting at 16:00 hrs. It will follow on Monday morning from 8:30 to 9:00 hrs.

For regular participants registration includes the Workshop materials, publication volume containing the contributions of participants, welcome reception, coffee break, lunches and banquet.

Student registration includes everything except publication volume. The registration for accompanying persons includes welcome reception, banquet and social activities.

COFFEE BREAKS AND MEALS

Coffee service will be served during the morning and the afternoon at the time indicated in the Workshop timetable. Lunches will be offered at restaurant Teatro Campo Alegre, located in the Conference site on Monday and Tuesday from 13:00 to 14:30 hrs.

TRANSPORTATION TO THE WORKSHOP LOCATION

Participants accommodated in the hotels of Porto city can reach the Teatro do Campo Alegre on foot (10 min walking).

Local transportation in Porto:

Rádio Táxi do Porto. (+351) 225 076 400.

Radio Taxis. (+351) 225 073 900.

SOCIAL PROGRAM

SUNDAY, April 17, 18:00 hrs. Welcome party. Place: Teatro Campo Alegre.

TUESDAY, April 20, 19:00 hrs. Conference dinner.

WEDNESDAY; April 21, 14:00hrs, Guided Tour of the City of Porto and Port Wine Cellars

Visit for accompanying persons.

PORTO AIRPORT

The Francisco Sá Carneiro Airport is located in the heart of the industrial north of the country, 11 km from the city of Oporto, making it a privileged access point to this valuable commercial area.

Having undergone intense renovation work, the Francisco Sá Carneiro Airport now receives passengers and other users in the greatest of comfort, taking up the role of primary travel hub for the north-western corner of the Iberian Peninsula.

Come discover this capital of the north with all its splendid traditions and in the company of friendly, outgoing locals. Along the banks of the River Douro lies the area where footwear, furniture and clothing companies have long been operating, bringing economic life to the country.

Oporto Airport

Telephone (+351) 229 432 400

oporto.airport@ana.pt

From airport to Conference location

Subway.

Line Violeta (Purple line). Connection to city downtown and Railways.

Airport - Casa da Música around 23 minutes. Ticket: 1.35 €

Bus Buses of the 601, ZA, 602 and 604 Lines link various parts of the city to the airport (Rotunda da Boavista/Campo Alegre).

Ticket: 1.30€

More about Porto:

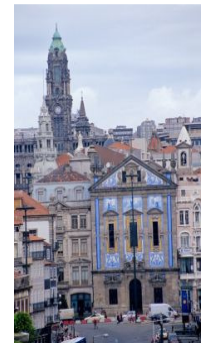
The Porto City Hall put forward a formal candidature to UNESCO in 1993 for the classification of the Porto Historic Centre as World Heritage, aware of the importance of this initiative for the international community and for the city as well. The process was given a decisive impulse in 1996, when UNESCO's World Heritage Committee gave its approval. The candidature was organised by CRUARB (Municipal Project for the Urban Renovation of the Porto Historic Centre), together with several specialised City Hall departments. UNESCO's decision was greatly influenced by the quality of the urban and social renovation works, especially those supporting the local population and boosting cultural and sport activities, which have been successfully introduced throughout the area now classified as World Heritage.

With around 267.000 inhabitants, the City of Porto has carefully preserved its architectonic treasures, including monuments in the Romanesque, Gothic, Baroque and Neo-classical style.

Stock-Exchange Palace 1. A national monument, the Stock-Exchange Palace is the headquarters of the Porto Commercial Association. It was built in neo-classical style in the second half of the 19th century. Located in the centre of the city, it is one of the most visited monuments, notably for its renowned Arabian Hall.



Cathedral See 2. As the main religious building of the diocese, the Sé Cathedral (the Cathedral See) presents itself as the gauge centre of aesthetic environments in successive transformation works. Those artistic solutions irradiate from here to its direct influence area.



In the long history of the Porto Cathedral, three stages stand out: in medieval times, the foundation, which granted it its architectural outline; in modern times, the transformation of the building, conditioned by the Catholic Reformation, makes it take on a coherent image where the interior arts – such as woodcarving, painting, plaster and others– are its main speech; the last one, dating from the 20 th century, consisted of the controversial interference of the National Monuments, which intended to purge it from its Baroque ambience, to lead it to the formal purism of the period that delineated it.

Clérigos Church 3. The buildings of the Confraternity of Clergymen comprise the Church, the House of the Clergymen (secretariat and infirmary) and the Tower, and are the most representative of the activity of the painter/architect Nicolau Nasoni in Porto, the city where he worked from 1725 to the time of his death in 1773. Born in Italy, Nasoni transferred to the city - after a stay in Rome - an artistic language that spread from painting to architecture. With the spatial conception of Clérigos, he asserted himself as a bearer of an expression that goes beyond what is merely ornamental, and thus became a full architect of the Roman Baroque as regards contents and form. The unusual elliptical nave of the church, among the other religious spaces of the city, alongside the careful treatment of the elevations and the covering system, justify his mastery of the art of conceiving spaces. He also knew how to take advantage of the building's localisation, by placing the rear tower on the highest side of the area, thus making it the greatest emblem of the city.



Real Companhia Velha Port Wine Cellars 4. Grape growing in the Douro Region dates back to pre-historic times. In Bronze Age burying-grounds, grape seeds and even carbonised vine-shoots have been found. With the Roman occupation, grape-growing underwent a large scale expansion-excavations carried out on the left bank of the Douro River clearly confirm the development and prosperity that the vine brought to the Douro Region. Porto has had acclaims as no other wine in the world. Over 300 years of a well established reputation give to Porto the recognition of being the wine that can age longer than any other.



In 2006 Real Companhia Velha celebrates 250 years of existence and uninterrupted activity on behalf of the Porto Wine trade. What makes Real Companhia Velha unique is the way its own history is intimately linked to the history of the Porto Wine trade and to the history of Portugal itself. Real Companhia Velha is the leading producer of Porto and the largest owner of Premium land in the Douro Valley. The Company owns some of the Douro's finest Quintas, located in the very best areas of the Region, having its cellars on the left bank of the Douro River, just facing Porto.

At the cellars the silence of its vaults, the wine is kept in barrels of noble wood, the work made by coopers, who have served the Company for many generations. There, asleep in a unique peacefulness, barrels and vats are lost in time... 10, 20... 30 years...The time it takes for each wine to reach its exact point of maturity.



For more information on Porto, please visit the website: <http://www.portoturismo.pt/>

Workshop Overview

Time	Sunday 27	Monday 28	Tuesday 29	Wednesday 30
8:30		REGISTRATION		
9:00		OPENING SESSION	Invited: M. Farle	Invited: L. Liz-Marzan
9:30		Invited: K. Hono	Invited: B. Heinrich	Invited: M. Miglierini
10:00		Invited: K. Suzuki	Invited: N. Skipper	Invited: I. Skorvánek
10:30		Invited: A. Yelon	Invited: R. Varga	Invited: L. Hennet
11:00		COFFEE BREAK	COFFEE BREAK	COFFEE BREAK
11:30		Invited: L. Battezzati	Invited: P. Salmon	Invited: H. Chiriac
12:00		Invited: S. Bossuyt	Invited: M. Vazquez	Invited: S. Flohrer
12:30		Invited: J. M. Greneche	Invited: E. Yelsukov	Invited: A. Glezer
13:00				Invited: K. L. Ngai
13:30		LUNCH	LUNCH	CLOSING SESSION
14:00				
14:30		14:30 (A) N. Cowlam (B) J. Barandiarán	14:30 (A) P. Gorria (B) A. Lancok	Guided Tour of the City of Porto and Port Wine Cellars
		14:45 (A) D. R. Tadjiev (B) J.C.R.E. Oliveira	14:45 (A) F. Vinai (B) J. Salado	
15:00		15:00 (A) J. Bonastre (B) J. Torrens-Serra	15:00 (A) M. L. Sánchez (B) M. Epifani	
		15:15 (A) Z. Sniadecki (B) J. Mira	15:15 (A) D. Ortega (B) E. Rozenberg	
15:30		15:30 (A) J. Bednarkík (B) A. M. L. Lopes	15:30 (A) H. A. Davies (B) M.Fernández-Garcia	
		15:45 (A) V. Cristiglio (B) J. S. Amaral	15:45 (A) J. Latuch (B) C. M. Mateo	
16:00	REGISTRATION	16:00 (A) P. Bruna (B) C. H. Lin	16:00 (A) M. T. Clavaguera-Mora (B) B. G. Almeida	
		16:15 (A) A. Conde (B) M. Insausti	16:15 (A) J. Ventura (B) J. M. González	
16:30		16:30 (A) J. Zhu (B) A. M. Pereira	16:30 (A) G. Attolini (B) V. M. Prida	
			16:45 (A) M. M. Tehranchi (B) J. Ordieres-Meré	
17:00	WELCOME PARTY			
17:30				
18:00				
18:30		POSTERS and Coffee break P-1 – P-40	POSTERS and Coffee break P-41 – P-79	
19:00				
19:30			Transportation	
20:00			CONFERENCE DINNER	

A – Room A: Teatro Campo Alegre

B – Room B: Planetário (Planetarium)

Posters: Foyer of Planetarium

Invited Communications

<i>Ref.</i>	<i>Title</i>	<i>Authors</i>	<i>Page</i>
I-01	NANOCRYSTALLINE STRUCTURE EVOLUTION IN FEB-CU SOFT MAGNETIC MATERIALS	Y.M. Chen, T. Ohkubo, M. Ohta, Y. Yoshizawa and K. Hono	23
I-02	LOCAL RANDOM MAGNETOCRYSTALLINE AND MACROSCOPIC UNIAXIAL ANISOTROPIES IN MAGNETIC NANOSTRUCTURES	K. Suzuki	23
I-03	NONLINEAR EFFECTS IN MAGNETOIMPEDANCE: MEASUREMENTS AND MODELS	D. Seddaoui, D. Ménard, B. Movaghar, and A. Yelon	23
I-04	ON THE RELATIONSHIP BETWEEN THERMO-PHYSICAL AND MECHANICAL PROPERTIES OF GLASS-FORMING ALLOYS	Livio Battezzati	24
I-05	APPLICATIONS OF INVERSE METHODS TO CHARACTERIZE METALLIC GLASSES	Sven Bossuyt	24
I-06	X-RAY AND NEUTRON SCATTERING FROM LEVITATED LIQUIDS	Louis Hennet	24
I-07	MAGNETISM AND CRYSTALLINE STRUCTURE OF FEPT NANOCUBES AND ICOSAHEDRA	M. Farle	25
I-08	SPIN CURRENT AND TWO MAGNON SCATTERING IN NANOSCALE SYSTEMS	B. Heinrich	25
I-09	LOW FIELD MAGNETISATION REVERSAL PROCESS OF SOFT/HARD BI-PHASE MAGNETIC MICROWIRES	M. Vazquez, G. A. Badini-Confalonieri, J. Torrejon and G. Infante	25
I-10	SINGLE DOMAIN WALL DYNAMICS IN THIN MAGNETIC WIRES	R. Varga, Y. Kostyk, R. Kornel, A. Zhukov, M. Vazquez	26
I-11	ORDERING IN NETWORK LIQUIDS AND GLASSES	Philip S. Salmon	26
I-12	STRUCTURE AND ELECTRONIC PROPERTIES OF METAL-AMMONIA "OGG-GLASSES"	N. Skipper	26
I-13	MECHANICAL ACTIVATION AS A WAY OF OBTAINING NON-EQUILIBRIUM STATES IN CONDENSED MATTER: FUNDAMENTAL PRINCIPLES AND POSSIBLE PRACTICAL APPLICATIONS	E.P. Yelsukov	27
I-14	SHAPE EVOLUTION, CRYSTALLINITY AND OPTICAL PROPERTIES OF GOLD NANOPARTICLES	Marcel Miglierini	27
I-15	CRYSTALLISATION OF NANOPERM TYPE ALLOYS	Liz-Marzan	28
I-16	RECENT ADVANCES IN SOFT MAGNETIC NANOCRYSTALLINE FE-CO AND FE-NI BASED ALLOYS	I. Škorvánek, J. Marcin, J. Turčanová, J. Kováč, P. Švec and D. Janičkovič	28
I-17	PHYSICAL PROPERTIES OF NANOCRYSTALLINE AND NANOSTRUCTURED FERRITES	J. M. Greneche	28

I-18	SINGLE AND MULTILAYERED MAGNETIC NANOWIRES: PREPARATION AND CHARACTERIZATION	H. Chiriac	29
I-19	MAGNETIC MICROSTRUCTURE OF NANOCRYSTALLINE MATERIALS	Sybille Flohrer	29
I-20	SEVERE PLASTIC DEFORMATION OF AMORPHOUS ALLOYS	A.M. Glezer, S.V. Dobatkin, M.R. Plotnikova, A.V. Shalimova, N.S. Perov	29
I-21	RECENT ADVANCES IN FUNDAMENTAL UNDERSTANDING OF THE GLASS TRANSITION	K.L. Ngai	30

Oral Communications

Ref.	Title	Authors	Page
C-01	NEUTRON DIFFRACTION STUDY OF THE STRUCTURES OF TWO CUHFTI BULK ALLOY GLASSES	N. Cowlam, I.A. Figueroa, G. Cuello, I.Todd, H.A. Davies	31
C-02	RESOLUTION FUNCTION FOR A DEDICATED TWO-AXIS DIFFRACTOMETER FOR THE STRUCTURE OF AMORPHOUS	G.J. Cuello	31
C-03	NON-ISTHERMAL, APPROACH TO CRYSTALLIZATION PROCESS OF SEVERAL CO RICH ALLOYS	J. Bonastre, LI. Escoda, J.J. Saurina, J.J. Sunol, J.D. Santos, M ^a L. Snachez, B.Hernando	31
C-04	KISSINGER ANALYSIS FOR DYMN6-XGE6-XFEXALX (0<X<6) ALLOYS	Z.Sniadecki, B. Idzkowski	32
C-05	INFLUENCE OF CRYOMILLING ON STRUCTURE OF COFEZRB ALLOY	J. Bednarcik, K. Saks1, R. Nicula, S. Roth, H. Franz	32
C-06	THE STRUCTURE OF LIQUID CALCIUM ALUMINATES: A COMBINED NEUTRON DIFFRACTION AND COMPUTER SIMULATION STUDY	V. Cristiglio, L. Hennem, G.J. Cuello, M.R. Johnson, I. Pozdnyakova, D.L. Price	33
C-07	MOSSBAUER CHARACTERIZATION OF AN AMORPHOUS STEEL ALLOY WITH OPTIMUM MO CONTENT	Laura Facchini, Pere Bruna, Eloi Pineda, Daniel Crespo	33
C-08	NANOCRYSTALLIZATION EFFECTS ON THE SPECIFIC HEAT OF FE-CO-NB-B AMORPHOUS ALLOY	J.S. Blazquez, M. Millán, C.F. Conde, V. Franco, A. Conde	33
C-09	WITHDRAWN		
C-10	METHODOLOGICAL STUDY ON PHASES TRANSITIONS AND NANOSTRUCTURE OF PHOPHATIDYLCHOLINE SINGLELAYER WITH SCANNING PROBE MICROSCOPES AND LANGMUIR-BLODGETT TECHNIQUES	Jie Zhu, Lianhong Guo, Guodong Wang	34
C-11	SPIN RELAXATION IN NANOPHASED MANGANITES	Javier Bermejo, Luís Fernández Barquín, Jon Gutiérrez and José Manuel Barandiarán	34
C-12	A NEW APPROACH TO DIFFUSION-LIKE RELAXATION PROCESSES	A. Fondado, J. Mira, J. Rivas	35
C-13	EFFECT OF NB IN THE NANOCRYSTALLIZATION AND MAGNETIC PROPERTIES OF FENBBCU AMORPHOUS ALLOYS	J. Torrens-Serra, S. Roth, J. Rodriguez-Viejo, M. T. Clavaguera-Mora	35

C-14	PREPARATION OF GD ₅ SI ₂ GE ₂ COMPOUNDS USING RF- INDUCTION	A.M. Pereira, J.R. Peixoto, P.B. Tavares, N. Martins, J.B. Sousa, J. P. Araújo	35
C-15	HYPERFINE FIELDS IN CHARGE ORDERED PR(1-X)CA(X)MNO ₃ MANGANITES	A. M. L. Lopes, T. M. Mendonça, J. S. Amaral, A. M. Pereira, P. B. Tavares, Y. Tomioka, Y. Tokura, J. G. Correia, V. S. Amaral, J. P. Araújo	36
C-16	THE EFFECT OF CHEMICAL INHOMOGENEITY ON THE MAGNETOCALORIC EFFECT OF (LA-ER-SR-MNO ₃)/ER-MNO ₃) SELF COMPOSITE	J. S. Amaral, P. B. Tavares, M. S. Reis, J. P. Araújo, T. M. Mendonça, V. S. Amaral and J. M. Vieira	36
C-17	NOVEL TRANSPORT BEHAVIOR OF YTTRIUM SUBSTITUTION IN POLYCRYSTALLINE LA _{0.7} PB _{0.3} MNO ₃	C. H. Lin, S. L. Young, H. Z. Chen, M. C. Kao, Lance Horng	37
C-18	MAGNETIC AND STRUCTURAL CHARACTERIZATION OF THE SILVER-IRON OXIDE NANOPARTICLES OBTAINED BY THE MICROEMULSION TECHNIQUE	E. Goikolea, M. Insausti, J. S. Garitaonandia and L. Lezama	37
C-19	SIMULATION OF THE SPINODAL PHASE SEPARATION DYNAMICS OF THE BI-ZN SYSTEM	J. C. R. E. Oliveira, M. H. Braga, Rui D. M. Travasso	37
C-20	COMPOSITION AND NEAR SURFACE MECHANICAL PROPERTIES OF SILICATE GLASSES	Damir R. Tadjiev, Russel J. Hand	38
C-21	MICROSTRUCTURAL AND MAGNETIC CHARACTERIZATION OF ND ₂ FE ₁₇ BALL MILLED	P. Álvarez, J.L. Sánchez Llamazares, M.J. Pérez, B. Hernandoa, J.D. Santos, J.Sanches-Marcos, J.A. Blanco, P. Gorria	38
C-22	EFFECT OF THERMAL TREATMENT ON HIGH-FREQUENCY MAGNETOIMPEDANCE IN FERROMAGNETIC/CU/FERROMAGNETIC TRILAYERS	F. Celegato, M. Coisson, P. Tiberto, F. Vinai	38
C-23	OFF-DIAGONAL MAGNETOIMPEDANCE EFFECT IN FEB AMORPHOUS RIBBONS	M .L. Sanchez, T. Sanchez, I. Ribot, M. J. Perez, J. D. Santos, V. M. Proda, B. Hernando, L. Escada, J. J. Sunol	39
C-24	SPECIFIC EFFECTS OF NANOMETER SCALE SIZE ON MAGNETIC ORDERING IN LA _{1-X} CA _X MNO ₃ (X=0.1, 0.3 AND 0.6) MANGANITES	E. Rozenberg, M. Auslender, A. I. Sharmes, Ya. Mukivskii, E. Sominski, A. Gedanken	39
C-25	GLASS FORMABILITY IN METALLIC MATERIALS	H.A. Davies, I.A. Figuerosa, I. Todd	40

C-26	FORMATION AND PROPERTIES OF THE NEW ZR75ALXNI10CU10AG5 BULK METALLIC GLASSES	J. Latuch, A. Abramczyk, T. Kulik	40
C-27	COMBINATORIAL ANALYSIS OF CA-MG-AL(CU) THIN FILM METALLIC GLASSES	J. Rodrigues-Viejo, R. Domenech-Ferrer, Gemma Garcia, M.T. Clavaquera-Mora	40
C-28	ASYMMETRY IN RESISTIVE SWITCHING IN MAGNETIC TUNNEL JUNCTIONS	J.Ventura, J.M. Teixeira, J.P. Araujo, J.B. Sousa, Z. Zhang, Y. Liu, P.P. Freitas	41
C-29	SYNTHESIS AND CHARACTERISATION OF 3C-SIC NANOWIRES	G. Attolini, F. Rossi, M. Bosi, B.E. Watts, G. Salviati	41
C-30	DESIGN OF A DOUBLE CORE LINEAR MAGNETOMETER BASED ON ASYMMETRIC MAGNETOIMPEDANCE EFFECT IN NANOSTRUCTURED FINEMENT RIBBONS	M.M. Tehranchi, M. Ghannatshoar, S.M. Mohseni, H. Eftekhari	41
C-31	STUDY OF HYPERFINE INTERACTIONS IN FE-CO NANOCOMPOSITE FILMS BY MOSSBAUER SPECTROSCOPY AND NMR	Adriana Lancok, Frantisek Fendrych, Marcel miglierini, Jaroslav Kohout	42
C-32	SYNTHESIS AND MAGNETIC PROPERTIES OF MONODISPERSIVE FE ₃ O ₄ NANOPARTICLES WITH CONTROLLED SIZES	J. Salado, M. insausti, I. Gil de Muro, L. Lezama, T. Rojo	42
C-33	ELECTRICAL AND OPTICAL PROPERTIES OF AMORPHOUS CR ₂ -XTIXO ₃ THIN FILMS	A. Conde-Gallardo, R. Escudero Derat, F. S. Aguirre-Tostado3.	43
C-34	RELATIONSHIP BETWEEN NANOPARTICLE GROWTH AND MAGNETIC PROPERTIES OF MAGNETIC NANOCOMPOSITES	D. Ortega, J.S: Garitaonandia, M.Ramirez-del-solar, C. Barrera-Solano, M. Dominguez	43
C-35	SUPERPARAMAGNETIC BEHAVIOUR OF FE NANOPARTICLES EMBEDDED IN A COMMERCIAL POROUS CARBON	M.P. Fernandez-Garcia, M. Sevilla, A.B. Fuertes, A.Silva, D.S. Schmool, P. Gorria, J.A. Blanco	43
C-36	SYNTHESIS AND CHARACTERIZATION OF COFE ₂ O ₄ -PVP NANOCOMPOSITES	Cintia Mateo Mateo, Carlos Vásquez Vásques, Maria del Carmen Buján Núñez, M. Arturo López Quintela, David Serantes Abalo, Daniel Baldomir Fernández, José Rivas	44
C-37	MAGNETIC ANISOTROPY OF BATIO ₃ -COFE ₂ O ₄ NANOGRANULAR COMPOSITE THIN FILMS	J. Barbosa, B.G. Almeida, J.A. Mendes, J.P.Araújo	44
C-38	MAGNETIZATION PROCESSES IN ARRAYS OF ANTIDOTS LITHOGRAPHED ON AMORPHOUS FEB FILMS	J. Gutiérrez, R. Yanes, F. Garcia, E. Paz, J. Haba, F. Cebollada, O. Chubykalo-Fesenko, F.J. Palomares,	44

		J.M. González	
C-39	ELECTROLYTE INFLUENCE ON THE ANODIC SYNTHESIS OF TIO ₂ NANOTUBE ARRAYS	V. Veja, M.A. Cerdeira, V.M. Prida, D. Alberts, N. Bordel, R. Pereiro, F. Mera, S. Garcia, M. Hernández-Vélez, M. Vázquez	45
C-40	FINITE ELEMENT ANALYSIS OF HYPERELASTIC CONTACT PROBLEM IN DOOR AUTOMOTIVE SEALING	J. Ordieres-Meré, A. Bello-Garcia, V. Muñoz-Munilla, JJ. Del-Coz-Diaz	45

Poster Communications

Ref.	Title	Authors	Page
P-01	AMORPHOUS NI ₅₉ ZR ₂₀ TI ₁₆ M ₅ (M=CU, AG) ALLOYS OBTAINED BY MELT SPINNING AND MECHANICAL	D. Oleszak, E. Zbrzezniak, T. Kulik	46
P-02	THE ROLE OF SURFACTANT IN SYNTHESIS OF MAGNETIC NANOCRYSTALLINE POWDER OF NIFE ₂ O ₄ BY SOL-GEL AUTO-BOMBUSTION METHOD	M.R. Barati, S.A. Seyyed Ebrahimil, A. Badiei	46
P-03	BULK GLASS FORMABILITY FOR CU-HF-ZR-AG AND CU-ZR-AG-SI ALLOYS	I.A. Figueroa, H. Zhao, S. González, H. A. Davies, I.Todd	46
P-04	RAPID THERMAL PROCESSING OF ZNO NANOCRYSTALLINE FILMS FOR APPLICATION IN DYE-SENSITIZED SOLAR CELLS	M.C. Kao, H.Z. Chen, S.L. Young, C.H. Lin	47
P-05	ANODIZATION PROCESS OF SELF-ORDERING NANOPOROUS ALUMINA MEMBRANES IN PHOSPHORIC ACID	M.P. Proença, C.T. Sousa, D.C. Leitão, J. Jentura, F. Carpinteiro, J.B. Sousa, J.P. Araújo	47
P-06	THE CRYSTALLINITY OF SIC GROWN FROM THE VAPOUR PHASE	B.E. Watts, G. Attolini, M.Bosi, G. Salviati, O. Martinez	47
P-07	INVESTIGATION OF THE EFFECTIVE PARAMETERS ON THE SYNTHESIS OF NI FERRITE NANOPOWDERS BY COPRECIPITATION METHOD	R. Dehghan, S.A. Seyyed Ebrahimi, A. Badiei	48
P-08	EPITAXY AND SURFACE MORPHOLOGY OF ZNO THIN FILMS GROWN BY RF_MAGNETRON SPUTTERING ON SAPPHIRE	A.C. Lourenço, S. Pereira, M. Peres, T. Monteiro, M.R. Correia, S. Magalhães, E. Alves	48
P-09	THE EVOLUTION OF BOND STRUCTURE IN GE ₃₃ AS ₁₂ SE ₅₅ FILMS UPON THERMAL ANNEALING	R.P. Wang, D.Y. Choi, A.V. Rode, S. Madden, B. Luther-Davies	48
P-10	PRIMARY CRYSTALLIZATION IN FE ₆₅ NB ₁₀ B ₂₅ METALLIC GLASS	M.T. Clavaguera-Mora, J. Torrens-Serra, J. Rodriguez-Viejo	48
P-11	EPR STUDY OF CRYSTALLINE AND GLASSY ETHANOL	Marina Kveder, Dalibor Merunka, Milan Jokić, Boris Rakvin	49
P-12	STRUCTURES OF LANTHANUM AND YTTRIUM ALUMINOSILICATE GLASSES	I. Pozdnyakova, L. Hennet, N. Sadiki, V. Cristiglio, A. Bytchkov, G. Cuello, J.P. Coutures, D.L. Price	49

P-13	THERMAL AND MAGNETIC BEHAVIOR OF COBALT-BASED ALLOYS	A. Rosales-Rivera, M. Gómez-Hermida, P. Pineda-Gómez	49
P-14	DIFFUSION PHENOMENA IN NON-CRYSTALLINE OBSIDIAN SAMPLES AND APPLICATIONS IN THE DATING OF ANCIENT OBSIDIAN TOOLS BY SIMS AND FT-IR	Th. Ganetsos, B. Kotsos, I. Liritzis, M. Novak, Nikos Laskaris	50
P-15	CRYSTALIZATION OF KNBO ₃ IN A B ₂ O ₃ GLASS NETWORK	R.C.C. Figueira, M.P.F. Graça, L.C. Costa, M.A. Valente	50
P-16	STRUCTURAL STUDY OF UNDOPED AND (MN,IN) DOPED SNO ₂ THIN FILMS GROWN BY RF SPUTTERING	A. Espinosa, N. Menéndez, J. Rubio-Zuazo, C. Prieto, A. De Andrés	50
P-17	STRUCTURAL AND OPTICAL SPECTROSCOPY OF LINBO ₃ :TM NANOCRYSTALS EMBEDDED IN A SIO ₂ GLASS MATRIX	M.P.F. Graça, M.A. Valente, T. Monteiro, A.J. Neves, M. Peres	51
P-18	ASYMMETRIC MAGNETIZATION REVERSAL OF PARTIALLY DEVITRIFIED CO ₆₆ SI ₁₅ B ₁₄ FE ₄ NI ₁ AMORPHOUS ALLOYS	J.C: Martinez-Garcia, J.A. Garcia, M. Rivas	51
P-19	NANOCRYSTALLIZATION AND FRACTURE CHARACTERISTICS IN CO-BASED RIBBONS	J.A. Garcia, J.A. Riba, R. Quintana, L. Elbaile	51
P-20	STRUCTURAL EVOLUTION OF METALLIC GLASSES DURING ANNEALING THROUGH IN-SITU SYNCHROTRON X-RAY DIFFRACTION	Eloi Pineda, Pere Bruna, Trinitat Pradell, Jorge Serrano, Ana Labrador, Daniel Crespo	52
P-21	DETECTION ON THE CURIE TRANSITION ON CO-BASED AMORPHOUS ALLOYS BY MEANS OF MICROWAVE ABSORPTION	H.Montiel, G. Alvarez, J.M. Saniger, R. Valenzuela	52
P-22	INFLUENCE OF MN ALLOYING ON THE DEVITRIFICATION PROCESS OF COFEMNNBB ALLOYS	M. Millán, J.S. Blazquez, C.F. Conde, A. Conde	53
P-23	ANALYSIS OF THE MECHANICALLY ALLOYED FE ₈₅ -NB ₅ -B ₁₀ POWDER USING NON UNIQUE LATTICE PARAMETER	J.J. Ipus, J.S. Blazquez, A. Conde, M. Krasnowki, T. Kulik	53
P-24	WITHDRAWN		
P-25	TRANSPORT PROPERTIES NEAR THE MAGNETO/STRUCTURAL TRANSITION OF TB ₅ SI ₂ GE ₂	A.M.Pereira, M.E. Braga, P.A. Algarabel, L. Morellon, C. Magen, R. Fermento, M.R. Ibarra, J.P. Araújo and J.B. Sousa	53
P-26	QUANTUM SPIN-RESONANT TUNNELING IN MAGNETIC JUNCTIONS WITH A DOUBLE-SPACER STRUCTURE	H. Silva, Y. Pogorelov	54

P-27	MAGNETOCALORIC EFFECT IN NANO- AND POLYCRYSTALLINE LA _{0.8} SR _{0.2} MNO ₃ MANGANITES	M. Pękała, V. Drozd	54
P-28	MAGNETIC PROPERTIES OF COMPACTED CAMNO ₃ -D NANOPARTICLES	V. Markovich, I. Fita, R. Puzniak, A. Wisniewski, D. Mogilyansky, L. Titelman, L. Vradman, M. Herskowitz and G. Gorodetsky	54
P-29	THE EFFECT OF CHEMICAL DISTRIBUTION ON ESTIMATING THE MAGNETOCALORIC EFFECT FROM MAGNETIC MEASUREMENTS	J.S. Amaral, N.J.O. Silva and V.S. Amaral	55
P-30	MAGNETIC AND MECHANICAL PROPERTIES FECONBB AMORPHOUS RIBBONS	I.Betancourt and R.Landa	55
P-31	DIELECTRIC, MORPHOLOGICAL AND THERMIC PROPERTIES OF TERNARY MELT-BLEND PROCESSING	C. R. Martins, C. P. L. Rubinger, L. C. Costa, R.M. Rubinger	56
P-32	THE STABILITY OF THE MAGNETIC DOMAINS INSIDE THE CORE OF AMORPHOUS METAL WIRE	A.A Gavriiliuk, A.Yu. Mokhovikova, A.V. Semirovb, A.L. Semenova, N.V. Turika, V.O. Kudrewcev	56
P-33	MAGNETIC AND TRANSPORT STUDIES OF THE A-S TRANSFORMATION IN AN FE ₅₀ V ₅₀ ALLOY	B.F.O. Costa, V.S. Amaral, G. Le Caër, M.E.Braga, M.M. Amado, and J.B. Sousa	56
P-34	CALCULATING GIANT MAGNETOIMPEDANCE IN ARBITRARY SHAPES	S. Sarkarati, M. H. Khaksaran, M. M. Tehranchi and S. M. Mohseni	57
P-35	ROOM TEMPERATURE FERROMAGNETISM WITH GIANT MAGNETIC MOMENT IN FE:ZNO	L.M.C. Pereira, J.P. Araújo, U. Wahl, J.G. Correia	57
P-36	ANGULAR DEPENDENCE OF FERROMAGNETIC RESONANCE IN AMORPHOUS CO-RICH RIBBONS	E. M. Mata-Zamora, H. Montiel, G. Alvarez, J. Saniger, and R. Valenzuela	57
P-37	PHOTO AND ELECTROLUMINESCENCE BEHAVIOR OF TB(ACAC) ₃ PHEN COMPLEX USED AS EMISSIVE LAYER ON ORGANIC LIGHT EMITTING DIODES	L. Rino, W. Simões, G. Santos, F.J. Fonseca, A.M. Andrade, V.A.F. Deichmann, L. Akcelrud, L. Pereira	58
P-38	MICROWAVE POWER ABSORPTION ANALYSIS OF THE DEVITRIFICATION PROCESS OF CO-BASED AMORPHOUS RIBBONS	R. Valenzuelaa, H. Montielb, R. Zamoranoc and G. Alvarez	58
P-39	THE INFLUENCE OF LASER ANNEALING IN THE PRESENCE OF LONGITUDINAL WEAK MAGNETIC FIELD ON ASYMETRICAL MAGNETOIMPEDANCE RESPONSE OF	M. Ghanaatshoar, N. Nabipour, M. M. Tehranchi, S. M. Hamidi, S. M. Mohseni	58

COFESIB AMORPHOUS RIBBONS

P-40	MAGNETO-OPTICAL KERR EFFECT IN GLASS/CU/COFESIB/SNO ₂ THIN FILMS	M. Ghanaatshoar, M. Moradi, M. M. Tehranchi, S. M. Hamidi	59
P-41	ANOMALOUS MAGNETIC PROPERTIES IN FE ₇₈ SI ₉ B ₁₃ THIN FILMS	S. M. Hamidi, M. M. Tehranchi, M. Ghanaatshoar, M. Moradi, S. M. Mohseni	59
P-42	PECULIARITIES OF THE TRANSPORT AND MAGNETIC PROPERTIES OF THE CATION-SUBSTITUTED MANGANESE SULPHIDE	O.B.Romanova, L.I. Ryabinkina	60
P-43	MAGNETIC BEHAVIOR AND MAGNETO IMPEDANCE EFFECT IN IRON-BASED RIBBONS	A. Rosales-Rivera, O. Moscoso-Londoño, A. A. Velásquez	60
P-44	A GRAPHICAL APPROACH FOR HAMILTONIAN OF T-J MODEL	C.R.Ou, S.L.Young, Chung-Ming Ou	60
P-45	LASER ACTION IN 1D AND 2D PHOTONIC CRYSTAL STRUCTURES WITH ACTIVATED GLASSES	Olga N. Kozina, Leonid A. Melnikov	61
P-46	MÖSSBAUER STUDY OF MULTIPHASE IRON OXIDE COMPOSITES	E. Goikolea, M. Insausti, J.S. Garitaonandia and L. Lezama	61
P-47	SURFACE AND BULK MAGNETIC PROPERTIES OF AMORPHOUS AND NANOCRYSTALLINE NI-SUBSTITUTED FINEMET SAMPLES	L. Elbailea, M ^a R. D. Crespoa, A. R. Piernab and J. A. Garcíaa	62
P-48	CAPPING LIGAND EFFECTS ON THE SIZE-DEPENDENT AMORPHOUS-TO-CRYSTALLINE TRANSITION OF CDSE NANOPARTICLES	Mauro Spifani, Eva Pellicer, Jordi Arbiol, Joan R. Morante	62
P-49	ANGULAR DEPENDENCE OF MICROWAVE ABSORPTION IN MULTILAYER FILMS	G. Alvarez, H. Montiel, D. de Cos, A. García-Arribas, R. Zamorano, J.M. Barandiarán, and R. Valenzuela	62
P-50	DIELECTRIC PROPERTIES OF POLYSTYRENE-CCTO COMPOSITE	F. Amaral, C.P. L. Rubinger, F. Henry, L.C.Costa, M.A. Valente	63
P-51	ON THE ENHANCEMENT OF METHANOL AND CO ELECTRO-OXIDATION BY AMORPHOUS (NINB)PTSNRU ALLOYS VERSUS BIFUNCTIONAL PTRU AND PTSN ALLOYS	A.R. Pierna, J. Barranco, F.F. Marzo, A. Lorenzo, B. Carton, M.M. Antxustegi, F. Lopez	63
P-52	ELECTROCATALYTIC ACTIVITY OF ORR AT AMORPHOUS NI ₅₉ NB ₄₀ PTXM _{1-X} ELECTRODES IN ACID MEDIUM	G. Ramos-Sanchez, O. Solorza-Feria, A.R. Pierna	63

P-53	SIMULATIONS ON THE REFRIGERATION OF INTEGRATED CIRCUITS USING MICRO-CHANNELS	A.M.Pereira, J.C.R.E. Oliveira, J. Ventura, J.B. Sousa, J.P. Araujo	64
P-54	DETERMINATION OF TRACE METAL RELEASE DURING CORROSION CHARACTERIZATION OF FECO-BASED AMORPHOUS METALLIC MATERIALS BY STRIPPING VOLTAMMETRY, NEW MATERIALS FOR GMI BIOSENSORS	F.F. Marzo, A.R. Pierna, J. Barranco, A. Lorenzo, J. Barroso, J.A. Garcia, A. Pérez	64
P-55	PRESSURE-INDUCED SUPPRESSION OF FERROMAGNETIC PHASE LACOO ₃ NANOPARTICLES	I. Fita, D. Mogilyansky, V. Markovich, R. Puzniak, A. Wisniewsky, L. Titelman, L.Vradman, M. Herskowitz, V.N. Varyukhin and G. Gorodestky	64
P-56	MAGNETIC CHARACTERIZATION OF FE, NI, CO NANOPARTICLES, DISPERSED IN PHYLLOSILICATE TYPE SILICON OXIDE	V.Sagredo, O. Peña, A. Loaiza-Gill, Marlin Villarroel, Maria La Cruz, José Balbuena	65
P-57	CARBON NANOCONES: A VARIETY OF NON-CRYSTALLINE GRAPHITE	H. Heiberg, A.T. Skjeltorp, Klaus Sattler	65
P-58	SYNTHESIS AND CHARACTERIZATION OF NANOCRYSTALLINE FE ₆₀ X ₂₀ P ₁₀ B ₁₀ (X=CO, NI) ALLOYS	M. Pilar, J.J. Suñol, L.Escoda, J.Saurina, B. Arcondo	66
P-59	PECULIARITIES OF MAGNETIC PROPERTIES OF HETEROGENEOUS NANOCRYSTALLINE MAGNETIC MATERIALS	E.E. Shalyguina, V.V. Molokanov, M.A. Komarova, V.A. Melnikov, A.N. Shalugin	66
P-60	INTERPLAY BETWEEN THE MAGNETIC FIELD AND THE DIPOLAR INTERACTION ON THE BLOCKING TEMPERATURE OF A MAGNETIC NANOPARTICLE SYSTEM: MONTE CARLO STUDY	D. Serantes, D. Baldomir, M.Pereiro, J.E. Arias, C. mateo-mateo, M.C. Buján-Núñez, C. Vásquez-Vásquez, J.Rivas	66
P-61	INFLUENCE OF NANOPARTICLE SIZE ON BLOCKING TEMPERATURE OF INTERACTING SYSTEM: MONTE CARLO SIMULATION	M.C. Buján Núñez, N. Fontaiña-Troitiño, C. Vázquez-Vázquez, M.A. López Quintela, Y. Piñeiro, D. Serantes, D. Baldomir, J. Rivas	67
P-62	HIGH PULSED MAGNETIC FIELD MAGNETORESISTANCE IN COFE(T)/AL ₂ O ₃ DISCONTINUOUS MULTILAYERS	J.M. Moreira, H. Silva, J.P. Araújo, Y.G. Pogorelov, A.M. Pereira, J.B. Sousa, P.P. Freitas, S. Cardoso, B. Raquet, H. Rakoto	67
P63	TIME-RESOLVED SYNCHROTRON RADIATION INVESTIGATION OG MAGNETITE GRAIN-GROWTH DURING MICROWAVE HEATING	M. Stir, R. Nicula, B. Schmitt, J.M. Catala-Civera and S. Vaucher	68

P-64	BROAD UHF FERROMAGNETIC RESONANCE OF IRON TICH ALUMINIUM PULSED LASER DEPOSITED THIN FILMS	V. Madurga, J. Vergara, C. Favieres	68
P-65	A PROTOTYPE LAYER ON AS ₂ S ₃ FILM FOR PHOTORESIST PATTERNING	Duk-Yong Choi, Steve Madden, Andrei Rode, Rongping Wang, Barry Luther-Davies	68
P-66	STRUCTURAL PROPERTIES OF EXCHANGE BIASING MNPT AND MNNI ANTIFERROMAGNETIC MATERIALS FOR SPINTRONIC	J. Ventura, J.M. Teixeira, J.P. Araújo, J.B. Sousa, V. Amaral, B. Negulescu, M. Rickart, P.P. Freitas	68
P-67	STRUCTURAL, MAGNETIC AND TRANSPORT PROPERTIES OF ION BEAM DEPOSITED NIFE THIN FILMS	J.Ventura, R. Fermento, D. Leitão, J.M. Teixeira, A.M. Pereira, J.P. Araujo, J.B. Sousa	69
P-68	PY ANTIDOT THIN FILMS: A TRANSPORT AND MAGNETIC CHARACTERIZATION AS A FUNCTION OF TEMPERATURE	D.C. Leitão, C.T. Sousa, J. Ventura, F. Carpinteiro, K.R. Pirota, M. Vazquez, J.B. Sousa, J.P. Araújo	69
P-69	STRUCTURAL AND MAGNETIC EVOLUTION OF MECHANICALLY ALLOYED FE ₃₀ CR ₇₀ ALLOYS STUDIED BY NEUTRON THERMO-DIFFRACTOMETRY AND X-RAY ABSORPTION SPECTROSCOPY	A. Fernandez-Martinez, D. Martinez-Blanco, M.J. Perez, G.J. Cuello, G. Castro, J.A. Blanco, P. Gorria	70
P-70	THEORETICAL STUDY OF MAGNETODYNAMICS IN FERROMAGNETIC NANOPARTICLES	N. Sousa, H. Kachkachi, D. S. Schmool	70
P-71	MEASURING MAGNETIC PROPERTIES IN EXCHANGE SPRING SYSTEMS USING FERROMAGNETIC RESONANCE	A. Apolinário, F. Casoli, L. Nasi, F. Albertini and D. S. Schmool	71
P-72	CHARACTERIZATION OF ELECTRODEPOSITED NI AND NI ₈₀ FE ₂₀ NANOWIRES	D. C. Leitao, C. T. Sousa, J. Ventura, J.Amaral, F. Carpinteiro, K.R.Pirota, M. Vazquez, J. B. Sousa, J. P. Araújo	71
P-73	ON THE ELECTROCHROMISM IN THE NON-CRYSTALLINE NIOBIUM PENTOXIDE ANODIC FILMS	L.Skatkov, V. Gomozov	71
P-74	STRUCTURAL AND MAGNETIC CHARACTERIZATION OF FE/FE ₃ O ₄ MIXED NANPOWDERS	O. Crisan, J.M. Greneche, I. Skorvanek, R. Nicula	72
P-75	FINITE VOLUME MODELLING OF THE NON-ISOTHERMAL FLOW OF A NON-NEWTONIAN FLUID IN RUBBER'S EXTRUSION DIE	J.J. del Coz, P.J: Garcia Nieto, J. Ordieres Meré, A. Bello Garcia	72
P-76	EVIDENCE OF INTRINSIC FERROMAGNETIC BEHAVIOUR OF THIOL CAPPED AU	E. Goikolea, J.S. Garitaonandia, M. Insausti, J. Lago, I. Gil de Muro, J.	73

	NANOPARTICLES BASED ON μ SR RESULTS	Salado, J. Bermejo, D.S. Schmool	
P-77	ELECTRON TRANSPORT IN HITPERM ALLOYS	K. Pekala	73
P-78	THERMAL AND MAGNETIC BEHAVIOR OF COBALT-BASED ALLOYS	A. Rosales-Rivera, M. Gomez-Hermida, P. Pineda- Gomez	73
P-79	MAGNETOTHERMOPOWER IN MAGNETIC NANOCOMPOSITES “AMORPHOUS FERROMAGNET $\text{Co}_{0.45}\text{Fe}_{4.5}\text{Zr}_{10}$ -AMORPHOUS DIELECTRIC Al_2O_n ”	A. Granovsky, Yu.Kalinin, V. Belousov, and A. Sitnikov	74

INVITED LECTURES

I-01

NANOCRYSTALLINE STRUCTURE EVOLUTION IN FE-B-CU SOFT MAGNETIC MATERIALS

Y. M. Chen^{1,2}, T. Ohkubo^{2,3}, M. Ohta⁴, Y. Yoshizawa⁴ and K. Hono^{1,2,3}

¹Graduate School of Pure and Applied Sciences, University of Tsukuba

²National Institute for Materials Science

³CREST, Japan Science and Technology Agency

⁴Advanced Electronics Research Lab., Hitachi Metals, Ltd.

More than 20 years have passed since the first nanocrystalline soft magnetic material was invented by Yoshizawa et al. Continuous effort has been devoted to improve the soft magnetic properties of Fe based nanocrystalline alloys, in particular saturation magnetic flux density (B_s). To keep the processability of wide melt-spun ribbons in air, which is essential to manufacture economically viable industrial products, a substantial amount of glass forming elements such as B and Nb had to be alloyed. However, Fe-B binary alloy is a marginal glass former, so the addition of Nb is not necessarily essential to obtain amorphous phase by melt-spinning. Ohta and Yoshizawa [1,2] have recently developed a new type of Fe-B-Cu and Fe-B-Si-Cu nanocrystalline soft magnetic materials without transition elements. Naturally, the saturation magnetization was improved ($\sim 1.84T$) compared to the highest B_s for the existing nanocrystalline soft magnetic materials ($\sim 1.7T$). In this work, we report the nanocrystalline structure evolution of $(Fe_{0.85}B_{0.15})_{100-x}Cu_x$ ($x=0, 1.0, 1.5$) melt-spun ribbons investigated by the three dimensional atom probe technique and discuss the mechanism of the nanocrystallization in comparison with those for the existing nanocrystalline soft magnets.

M. Ohta and Y. Yoshizawa, JJAP 46, L477 (2007).

M. Ohta and Y. Yoshizawa, APL 91, 0625171 (2007).

I-02

LOCAL RANDOM MAGNETOCRYSTALLINE AND MACROSCOPIC UNIAXIAL ANISOTROPIES IN MAGNETIC NANOSTRUCTURES

K. Suzuki

Department of Materials Engineering, Monash University, Clayton, Victoria 3800, Australia

When the domain wall displacement is the primary mechanism of technical magnetization, the coercivity is governed by the fluctuation amplitude of the magnetic anisotropy energy. This fluctuation amplitude in nanocrystalline soft magnetic materials is predicted to be proportional to the 6th power of the mean grain size (D) in

the framework of the random anisotropy model (RAM). This D^6 power law was confirmed through the grain size dependence of the coercivity in nanocrystalline Fe-Si-B-Nb-Cu alloys (Finemet). However, a lower D -power exponent of approximately 3 was also reported for nanocrystalline Fe-Zr-B alloys (Nanoperm). In this paper the effect of induced K_u on the coercivity of soft magnetic nanostructures is studied with a view to answer the question: Why does the D -power dependence differ between the two nanocrystalline alloy families? In order to isolate the effects of annealing induced K_u from other influential material parameters, we have employed rotating magnetic field annealing, an established technique, but which is new to nanocrystalline soft magnetic ribbons. The coercivity (H_c) of nanocrystalline $Fe_{84}Nb_6B_{10}$ was found to decrease from 10 A/m to 5.9 A/m by applying a static magnetic field of 640 kA/m during annealing. This decrease in H_c is well understood by a higher coherence of K_u after the static field annealing. Furthermore, the lowest H_c value 3 A/m was obtained by rotating the applied field during annealing, implying that lifting K_u from the sample is effective in suppressing the random magnetocrystalline anisotropy ($\langle K_1 \rangle$). The suppression of H_c by rotating field annealing may well be understood by the change in the D dependence of $\langle K_1 \rangle$ from the 3rd power to the 6th power. It has also been found in our simulation based on RAM with K_u (i.e. RAM where the exchange length is governed both by $\langle K_1 \rangle$ and K_u) that the ratio of K_u to $\langle K_1 \rangle$ required for the changeover from the D^6 to D^3 dependence is about 2. This explains why Nanoperm reveals the D^3 dependence whereas the dependence in Finemet remains D^6 . The key to understanding the difference in the scaling behavior between these two alloy families is their K_u values. The annealing induced K_u in Finemet is an order of magnitude smaller than that of Nanoperm. Hence, the crossover from the D^6 to D^3 dependence in Finemet could only be possible in a very small $\langle K_1 \rangle$ range where the effective anisotropy density of ribbon specimens tends to be governed by extrinsic mechanisms. Consequently, the grain size dependence of H_c in Finemet is likely to be lost before this crossover takes place.

I-03

NONLINEAR EFFECTS IN MAGNETOIMPEDANCE: MEASUREMENTS AND MODELS

D. Seddaoui, D. Ménard, B. Movaghar, and A. Yelon
Département de génie physique and Réseau québécois des matériaux de pointe, École Polytechnique de Montréal, P.O. Box 6079, Station C.-V., Montréal, QC H3C3A7, Canada

The giant magnetoimpedance (GMI) effect, observed especially in soft amorphous magnetic metallic ribbons and wires is now well known. For linear response, the behavior is reasonably well understood. However, beginning at

relatively small values of alternating current, the voltage response becomes non-linear. If the hysteresis loop, transverse to the current, is asymmetric, even harmonics are observed, and may be quite sensitive and exhibit complex structure as a function of static magnetic field, at small values of field and frequencies up to hundreds of kHz. A quasistatic model of the nonlinearity, assuming uniform magnetization and rotational switching, predicts behavior similar to that observed, but does not yield quantitative agreement, and of course, does not predict frequency dependence. This encouraged us to develop a fully dynamic model, involving simultaneous solution of the Landau-Lifschitz equation and Maxwell's equations, and satisfaction of boundary conditions on fields and on magnetization. Unlike the calculation of the fundamental in GMI, which may be done analytically up to the last steps, we are obliged to do these calculations entirely numerically. The parameters involved are the size of the anisotropy and axis direction, magnitude of static field, current magnitude and frequency, and surface anisotropy. In the linear regime, the predictions of the numerical calculations are in full agreement with the analytical model. Its predictions in the non-linear regime are explained and the results are compared with experimental results on microwires, including measurements in which the anisotropy is modified by the application of mechanical strain. A preliminary evaluation of potential applications of harmonics is presented. The possibility of chaotic behavior is discussed briefly.

I-04

ON THE RELATIONSHIP BETWEEN THERMO-PHYSICAL AND MECHANICAL PROPERTIES OF GLASS-FORMING ALLOYS

Livio Battezzati

Dipartimento di Chimica IFM e Centro di Eccellenza NIS, Università di Torino, Via P. Giuria 7, 10125 Torino, Italy,

This contribution initially reviews the relationship between thermophysical properties of glass-forming alloys: glass transition, specific heat, entropy of fusion, fragility indexes, using recent models for ranking undercooled liquids and glasses. These rely on both empirical correlations and the statistics of local minima in the potential energy landscape of the material.

Then, the relationship between mechanical properties and some of the above quantities is discussed to get insight into the mechanism of shear band propagation during mechanical failure when, following up a shear offset event, a local temperature rise occurs. The mechanism is supported by evaluating the energy content of the shear band, as well as finite element modelling of temperature profiles around it.

A comparison with properties of other families of glass-formers is finally performed.

I-05

APPLICATIONS OF INVERSE METHODS TO CHARACTERIZE METALLIC GLASSES

Sven Bossuyt

Department of Mechanics of Materials and Constructions, Vrije Universiteit Brussel, Belgium

Using inverse methods, material properties are determined from measurements that are easy to perform accurately, but do not correspond directly to the properties of interest. Instead, an iterative numerical calculation finds those values of the unknown properties that provide good agreement with the experimental data. Thus, numerical modelling of the experiment, in preparation for the experiment as well as in processing the results, is an important part of the method. Several examples of inverse methods in experimental mechanics, applied to problems of interest in the characterization of metallic glasses, will be discussed.

Vibration frequencies of a specimen depend sensitively on the stiffness of the material. Measuring, within a furnace, the vibrations of metallic glass beams after impact excitation, the temperature dependence of the elastic constants near the glass transition was determined. Observed changes in modulus are in agreement with calorimetric studies of relaxation and crystallization behaviour.

For studies of shear banding, optical full-field techniques for displacement measurements are investigated. These use CCD sensors to measure simultaneously at different points across the field of view of the camera. As a result, detailed information about the shear bands and the displacement field between them can be obtained, even if it is not known beforehand where the shear bands will be located. Novel implementations of these techniques are required, however, to avoid complications with the discontinuity of the displacement field at shear bands. The same techniques are also being used to investigate processing issues related to non-uniform plastic deformation.

I-06

X-RAY AND NEUTRON SCATTERING FROM LEVITATED LIQUIDS

Louis Hennet

Centre de Recherche sur les Matériaux à Haute Température (CRMHT) 45071 Orléans cedex 2, France. Email:

Studies of high temperature liquids are interesting from a fundamental point of view and have technological importance since the molten state is an essential stage in various industrial processes.

Most of the physical properties of a high temperature liquid are related to its atomic structure. It is therefore important to develop experimental techniques capable of probing the local environment of the atoms in a molten sample. At very high temperature, it is difficult to use conventional furnaces, which present various problems. In particular, the sample can react with the container and become

contaminated. Furthermore it is difficult to reach very high temperatures. This has led to the development of containerless techniques and their use at synchrotron and neutron sources for studying the structure and dynamics of molten materials.

Several levitation techniques have been developed by various groups around the world. Our group has chosen to work with aerodynamic levitation associated with CO₂ laser heating. With this method it is possible to design relatively simple and compact devices that can be integrated easily into different instruments at neutron and synchrotron sources.

In this talk, I will present some of our experimental setups installed at the ESRF (European Synchrotron Radiation Facility) and the ILL (Institut Laue Langevin) in Grenoble (France). I will give also an overview of various x-ray and neutron techniques that we have used for studying the structure and dynamics of high temperature liquids. This will be illustrated by experimental results on different high-temperature liquids.

I-07

MAGNETISM AND CRYSTALLINE STRUCTURE OF FEPT NANOCUBES AND ICOSAHEDRA

M. Farle

Universität Duisburg-Essen, Fachbereich Physik, Lotharstr. 1, 47048 Duisburg, Germany.

Element-specific magnetism and interface properties inside a nanoparticle can be studied by combining superparamagnetic resonance and different x-ray absorption spectroscopies [1]. Different shapes and structures of nanoparticles are obtained by different organometallic synthesis routes or by enhancing diffusion processes during the formation of particles in gas-phase condensation methods [2]. Using the magnetic alloy FePt as an example the possibilities will be discussed. In ligand and oxide free Fe_xPt_{1-x} icosahedral particles (6 nm), which have been annealed to 800 K, we find enhanced (330 %) orbital magnetism at the Fe site [1,2] and a reduced orbital magnetism at the Pt site. Modifications of the magnon excitation spectrum due to size effects in FePt nanocubes [3] lead to changes of the temperature dependence of the magnetization and can be experimentally determined. The special importance of correlating experimental structural and magnetic findings with ab-initio calculations will be demonstrated by showing experimentally resolved surface reconstructions of few percent [4] and theoretical results confirming that below 3 nm diameter the formation of fct L10 chemically ordered FePt nanoparticles is energetically not favored [5].

- [1] C. Antoniak *et al.* Phys. Rev. Lett. 97 (2006) 117201
 [2] O. Dmitrieva, *et al.* Phys. Rev. B 76 (2007) 064414
 [3] O. Margeat, *et al.* Phys. Rev. B 75 (2007) 134410
 [4] Rongming Wang, *et al.* Phys. Rev. Lett. 100 (2008) 017205
 [5] M. E. Gruner, *et al.* Phys. Rev. Lett. 101 (2008) in press

I-08

SPIN CURRENT AND TWO MAGNON SCATTERING IN NANOSCALE SYSTEMS

B. Heinrich

Physics Department, Simon Fraser University, Burnaby, BC, Canada

Research interest in magnetic nanostructures and spintronics has shifted increasingly from the static to dynamic properties of magnetic nanostructures. This is motivated by the fact that the switching time of magnetic hybrid multilayers used in mass data storage devices and magnetic random access memories (MRAM) is a real technological issue. The crystalline Fe/Au, Pd/Fe/Au (001) nano-structures were prepared by Molecular Beam Epitaxy (MBE) technique using 4x6 reconstructed GaAs(001) substrates. A gyrating magnetic moment creates a spin current in surrounding normal metal layers and leads to non-local interface spin damping. The precessing magnetization acts as a peristaltic spin pump, which transports the spin momentum and allows one to establish a transfer of information between the magnetic layers separated over thick nonmagnetic metallic spacers. Modified Landau-Lifshitz-Gilbert (LLG) equations of motion are modified by spin pumping and spin sink effects. Time Resolved Magneto-Optical Kerr effect (TRMOKE) is an ideal tool to investigate propagation of spin currents. The stroboscopic time-resolved measurements (with the time resolution of 1 ps and sub micron spatial resolution) were carried out using a slotted transmission line with repetitive ps magnetic pulses. Spin currents generated by spin pumping propagate across the Au spacer in ballistic manner and result in rf excitations of the surrounding magnetic films.

The Pd lattice has a large lattice mismatch with respect to Fe. The lattice strain is partially released by a self-assembled rectangular network of misfit dislocations. It will be shown that the nano-network of misfit dislocations leads to a strong extrinsic magnetic damping. This system provides an ideal opportunity to investigate the role of two magnon scattering in a wide range of microwave frequencies. FMR measurements were carried out from 4 GHz to 73 GHz. The contribution to the FMR linewidth from this two magnon scattering is strongly anisotropic and follows the rectangular symmetry of the glide planes of the misfit dislocation network. The angular dependence of the FMR linewidth is a consequence of channeling of the scattered spinwaves along the misfit dislocation glide planes.

I-09

LOW FIELD MAGNETISATION REVERSAL PROCESS OF SOFT/HARD BI-PHASE MAGNETIC MICROWIRES

M. Vazquez, G. A. Badini-Confalonieri, J. Torrejon and G. Infante
Instituto de Ciencias de Materiales, 28049, Madrid, Spain

A novel family of soft/hard magnetic microwires have been recently introduced consisting of an ultrasoft nucleus (CoFeSiB amorphous alloy) prepared by quenching and drawing techniques and an electroplated outer harder magnetic shell (CoNi) (1). The low-field magnetization reversal process of the soft nucleus is determined by the magnetoelastic anisotropy introduced during the fabrication and the outer microtubes. Furthermore, a magnetostatic bias field has been proved to be effective to shift that low-field reversal. This magnetization reversal process involving magnetization rotation or switching of a single domain wall depends on whether magnetostriction of the soft nucleus is positive or negative (2). Furthermore, new improvement of the fabrication process has allowed to introduce FePt based hard nucleus covered by a soft FeNi electroplated alloy. In the present work we will introduce the latest results involving the micromagnetics of that reversal process as well as the perspectives to apply such bimagnetic microwires as sensing elements in various devices (3).

(1) K. Pirota *et al.*, *Adv Funct, Mater.* 14 (2004) 266 ; (2) R. Varga *et al.*, *Phys. Rev. Lett* 94 (2005) 017201; (3) M. Vázquez *et al.*, PCT/ES200502760.

I-10

SINGLE DOMAIN WALL DYNAMICS IN THIN MAGNETIC WIRES

R. Varga^{1*}, Y. Kostyk¹, R. Kornel¹, A. Zhukov², M. Vazquez³

¹⁾ *Inst. Phys., Fac. Sci., UPJS, Park Angelinum 9, 041 54 Kosice, Slovakia*

²⁾ *Dpto. Fis. Mater., Fac. Química, UPV/EHU, 1072, 20080, San Sebastian, Spain*

³⁾ *ICMM CSIC Cantoblanco 28049 Madrid, Spain.*

Single domain wall propagation is used in many magnetic devices like Magnetic Random Access Memory, different spintronic equipment or sensors [1,2]. Although the domain wall dynamics was studied for a long time, new phenomena arise when the dimensions of the applied elements decreases. Firstly, it is the domain wall velocity that determines the speed of such devices. Moreover, understanding the domain wall propagation through a real material containing defects will help us in controlling of such devices.

Amorphous glass-coated magnetic microwires are novel materials with very interesting magnetic properties [3]. In the case of microwires with positive magnetostriction, the magnetization process runs through the depinning and subsequent propagation of the single domain wall along entire microwire [4].

Generally, the domain wall dynamics is described by the linear dependence of the domain wall velocity v on applied magnetic field H ($v = S(H - H_0)$), S - domain wall mobility, H_0 - critical propagation field). Although looking simple, the domain wall dynamics in magnetic microwires brings very

surprising results. Firstly it is a negative critical propagation field H_0 [4]. Moreover, new contribution to the domain wall damping has been found that arises from the domain wall pinning on the local defects and their structural relaxation. At low fields, the adiabatic domain wall dynamics was found to be described by the power law ($v = S'(H - H_0)^\square$). Although it was predicted theoretically, no clear measurements were done before that confirms such law in magnetic wires. The temperature dependence of the power exponent \square is explained by the change of the domain wall roughness due to its pinning on the defects. Finally, very fast domain wall were observed in magnetic microwires [5] that even exceeded the sound velocity [6] as a result of very low anisotropy of amorphous microwires and of the presence of two perpendicular anisotropies. The presence of second, perpendicular anisotropy helps to increase the domain wall velocity even at very low fields. Moreover, the interaction of the domain wall with phonons can be recognized when it achieves the sound velocity.

[1] D. A. Allwood, G. Xiong, C. C. Faulkner, D. Atkinson, D. Petit, and R. P. Cowburn, *Science* 309 (2005), 1688.

[2] D. Atkinson, C.C. Faulkner, D.A. Allwood, and R.P. Cowburn, *Topics Appl. Physics* 101, (2006), 207.

[3] M. Vázquez, “Advanced magnetic microwires” in *Handbook of Magnetism and Advanced Magnetic Materials* ed. H. Kronmuller and S. Parkin, John Wiley & Sons (2007), pp.2193;

[4] R. Varga, K.L. Garcia, M. Vázquez, P. Vojtanik, *Phys. Rev. Lett.* 94 (2005), 017201.

[5] R. Varga, A. Zhukov, J.M. Blanco, M. Ipatov, V. Zhukova, J. Gonzalez, P. Vojtaník, *Phys. Rev. B* 74 (2006), 212405.

[6] R. Varga, A. Zhukov, V. Zhukova, J.M. Blanco, J. Gonzalez, *Phys. Rev. B* 76 (2007), 132406.

I-11

ORDERING IN NETWORK LIQUIDS AND GLASSES

Philip S. Salmon

Department of Physics, University of Bath, Bath BA2 7AY, UK

The structure of liquid and glassy materials is a formidable problem to solve because the atomic sites are topologically disordered and the presence of two or more chemical species adds further complexity. In this talk, some new inroads are reported that have emanated from the application of neutron and x-ray diffraction methods. Specifically, it is found that the topological and chemical ordering are both described by at least two different length scales at distances greater than the nearest-neighbour. The interplay between the ordering on these length scales and the physical properties of liquid and glassy networks is discussed.

I-12

THE STRUCTURE AND ELECTRONIC PROPERTIES OF METAL-AMMONIA “OGG-GLASSES”

Cecilia Gejke¹, Helen Thompson¹, Mark Ellerby¹, Chris Howard¹,
Jonathan Wasse¹, Robert Delaplane² & Neal Skipper¹

¹Department of Physics & Astronomy, University College London,
Gower Street, London WC1E 6BT, UK.

²Studsvik Neutron Research Facility, P.O. Box 256, 82 Nyköping
611, Sweden.

Dissolution of metals, such as lithium, into liquid ammonia produces highly coloured conducting solutions, in which solvation of the metal ions releases the valence electrons into the liquid. These complex and important electronic liquids contain a fascinating variety of solvated ionic and electronic species, including isolated polarons, spin-paired bipolarons, excitonic atoms, metal anions, and truly delocalised (itinerant) electrons. These species in turn give rise to remarkable bulk properties. For example; the time-honoured metal-nonmetal (M-NM) transition, liquid-liquid phase separation, and high redox reactivity. At saturation compositions the solutions are class A metals, with electrical conductivities $\sim 15,000\Omega^{-1}\text{cm}^{-1}$. The deep pseudoeutectic at this point gives rise to some of the lowest temperature and lowest density liquid metals known. We have shown that fast quenching of the liquids produces amorphous materials, which were first reported in 1946 by RA Ogg, hence the name "Ogg Glasses". In spite of Ogg's controversial, and unproven, claim of superconductivity at around 200K, these amorphous materials have remained relatively unstudied. Here we will present results from our neutron scattering studies of these systems, which show that glasses can be formed at all compositions with overall density slightly lower than the parent liquids. SQUID magnetometry shows evidence for weak diamagnetism in field-quenched samples of composition close to the metal-nonmetal transition.

I-13

MECHANICAL ACTIVATION AS A WAY OF OBTAINING NON-EQUILIBRIUM STATES IN CONDENSED MATTER: FUNDAMENTAL PRINCIPLES AND POSSIBLE PRACTICAL APPLICATIONS

E.P.Yelsukov

Physical-Technical Institute UrB RAS, 132 Kirov St., 426000

Izhevsk, Russia

Results on mechanical activation (mechanical grinding and mechanical alloying) of Fe-based systems and Ca gluconate medicinal preparation are presented in this report.

The following topics are considered:

- Types of solid state reaction under mechanical grinding (MG) and mechanical alloying (MA)
- "order-disorder" transition during MG of Fe₃Si alloy, accompanying nanocrystalline state formation;
- nanocrystalline Fe carbides formation during MG of Fe powder in liquid organic media;

- amorphous Fe-Si-C alloy obtained by MA as a precursor for the metastable Fe₅SiC intermetallic formation;
- deformation-induced nanocrystallization of the Fe₉₀Zr₁₀ amorphous ribbon;
- Microscopic mechanism of MA in the binary Fe-sp-element (M) systems. M = B, C, Mg, Al, Si, Ge, Sn, Pb;
- Deformation-induced dissolution of the Fe₃C and Fe₂B in nanocrystalline α -Fe with the formation nanocomposites consisting of α -Fe and amorphous Fe-C(B);
- Thermally induced structure-phase transformations in non-equilibrium nanosystems (α -Fe amorphous Fe-C nanocomposite);
- Properties of mechanically activated materials - magnetic moments and hyperfine magnetic fields in disordered systems (nanocrystalline Fe-Si disordered and amorphous Fe₇₀(Si, C)₃₀ alloys:
- coercivity of Fe-C and Fe-Si-C systems;
- microwave magnetic parameters of bulk composites with mechanically activated Fe and Fe-Si powders;
- morphology, density and microhardness of Fe-C bulk nanocomposites obtained by MA and magnetic pulse compaction;
- Mechanically activated amorphous Ca gluconate as a medicinal preparation for therapy of osteoporosis and stomatologic diseases.

The principal role of nanostructure in formation on non-equilibrium phases and properties, transition toward equilibrium is especially pointed out in the report.

I-14

SHAPE EVOLUTION, CRYSTALLINITY AND OPTICAL PROPERTIES OF GOLD NANOPARTICLES

I. Pastoriza-Santos, J. Pérez-Juste, B. Rodríguez-González, L. M. Liz-Marzán

Department of Physical Chemistry, University of Vigo, 36310,

Vigo, Spain

Size and shape control are hot topics in both Colloid Science and Nanotechnology. In the case of metals, size and shape control can be used as a means to tailor the optical properties through modification of the plasmon resonance condition. Many synthetic protocols have been published for metal nanoparticle synthesis, though simultaneous size and shape control are still rare. We present here the controlled synthesis of extremely regular gold nanocrystals through ultrasound-induced reduction of HAuCl₄ on pre-synthesized seeds, using PVP as a stabilizing polymer. A strict relationship between the final morphology and the crystalline structure of the seeds has been observed, with formation of decahedra (pentagonal bipyramids) using penta-twinned Au seeds but single crystalline octahedra using single crystal Pt seeds. The dimensions can be strictly controlled through the ratio

between the amount of seed and the HAuCl_4 concentration, and the monodispersity is as good as 10%. The optical properties of these particles can be reproduced with a very good agreement by means of a boundary element method for the resolution of Maxwell's equations, so that a good correlation between particle size and optical response can be established.

I-15

CRYSTALLISATION OF NANOPERM TYPE ALLOYS

Marcel Miglierini

Slovak University of Technology, Bratislava, Slovakia

Disordered nature of structural arrangement in Fe-based metallic alloys gives rise to advantageous (from a practical application point of view) magnetic properties. Suitable heat treatment of metallic glasses produces the so-called nanocrystalline alloys. The latter attract a lot of scientific interest because, contrary to their amorphous counterparts, their magnetic parameters do not substantially deteriorate at elevated temperatures during the process of their practical exploitation. To benefit from their unique magnetic properties, the mechanism of stability comprising crystallization should be known.

Here, we present a study case of Fe-Mo-Cu-B NANOPERM-type alloys. The progress of crystallization with special emphasis on its early stages was investigated by the help of Mössbauer effect techniques, conventional X-ray diffraction as well as by *in situ* (during continuous heat treatment) diffraction of synchrotron radiation. Additional information is provided by atomic force microscopy, transmission electron microscopy, high resolution electron microscopy, differential scanning calorimetry, positron annihilation spectroscopy, and magnetic force microscopy. Differences between both surfaces of the inspected ribbons are also discussed.

I-16

RECENT ADVANCES IN SOFT MAGNETIC NANOCRYSTALLINE FE-CO AND FE-NI BASED ALLOYS

I. Škorvánek^{1*}, J. Marcin¹, J. Turčanová¹, J. Kováč¹, P. Švec² and D. Janičkovič²

¹*Institute of Experimental Physics, Slovak Academy of Sciences, SK-040 01 Košice, Slovakia*

²*Institute of Physics, Slovak Academy of Sciences, SK-842 28 Bratislava, Slovakia*

* IEP SAS, Watsonova 47, 040 01 Košice, Slovakia.

e-mail: skorvi@saske.sk

The reduction of the grain sizes to the nanometer range may vary drastically the functional properties of materials, including the magnetic behavior. Typical examples of such systems are nanocrystalline Fe-based alloys prepared by devitrification of melt-spun amorphous precursors, which

belong to an important group of soft magnetic materials. The properties of these materials can vary widely, depending on the size and volume fraction of the nanocrystalline grains as well as on the magnetic properties of the intergranular amorphous matrix. In order to further optimize the magnetic performance of the nanocrystalline alloys it is important to deepen knowledge about the influence of the alloying elements and processing techniques that can be used to tailor their properties for specific applications.

A special attention of this talk is devoted to the study of the effects of the annealing under a presence of external magnetic field in order to produce a controllable uniaxial anisotropy in the nanocrystalline soft magnetic materials. We report on the effects of both longitudinal and transverse magnetic field applied during the heat treatment on the magnetic behaviour in the series of Fe-Co-M-B type (M=Nb, Zr and Mo) nanocrystalline alloys. A heat treatment under the presence of longitudinal magnetic field results for the Mo-containing samples in squared hysteresis loops characterized by coercive field values in the range of 3 - 8 Am⁻¹. These values are superior to those previously reported for Fe-Co based nanocrystalline alloys. Sheared loops with good field linearity were achieved for all investigated alloys after annealing in transverse magnetic field. Such soft magnetic characteristics are of particular interest for various sensors and high frequency devices. The stronger response to the transverse field-annealing is observed for the alloys containing Nb and Zr. Here, the values of the induced anisotropy constant up to ~ 1350 Jm⁻³ can be reached. We also investigate the effect of Fe replacement by Ni on the formation of nanocrystalline structure and on the magnetic properties in the series of Fe-Ni-Nb-B alloys. Our attention is focused on the relationship between the microstructure and magnetic properties studied under the angle of the BCC-FCC phase transition in the nanograins. We show that an addition of the proper amount of Ni to the ternary FeNbB alloy results in a marked improvement of the magnetic softness and it has also a beneficial effect on the bend ductility of the optimally heat treated nanocrystalline samples.

I-17

PHYSICAL PROPERTIES OF NANOCRYSTALLINE AND NANOSTRUCTURED FERRITES

J.M. Greneche

Laboratoire de Physique de l'Etat Condensé LPEC, UMR CNRS 6087, Université du Maine,

Institut de Recherche en Ingénierie Moléculaire et Matériaux Fonctionnels IRIM2F, FR CNRS 2575

72085 Le Mans, Cedex 9, France.

Email : greneche@univ-lemans.fr

Great attention is devoted to the understanding of the physical properties of nanostructures. Indeed, some properties are rather unusual and in the case of magnetic nanostructures, the interest of numerous systems is based

on their technological interest in magnetic recording, catalysis, biomedicine, The modelling of their physical properties require a good knowledge of their structure at both microscopic and nanoscopic scales. Indeed, the samples consist of nanoparticles, it is first important to control their (distribution of) size, their morphology, their surface state and their aggregation or their dispersion, all these parameters being strongly dependent on the procedure and conditions of synthesis. In the case of nanostructured powders prepared either by high energy ball milling or chemical routes, the grain boundaries could contribute as a large atomic fraction while their structure strongly depends on the preparation conditions.

Ferrites can be found as nanoparticles when synthesized by chemical processes or nanostructured powders when prepared by mechanical route. It is also clear that the chemical, magnetic and transport properties of microcrystalline and nanocrystalline ferrites are strongly dependent on the cationic distribution within the crystalline grains.

The aim of the presentation is to review recent studies on magnetic nanoferrites dealing with a complete description of the structural properties obtained using experimental features combining X-ray diffraction, magnetic measurements and ^{57}Fe Mössbauer spectrometry (as a function of temperature and external applied field). A modelling of structural and magnetic properties is finally proposed in the case of nanostructured ferrites, ferrite nanoparticles and functionalized ferrite nanoparticles.

I-18

SINGLE AND MULTILAYERED MAGNETIC NANOWIRES: PREPARATION AND CHARACTERIZATION

H. Chiriac

National Institute of Research and Development for Technical Physics, Iasi, Rumania

Nowadays, there is an increasing demand for new types of materials with different structures and improved physical properties to be used in miniaturized devices. Recently, the nanowire arrays have been studied extensively because of their specific physical properties, with huge potential for multiple applications [1]. The multilayered nanowires, in particular, are very interesting for their d.c. magnetoresistive effect, especially in connection with the spin-valves applications [2].

Results on different magnetic nanowires as single or multilayered structures, with different compositions (NiFe/Cu, Co/Cu, NiFe/Cu/Co, FeGa/NiFe, CoFeB/Cu, CoNiP/Cu, etc.), prepared by electrodeposition, will be presented. The differences between the magnetic crystalline (NiFe, Ni, Fe, Co, FeGa) and amorphous (CoNiP, NiP [3], CoNiB, etc.) nanowires formation and properties will be presented. The influence of the electrodeposition conditions (pH of the deposition bath, deposition voltage/current,

deposition time, bath composition, additives) on the morphology and magnetic/magneto-transport properties of single and multilayered magnetic nanowires arrays will be discussed in detail. The influence of the nanopores distribution and size, as well as the influence of the non-magnetic layer, on the magnetic interactions between nanowires or/and at the interface between different layers in multilayered structures will be presented, too.

[1] A. Fert, L. Piroux, J. Magn. Mater. 200 (1999) 338.

[2] S. Fusil *et al.*, Nanotechnology 16 (2005) 2936.

[3] H. Chiriac *et al.*, J. Magn. Mater. 272 (2004) 1678.

I-19

MAGNETIC MICROSTRUCTURE OF NANOCRYSTALLINE MATERIALS

Sybille Flohrer*, Giselher Herzer

VACUUMSCHMELZE GmbH & Co. KG, Grüner Weg 37, D-63450 Hanau, Germany

The analysis of the magnetic microstructure by magneto-optical technique is a basic tool for understanding the magnetization process of magnetic materials. Insight into the magnetization process of soft-magnetic nanocrystalline ribbons of the FeCuNbSiB type is given for two examples: (1) the interplay between uniform and random anisotropy and (2) excess loss mechanisms:

1. The magnetic microstructure of field annealed nanocrystalline ribbons usually resembles that of amorphous ribbons. However, if annealing time and temperature are set to tailor lowest induced anisotropies, an irregular patch substructure of the wide regular magnetic domains is found in the nanocrystalline material. These patches reflect the contribution of the random magneto-crystalline anisotropy.

2. It is well known that excess loss is an important loss component of soft magnets with square hysteresis loop. It will be shown that even cores of flat type loop possess significant excess loss if magnetization is driven close to saturation

I-20

SEVERE PLASTIC DEFORMATION OF AMORPHOUS ALLOYS

A.M.Glezer¹, S.V.Dobatkin², M.R.Plotnikova¹, A.V.Shalimova¹, N.S.Perov

¹*G.V.Kurdyumov Institute for Physical Metallurgy, Moscow, Russia;*

²*A.A.Baikov Institute for Metallurgy and Material Science; Moscow, Russia*

³*M.V.Lomonosov Moscow State University, Moscow, Russia*

Amorphous alloys Ni-Fe-Co-Si-B have been deformed by Bridgman camera at the different temperatures and degrees of severe deformation ($\epsilon \geq 1,0$). X-Ray diffraction, transmission electron microscopy and measuring of magnetic and mechanical properties have been used. It was shown that a new structural state with the very high saturation magnetization forms at 77 K. Severe deformation at the room temperature leads to amorphous state with 5-10 % volume fraction of nanocrystalline fcc-particle with the $d < 10$ nm. The cycling mode of severe plastic deformation has been predicted. The nature of unusual magnetic parameters after cryogenic deformation is now under active investigation.

I-21

**RECENT ADVANCES IN FUNDAMENTAL
UNDERSTANDING OF THE GLASS TRANSITION**

K.L. Ngai

Naval Research Laboratory, Washington DC 20375-5320 USA

Several remarkable dynamic properties of glass-forming materials have recently been discovered experimentally, some of them by the application of pressure. These properties have great impact on the research field of glass transition because they are general and fundamental, and not easy to explain. I review some of these experimental facts and show that they originate from intermolecular interaction and many-body relaxation dynamics of the structural α -relaxation. While these properties are either not explained or not explainable by conventional theories and models, they can be rationalized by the coupling model of the author. The results can be used as guide to a viable solution of the long-standing glass transition problem.

ORAL CONTRIBUTION

C-01

NEUTRON DIFFRACTION STUDY OF THE STRUCTURES OF TWO CUHFTI BULK ALLOY GLASSES

N.Cowlam¹, I.A.Figueroa², G.Cuello³, I.Todd² and H.A.Davies²
 1. Department of Physics and Astronomy, University of Sheffield,
 Sheffield S3 7RH, U.K.

2. Department of Engineering Materials, University of Sheffield,
 Sheffield S1 3JD, U.K.

3. Institut Laue-Langevin, 6 rue Jules Horowitz, 38042 Grenoble
 cedex, France

A number of alloy systems based on Cu, generally with two or more of the group IVB metals Ti, Zr and Hf, have been shown to be bulk glass formers (*i.e.* capable of being fully vitrified in section thicknesses $> \sim 0.5$ mm) over certain composition ranges. It has been proposed that easy glass formation in alloys typified by these Cu-IVB metal systems is promoted by the existence of specifically coordinated atomic groupings and, as part of a more general investigation of bulk Cu-based alloy glasses at Sheffield, we have initiated neutron and x-ray diffraction studies of these materials, partly to investigate the extent to which there is any evidence for the existence of such structural elements.

Neutron diffraction measurements have been made on $\text{Cu}_{55}\text{Hf}_{25}\text{Ti}_{20}$ and $\text{Cu}_{60}\text{Hf}_{20}\text{Ti}_{20}$ rod samples of diameter up to 3 mm, using the D4 diffractometer at the I.L.L. Grenoble, which has provided data of exceptional statistical quality. Neutrons easily penetrate these samples and demonstrate that they are fully amorphous with no crystalline core. The structure factors obtained to $Q_{\text{max}} \approx 17 \text{ \AA}^{-1}$ show the classic features expected for the $S(Q)$ of a metallic glass. The radial distribution functions have been obtained by the usual Fourier transform. The position of the first neighbour peak in these RDF's can be interpreted in terms of the Goldschmidt diameters of the constituents and its shape in terms of the weighting factors of the six atomic pair correlation functions. The coordination numbers obtained are ≈ 11.1 from the first peak alone and ≈ 12.2 , if a clear contribution at greater radial distance $r \approx 3.2 \text{ \AA}$ is included. There are subtle differences between the $S(Q)$'s and the RDF's of the two samples, but at present, they do not provide sufficient evidence for any special form of local coordination, *i.e.* they suggest a structure based on dense topologically random packing of hard spheres.

C-02

RESOLUTION FUNCTION FOR A DEDICATED TWO-AXIS DIFFRACTOMETER FOR THE STRUCTURE OF AMORPHOUS

G. J. Cuello

Institut Laue Langevin, 6, rue Jules Horowitz, B.P. 156
 F-38042 Grenoble Cedex 9, France

In a diffraction experiment the observed intensity is a convolution of the real intensity produced by the sample and the instrumental resolution. In a powder diffraction experiment on a polycrystalline material, this convolution produces larger Bragg peaks and the standard Rietveld tools takes into account the effect, usually through the Caglioti's formula. In the case of diffraction on liquid or amorphous systems, this procedure can not easily be applied and a deconvolution is necessary. In order to perform this mathematical operation, a well known resolution function is needed. This resolution function is also necessary when numerical simulations are compared with experimental data. This can be done by convoluting the simulated data with the instrumental resolution. The dedicated two-axis diffractometer (D4) for the structure of liquids and amorphous systems at the Institut Laue Langevin operates at three standard wavelengths (0.7, 0.5 and 0.35 Å) providing a good range in the reciprocal space for PDF (Partial Distribution Function) analysis. This work presents the experimental resolution functions corresponding to three different copper monochromators (Cu200, Cu220 and Cu331) for several wavelengths. This information is crucial for a proper data treatment of the diffraction spectra. It will be also useful for a developing field like the PDF analysis on polycrystalline or quasicrystalline samples, for which a good choice of neutron flux and resolution is extremely important.

C-03

NON-ISOTHERMAL APPROACH TO CRYSTALLIZATION PROCESS OF SEVERAL CO RICH ALLOYS

J. Bonastre¹, Ll. Escoda¹, J.J. Saurina¹, J.J. Suñol¹, J.D. Santos²,
 M.L. Sanchez², B. Hernando²

¹ Universidad de Girona, Campus de Montilivi, edifici PII. Lluís
 Santaló s/n. 17003 Girona, Spain

² Universidad de Oviedo, Departamento de Física. C/ Calvo
 Sotelo, s/n. 33007 Oviedo, Spain

In this work we have investigated the crystallization behaviour of several Co-rich alloys obtained by melt-spinning in ribbon form. The as-quenched ribbons are amorphous as determined by X-ray diffraction patterns. Several ribbons were annealed. The procedure of quenching and subsequent annealing is a basic approach to control the microstructure of materials and thereby to achieve the optimal physical properties for the final product. It is known that the controlled heat treatment of certain amorphous alloys can produce nanocrystalline or quasicrystalline structures. The kinetics of transformation

gives information relative to the stability and applicability of these materials. Non-isothermal experiments were carried out by differential scanning calorimetry. An isoconversional method is applied to perform the kinetic analysis in order to obtain the temperature – heating rate transformation diagrams. A good concordance was observed between the diagram curves obtained by calculation and the experimental data, which verifies the reliability of the method and the validity of the rate constant model description. Furthermore, the as quenched amorphous ribbons were subjected to mechanical alloying in a planetary ball-milling device under Ar atmosphere. The MA of bulk amorphous metallic glasses may be a two-step procedure prior to the consolidation or compacting of complicated shape materials. The milling conditions were chosen to develop a material in a like-powdered form. It was found a decrease of 16-18 % in the activation energy of the main crystallization process.

C-04

KISSINGER ANALYSIS FOR DYMn6-XGE6-XFEXALX ($0 \leq X \leq 6$) ALLOYS

Z. Śniadecki, B. Idzikowski

*Institute of Molecular Physics, Polish Academy of Sciences, M.
Smoluchowskiego 17, 60-179 Poznań, Poland*

The multicomponent DyMn_{6-x}Ge_{6-x}Fe_xAl_x ($0 \leq x \leq 6$) alloy series, which is derived from a system combining transition metals (TM) Fe and Mn, rare-earths element (R) Dy, and metalloid or other metal (M) Ge and Al, belongs to a group of magnetic compounds with complex magnetic ordering. Some compositions of this series were obtained in fully amorphous state [1]. Alloys were prepared by arc-melting and subsequent melt-spinning in the form of ribbons (50 - 70 μm thick).

Here, we report results obtained with the use of differential scanning calorimetry (DSC) technique. DSC curves were recorded at different constant heating rates from 10 to 120 K/min. Fig. 1. presents two well defined exothermic effects which are connected with crystallization. For the heating rates up to 120 K/min no signs of endothermic glass transition effect were observed as it was reported earlier for the heating rates up to 50 K/min [1]. Activation energies for primary crystallization (first event) were calculated from the Kissinger relation [2]. Determined parameters were used to discuss thermal stability of these metallic glasses, which is higher for the alloys with high Fe and Al content. For some compositions short isothermal heat treatment at temperatures below first exothermic effect leads to formation of nanocrystalline state which was confirmed by the X-ray diffraction analysis.

[1] P. Kersch, U.K. Rössler, T. Gemming, K.H. Müller, Z. Śniadecki, B. Idzikowski, *Appl. Phys. Lett.* 90 (2007) 031903

[2] H.G. Kissinger, *J. Res. Natl. Bur. Stand.* 57 (1956) 217

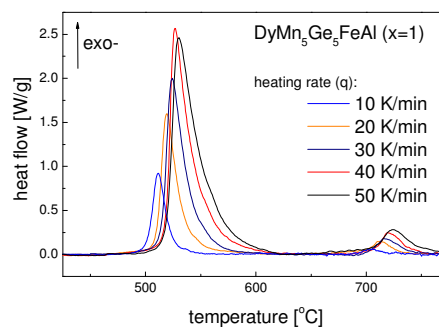


Fig. 1. Heat flow (DSC signal) for DyMn₅Ge₅FeAl sample measured with different heating rates.

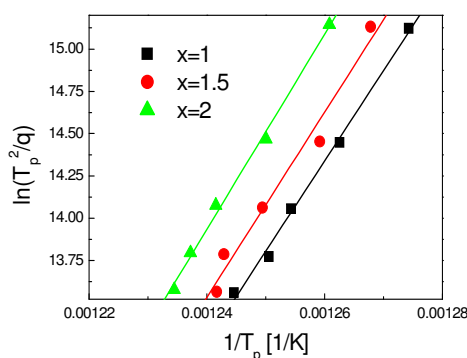


Fig. 2. Kissinger plots of DyMn_{6-x}Ge_{6-x}Fe_xAl_x ($0 \leq x \leq 6$) series amorphous alloys.

C-05

INFLUENCE OF CRYOMILLING ON STRUCTURE OF COFEZRB ALLOY

J. Bednarčík¹, K. Saks², R. Nicula³, S. Roth⁴, and H. Franz¹

¹ *Deutsches Elektronen-Synchrotron (HASYLAB), Notkestr. 85, D-22607 Hamburg, Germany*

² *Institute of Materials Research, Slovak Academy of Sciences, Watsonova 47, 043 53 Košice, Slovakia*

³ *EMPA, Feuerwerkerstrasse 39, CH-3602 Thun, Switzerland*

⁴ *IFW Dresden, Institut für Metalische Werkstoffe, Helmholtzstraße 20, D-01069 Dresden, Germany*

Ball milling (BM) is a simple and versatile processing technique to synthesize nonequilibrium materials such as amorphous phases, nanocrystalline phases, and extended solid solutions. In this contribution we report how the short-time ball milling, and specially the cryomilling, influences the phase stability of Co₅₆Fe₁₆Zr₈B₂₀ (at.%) metallic glass. Two independent sets of powder samples were obtained by BM of CoFeZrB alloy with and without additional cooling using LN₂ bath. The changes in the structure upon milling were monitored using hard x-ray diffraction and magnetic measurements. High-energy x-ray diffraction measurements were performed at the BW5 beamline of DORIS positron storage ring (Hamburg, Germany). X-ray diffraction (XRD) experiments were performed in Debye-Scherrer geometry using monochromatic beam with energy of 100 keV. Thermomagnetic curves were measured in constant magnetic field with 10 K/min heating rate using Faraday magnetic balance. XRD experiments indicate that the

originally amorphous CoFeZrB alloy is progressively crystallising when milled without additional cooling. After 12 hours of such milling the Bragg peaks belonging to bcc-Fe are identified. On the other hand, keeping the vials during milling at a sufficiently low temperature (case of cryomilling) helps to prevent crystallisation induced by BM. XRD patterns at different stages of cryomilling do not show significant changes and indicate fully amorphous nature of milled powders. However, magnetic measurements reveal relatively strong impact of cryomilling on amorphous structure of CoFeZrB powders, manifested by relatively high increase (15 %) of Curie temperature of amorphous phase.

C-06

**THE STRUCTURE OF LIQUID CALCIUM ALUMINATES:
A COMBINED NEUTRON DIFFRACTION AND
COMPUTER SIMULATION STUDY**

Cristiglio^{1,2*}, L. Hennes², G. J. Cuello¹, M.R. Johnson¹, I. Pozdnyakova², D. L. Price²

¹Institut Laue Langevin, 6, rue Jules Horowitz BP 156 - 38042
Grenoble Cedex 9 - France

²CNRS-CRMHT, 1d av. de la Recherche Scientifique, 45071
Orléans cedex 2, France

Over the past ten years an increasing number of studies on molten materials have been carried out thanks to the development of containerless methods. These techniques allow studies of high-temperature liquids with a very high degree of control. In particular, they eliminate the problems of sample-container interactions and contamination and make it possible to access very high temperatures. The CRMHT has chosen to combine aerodynamic levitation with CO₂ laser heating and has developed various devices for making diffraction measurements at synchrotron and neutron sources [1-3].

From the structure factor $S(Q)$ and the corresponding pair correlation function $g(r)$ obtained with x-ray or neutron diffraction experiments, it is possible to get information on the local structure of liquid materials. But very often the material studied is a polyatomic system and both $S(Q)$ and $g(r)$ are weighted sums of the partial functions for all atomic pairs, so that a single diffraction measurement gives an incomplete representation of the structure.

In order to go further in structural studies, the combination of experimental methods with simulation techniques becomes indispensable. This makes it possible to derive partial $S(Q)$ and $g(r)$ functions for all atomic pairs and to determine reliable structural models to compare with the experimental results. At the ILL we have developed ab initio molecular dynamics (AIMD) simulations using the VASP code [4] where interatomic forces are obtained from density functional theory.

We present here a structural analysis of liquid calcium aluminates (CaO-Al₂O₃), showing a good agreement between the AIMD simulations and the experimental data.

[1] L. Hennes et al., Appl. Phys. Lett. 83, 3305 (2003)

[2] C. Landron et al., Phys. Rev. Lett. 86, 4839 (2001)

[3] L. Hennes et al., Rev. Sci. Instrum. 77, 53903 (2006)

[4] G. Kresse and J. Furthmüller, Phys. Rev. B 54, 11169 (1996)

C-07

**MÖSSBAUER CHARACTERIZATION OF AN
AMORPHOUS STEEL ALLOY WITH OPTIMUM MO
CONTENT**

Laura Facchini¹, Pere Bruna^{1,3}, Eloi Pineda^{2,4}
and Daniel Crespo^{1,4}

¹Departament de Física Aplicada, EPSC, and ²Departament de
Física i Enginyeria Nuclear, ESAB

Universitat Politècnica de Catalunya, Avda. del Canal Olímpic
15, 08860 Castelldefels, Spain

³ Centre de Recerca en Nanoenginyeria and ⁴ Centre de Recerca
de l'Aeronàutica i de l'Espai, UPC

Fe-based bulk metallic glasses (BMGs) are of great interest for its potential use in structural applications. The enhancement of the glass forming ability (GFA) of these alloys has been generally achieved by adding small amounts of rare earths or high-purity elements, thus increasing the cost of fabrication and reducing the possibility of industrial production. Recently, Fe-based BMGs were developed by using commercial raw materials and with a optimized GFA through the small substitution of Fe by Mo [1]. These BMGs can be produced in large quantities and cost-effectively. In the present study, three of these alloys, Fe_{71.2-x}C_{7.0}Si_{3.3}B_{5.5}P_{8.7}Cr_{2.3}Al_{2.0}Mo_x (x=0, 4.5 and 6.5 at%), have been produced by the melt-spinning technique and characterized by X-ray diffraction and transmission Mössbauer spectrometry (TMS). TMS allows us to study the local environments of the Fe atoms in the glassy state, showing the changes in the amorphous structure due to the addition of Mo. A reduction of the mean hyperfine field is observed as the amount of Mo increases. With intermediate Mo content, this reduction is associated to the substitution of Fe by Mo in a disordered magnetic Fe-rich structure, whereas for high Mo content, this structure is destroyed leading to an increase of paramagnetic environments. Finally, the relationship between the GFA of these alloys and its local structure determined by TMS will be discussed.

[1] H.X. Li, K.B. Kim and S. Yi, Scripta Materialia 56 (2007) 1035-1038

C-08

**NANOCRYSTALLIZATION EFFECTS ON THE SPECIFIC
HEAT OF FE-CO-NB-B AMORPHOUS ALLOY**

J.S. Blázquez, M. Millán, C.F. Conde, V. Franco, A. Conde*.
Dpto. Física de la Materia Condensada, ICMSE-CSIC,

Universidad de Sevilla,

P.O. Box 1065, 41080, Sevilla, Spain.

Amorphous samples of Fe₆₀Co₁₈Nb₆B₁₆ alloy were heated up to different temperatures in order to produce structurally

relaxed amorphous, nanocrystalline and fully crystallized microstructures. Afterwards, measurements of the specific heat at constant pressure, C_p , were performed in a DSC7 calorimeter of Perkin-Elmer at temperatures low enough to assure the stability of the metastable microstructures produced. For amorphous samples, C_p curves show a clear and broad maximum at 662 K ascribed to the Curie transition of the amorphous phase. As nanocrystallization progresses this maximum is reduced, being undetected for crystalline volume fractions above ~ 0.45 . For amorphous samples at 550 K, a clear enhancement of 25 % in the C_p value with respect to the Dulong-Pettit limit is observed. This enhancement reduces as the nanocrystallization progresses, saturating at about 14 % for nanocrystalline samples with crystalline fractions above ~ 0.45 . The C_p enhancement and its observed trend are consistent with a reduction of the free volume as the crystalline fraction increases. On the other hand, the magnetic contribution to C_p could also influence this enhancement.

C-09

WITHDRAWN

C-10

METHODOLOGICAL STUDY ON PHASES TRANSITIONS AND NANOSTRUCTURE OF PHOSPHATIDYLCHOLINE SINGLELAYER WITH SCANNING PROBE MICROSCOPES AND LANGMUIR-BLODGETT TECHNIQUES

Jie Zhu^{1,2}, Lianhong Guo¹, Guodong Wang¹

¹College of Science, Northwest A&F University, Yangling, 712100 China

²BioCAT, APS, Argonne National Laboratory, Argonne, IL, 60439 USA

Abstract: Aims: Biologic simulated membranes in high stability and integrality are propitious to the advancement of the repetition-needing experiments in biology. Deep discussion on the influence of the preparation methods to the phase transformations of single molecular Phosphatidylcholine film could reach the optimum parameters in special laboratory^[1-2].

Methods: Based on the analysis results of the π -A curves of Phosphatidylcholine film and the theoretic on the phase transformations, we study on the main seven factors or parameters by the numbers to the quality of the LB film such as inserting quantity and concentration of Phosphatidylcholine molecules, the solvents, expanding time, the compression velocity of the barriers, the temperature and pH value of the subphase and so forth. Scanning probe microscope (SPM) also be used to check film morphology. **Results:** Experimental results from the seven different conditions indicate that the influence of inserting quantity, the temperature and pH value of the subphase are biggest, and the concentration of Phosphatidylcholine molecules, the solvents and the expanding time are smaller, and the compression velocity

of the barriers smallest. SPM results gave a good testimony to the LB. Conclusion: According to the analysis combined with the feasibility in special laboratory environments, we reach to the best parameters in film preparations: 50 μ L, 0.67mmol/ml Phosphatidylcholine / ether on the subphase in pH6.8 expanded 20min can get a intact π -A curves when film is compressed by barriers in about 5mm/min vibration speed.

[1] Roubeau O, Natividad E, Agricole B, et al. Formation, structure, and morphology of triazole-based Langmuir-Blodgett films [J].LANGMUIR, 2007, 23 (6): 3110-3117

[2] Fleming BD, Zhang J, Elton D, et al. Detailed analysis of the electron-transfer properties of azurin adsorbed on graphite electrodes using dc and large-amplitude Fourier transformed ac voltammetry [J].ANALYTICAL CHEMISTRY, 2007, 79 (17): 6515-6526

C-11

SPIN RELAXATION IN NANOPHASED MANGANITES

Javier Bermejo¹, Luis Fernández Barquín², Jon Gutiérrez¹ and Jose Manuel Barandiarán¹

¹ Universidad del País Vasco UPV/EHU, Facultad de Ciencia y Tecnología y Unidad Asociada al CSIC, P.O. Box 644, E-48080 Bilbao, Spain

² Universidad de Cantabria, CITIMAC, Facultad de Ciencias, E-39005 Santander, Spain

Manganites or mixed manganese oxides of the formula $La_{1-x}M_xMnO_3$ where M is a divalent cation like Pb in our case, are Double Exchange (DE) ferromagnets (FM) that attract great interest in view of their colossal magnetoresistance around the magnetic order temperature. They have a strong tendency to grow in small coherent regions due to the coupling of the magnetic and charge carriers and local distortions like Jahn-Teller or charge ordering. Such a tendency is enhanced by doping the Mn with other 3d-metals, like Fe, that break up the FM chains by suppressing the DE between Mn ions, and can eventually give rise to spin glass-like structures. Dynamic spin methods can therefore give insight into the magnetic coupling and their range in such materials.

In this work we present a survey of recent results obtained by AC magnetic susceptibility, muon spin relaxation (μ SR) and Neutron Spin Echo (NSE) experiments in $La_{0.7}Pb_{0.3}MnO_3$ and $La_{0.7}Pb_{0.3}Mn_{0.8}Fe_{0.2}O_3$, aimed to cover an extraordinary equivalent frequency range (from quasi-DC experiments to almost the THz region) and to give an overall picture of the processes within. The results indicate that undoped manganites behave like strong FM while Fe-doped compounds display two different relaxation mechanisms that can be correlated with the FM regions and frustrated magnetic regions of nearly spin glass structure. This is a situation intimately related to a magnetically disordered state.

C-12

A NEW APPROACH TO DIFFUSION-LIKE RELAXATION PROCESSES

A. Fondado, J. Mira, J. Rivas
*Departamento de Física Aplicada – Faculdade de Física
 Universidade de Santiago de Compostela
 15782 Santiago de Compostela – Spain*

Relaxation phenomena with long-term decay behaviour are found in systems of very different nature, ranging from socioeconomics to materials science. Despite this, some characteristics are similar. The problem is that the time dependence of the measured magnitude can be fitted to several models. Which is the real one?

To answer this question we have focused on diffusion-like relaxation processes, specifically on the stationary part, i.e., that phase of the time decay described by time-independent parameters. With this premises we were able to demonstrate analytically that in such a case the decay ends up by following a power law [1]. Our formalism also suggests a graphical representation that allows an easy identification of different dynamics within the same process. We check the validity of our results both on real systems and on computer simulations of a linear chain of elements that relax through nonlinear interactions with nearest neighbours.

But, at this stage, from an inspection of the different values taken by the individual elements, we observed the onset of a fixed shape of the configuration after some time [2]. When the runs of the simulations enter the stationary phase, the time evolution of the system is simply a change of scale of this shape. Based on this we have obtained analytically some laws of scale that should apply to these dynamics. These scaling properties are now checked in magnetic and dielectric materials.

[1] A. Fondado, J. Mira, J. Rivas; *Phys. Rev. B* 72, 024302 (2005).

[2] A. Fondado, J. Mira, J. Rivas; *Physica D* 228, 107 (2007).

C-13

EFFECT OF NB IN THE NANOCRYSTALLIZATION AND MAGNETIC PROPERTIES OF FENBBCU AMORPHOUS ALLOYS

J. Torrens-Serra^{1,2}, S. Roth², J. Rodriguez-Viejo¹, M.T. Clavaguera-Mora¹

¹*Grup de Nanomaterials i Microsistemes. Departament de Física. Universitat Autònoma de Barcelona. Edifici Cc, 08193 Bellaterra. Spain*

²*Institut für Metallische Werkstoffe. Leibniz Institut für Festkörper und Werkstofforschung Dresden. Helmholtzstraße 20, Dresden, D-01069. Germany*

The crystallization of melt-spun $\text{Fe}_{79-x}\text{Nb}_{5+x}\text{B}_{15}\text{Cu}_1$ ($x=0,2,4$) ribbons has been studied by means of differential

scanning calorimetry and X-ray diffraction. The results show a primary crystallization of bcc-Fe embedded in a residual amorphous matrix. At higher temperatures a secondary crystallization event shows the precipitation of metastable borides from the residual matrix. The characteristic temperatures of crystallization events change with Nb concentration. The results obtained from thermal and structural characterisation are related to magnetic properties of the sample. A dependence of magnetic behaviour with Fe/Nb content in the alloy is observed. The results show an enhancement of both the saturation polarization and the Curie temperature when decreasing the Nb content, due to the changes in the exchange coupling between Fe atoms. In nanocrystalline samples the differences in the nanocrystalline transformed fraction seems to be the main cause of the change in the saturation polarisation of the sample.

C-14

PREPARATION OF $\text{Gd}_5\text{Si}_2\text{Ge}_2$ COMPOUNDS USING RF-INDUCTION

A.M.Pereira¹, J. R. Peixoto¹, P. B. Tavares², N. Martins², J.B. Sousa¹ and J. P. Araújo¹

*IFIMUP unit and Physics Department of FCUP, University of Porto, R. Campo Alegre 687, 4169-007 Porto, Portugal;
 Departamento de Química and CQ-VR, Universidade de Trás-os-Montes e Alto Douro, 5001-911 Vila Real, Portugal*

The recent increase of the basic research and development of materials with near room-temperature large magnetocaloric effect (MCE) has enhanced the possibility of commercialization of magnetic refrigeration (MR) in the near future [1].

The $\text{Gd}_5\text{Si}_2\text{Ge}_2$ compound is a promising material to be used in MR because it presents a giant MCE, which is associated with a first-order phase transformation in the as-prepared $\text{Gd}_5\text{Si}_2\text{Ge}_2$ alloy. However, sample preparation techniques and conditions are still under discussion, because this first-order phase transformation is largely dependent on the purity of the chemical elements, atmospheric conditions and quenching rates [2].

In the present work we re-melt, using RF-induction, $\text{Gd}_5\text{Si}_2\text{Ge}_2$ samples previously prepared by arc-melting discharge. Scanning electron microscopy and energy dispersive spectrometry measurements confirm that the chemical stoichiometry of the re-melted sample is kept when compared with the as-cast material.

Analysis of the $\text{Gd}_5\text{Si}_2\text{Ge}_2$ crystal structure shows that the two samples present different space group symmetry, namely a $Pnma$ structure for the re-melted sample and, mostly a $P1121/a$ structure in the as-cast material. This is confirmed by our magnetic measurements, where we observed a single magnetic transition at $T_C \sim 300\text{K}$ (without thermal hysteresis) and two magnetic phase transitions at $T_C \sim 300\text{K}$ and $T_S \sim 279\text{K}$ for the re-melted and as-cast samples, respectively.

The aim of this work is the discussion of the microstructural results, namely the roles of impurities, quenching rates and atmospheric conditions.

[1] V.K. Pecharsky and K.A. Gschneidner Jr., *Adv. Mater.* 13, 683 (2001).

[2] A. O. Pecharsky, K. A. Gschneidner, Jr. and V. K. Pecharsky, *J. Appl. Phys.* 93, 4722 (2003)

C-15

HYPERFINE FIELDS IN CHARGE ORDERED $\text{Pr}_{1-x}\text{Ca}_x\text{MnO}_3$ MANGANITES

A.M.L. Lopes^{1,2}, T.M. Mendonça^{1,2}, J.S. Amaral³, A.M. Pereira¹, P.B. Tavares⁴, Y. Tomioka⁵, Y. Tokura^{5,6}, J.G. Correia^{2,7}, V.S. Amaral³, J.P. Araújo¹

¹ Departamento de Física, IFIMUP, Universidade do Porto, 4169-007 Porto, Portugal.

² CERN EP, CH 1211 Geneva 23, Switzerland

³ Departamento de Física and CICECO, Universidade de Aveiro, 3810-193 Aveiro, Portugal.

⁴ Dep. de Química and CQ-VR, Univ. de Trás-os-Montes e Alto Douro, 5000-911 Vila Real Portugal

⁵ CERC, National Institute of Advanced Industrial Science and Technology, Tsukuba, Ibaraki 305-8562, Japan

⁶ Department of Applied Physics, University of Tokyo, Tokyo, 113-8656, Japan

⁷ Instituto Tecnológico Nuclear, E.N. 10, 2686-953 Sacavém, Portugal.

The physical phenomena behind the phase diagram of manganites still challenges our understanding. In fact, much attention has been devoted to these compounds due to the peculiar entanglement between several degrees of freedom leading to phenomena like phase separation and charge ordering (CO). In this work local scale information on the different magnetic and electronic states along the $\text{Pr}_{1-x}\text{Ca}_x\text{MnO}_3$ phase diagram was obtained via Perturbed Angular Correlation spectroscopy. The Electrical Field Gradient (EFG) and the Magnetic Hyperfine Field (MHF) measurements, at the Ca/Pr site, were performed in samples ranging from $x=0$ to 1, in the 10 K to 1000 K temperature range.

We show that at room temperature the principal component of the EFG, V_{zz} , decreases with increasing Ca content, i.e., with the decrease of the orthorhombic distortion. Moreover, we found that the CO region of the phase diagram delimits distinct EFG regimes. This behaviour can be understood when the temperature dependence of the EFG for the whole system is considered. This study reveals that samples outside the CO region of the phase diagram have the expected increase of V_{zz} with decreasing temperature. While for samples within the CO region, the common increase of $V_{zz}(T)$ is only observed for temperatures above $T \gg T_{CO}$. Below T a clear anomalous decrease of V_{zz} is found when decreasing temperature. This feature remains till the charge-order temperature is reached, showing that CO is preceded by anomalous lattice dynamics. The nature

of this anomaly is discussed. Moreover, the study of the MHF is also presented and correlated with macroscopic magnetic data.

C-16

THE EFFECT OF CHEMICAL INHOMOGENEITY ON THE MAGNETOCALORIC EFFECT OF (LA-ER-SR-MNO₃ / ER-MNO₃) SELF-COMPOSITE

J.S. Amaral¹, P.B. Tavares², M.S. Reis¹, J.P. Araújo³, T.M. Mendonça³, V.S. Amaral¹ and J.M. Vieira⁴

¹ Departamento de Física da Universidade de Aveiro and CICECO, Aveiro, Portugal

² CQ-VR, Departamento de Química, Universidade de Trás-os-Montes e Alto Douro, Vila Real, Portugal

³ Departamento de Física da Universidade do Porto and IFIMUP, Porto, Portugal

⁴ Departamento de Cerâmica e Vidro da Universidade de Aveiro and CICECO, Aveiro, Portugal

Manganites of general formula ABMnO_3 (where A is a trivalent rare-earth ion and B is a divalent dopant) have numerous interesting properties [1], including their applicability as materials for active magnetic regenerators [2]. $\text{La}_{0.70}\text{Sr}_{0.30}\text{MnO}_3$ (LSMO) is a ferromagnet with $T_C \sim 370$ K and magnetic entropy variation comparable to pure Gadolinium. The high value of T_C makes LSMO unsuitable for room-temperature magnetic refrigeration applications, but by substituting La with the high-magnetic moment ion Er, T_C is lowered and total magnetic entropy increases. We have found a limit of solid solubility of Er ions in LSMO, in samples prepared by either solid state or sol-gel techniques in previous works [3], in accordance with other authors [4]. We now present a more detailed study of this limit of solubility, with more samples prepared with Er substitution close to the solubility limit and SEM microscopy clearly showing the changes in microstructure caused by the formation of a secondary ErMnO_3 phase, in accordance with X-ray diffraction data and T_C variation along the series. The magnetocaloric properties of the series are also presented, showing the increase of Relative Cooling Power along the series, in applied magnetic fields up to 1 T.

[1] Colossal Magnetoresistance, Charge Ordering and Related Properties of Manganese Oxides, C.N.R. Rao and B. Raveau (eds.), World Scientific (1998).

[2] K.A. Gschneidner Jr., V.K. Pecharsky and A.O. Tsokol, *Rep. Prog. Phys.* 68 (2005) 1479–1539.

[3] J. S. Amaral, M. S. Reis, V. S. Amaral, T. M. Mendonça, J. P. Araújo, P. B. Tavares and J. M. Vieira: *Mater. Sci. Forum* Vol. 514-516 (2006), 299-303.

[4] V. Ravindranath, M. S. Ramachandra Rao, R. Suryanarayanan and G. Rangarajan: *Appl. Phys. Lett.*, Vol. 82 (2003), 2865-2867.

C-17

NOVEL TRANSPORT BEHAVIOR OF YTTRIUM SUBSTITUTION IN POLYCRYSTALLINE $\text{La}_{0.7}\text{Pb}_{0.3}\text{MnO}_3$

C. H. Lin¹, S. L. Young¹, H. Z. Chen¹, M. C. Kao², Lance Horng³
¹Department of Electrical Engineering, Hsiuping Institute of
 Technology, Taichung, Taiwan

²Department of Electronic Engineering, Hsiuping Institute of
 Technology, Taichung, Taiwan

³Department of Physics, Changhua University of Education,
 Chunghua, Taiwan

The transport properties in polycrystalline manganites $\text{La}_{0.7-x}\text{Y}_x\text{Pb}_{0.3}\text{MnO}_3$ ($0.0 \leq x \leq 0.2$) have been investigated. The substitution of La^{3+} ions by smaller nonmagnetic Y^{3+} leads to greater spin disorder and induces variation of magnetotransport behavior. Resistivity versus temperature curves reveal a metal-insulator transition phenomenon and the transition temperature T_p decreases as the Y content increases. At high temperature the resistivity can be fitted well with $\rho(T) \propto \exp\left[\left(T_1/T\right)^{1/2}\right]$, a characteristic temperature T_1 varies with Y content in a manner consistent with a localization model of variable range hopping with Coulomb effects. Below T_p , resistivity varies as a function of power law contributions, $\sum \rho_n T^n$, represents the electron scattering process in ferromagnetic phase. The magnetoresistance ratio enhances with the increase of Y-doped due to the suppression of spin scattering in the presence of applied magnetic field. Additionally, novel transport behavior of two distinct resistivity peaks, the double-peaks behavior, with the introduction of yttrium can be explained by extrinsic magnetotransport induced by the grain boundary effect.

C-18

MAGNETIC AND STRUCTURAL CHARACTERIZATION OF THE SILVER-IRON OXIDE NANOPARTICLES OBTAINED BY THE MICROEMULSION TECHNIQUE

E. Goikolea, M. Insausti, J.S. Garitaonandia and L. Lezama
 Zientzia eta Teknologia Fakultatea, Euskal Heriko Unibertsitatea
 (UPV/EHU), 644 pk, 48080 Bilbao (Spain).

Among the chemical routes of synthesis of inorganic nanoparticles, the use of microemulsions has become very popular in the last years. One of the main advantages of this method is the ability to control the formation of different kind of microstructures with nanometric sizes. The known core-shell (CS) type nanoparticles are usually obtained by this procedure. Normally, they are composed by a core and a shell of metals or phases of different nature but with a close physical and chemical interactions between them [1]. The sizes of the core and the shell and the structure of the final CS nanoparticles are controlled by an adequate selection of the initial compositions and/or the concentration of the metal precursors. So, based in this procedure, a suitable selection of these parameters should allow the obtaining of a microstructure composed by a continuous matrix created by expanded shells in where the cores are embedded

Following this idea, we have obtained cores of Ag of 8 nm size embedded in a continuous matrix of quasicrystalline $\gamma\text{-Fe}_2\text{O}_3$ phase. Zero-field cooling and field cooling magnetic measurements obtained at very low external fields show a transition temperature at $T_B = 50$ K which is identified by Mössbauer measurements as a blocking temperature of the magnetic moments of the $\gamma\text{-Fe}_2\text{O}_3$ phase. The analysis of these data reveals that the matrix presents a structural order length of ~ 2 nm. Above T_B the coercive field is practically zero, characteristic of a superparamagnetic behaviour. However, $M(H)$ curves obtained up to 7 Tesla show a very high susceptibilities and saturation magnetizations, similar to those obtained at low temperatures in the blocked state which would suggest a possible magnetic exchange, induced by the external fields, among the moments of the $\gamma\text{-Fe}_2\text{O}_3$ matrix.

[1] J.J. Schneider, Adv. Mater., 13 (2001) 529

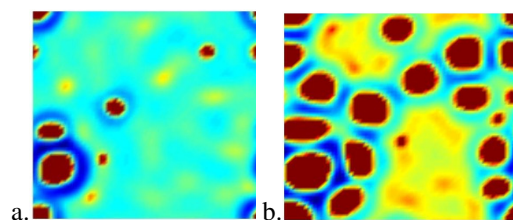
C-19

SIMULATION OF THE SPINODAL PHASE SEPARATION DYNAMICS OF THE BI-ZN SYSTEM

J. C. R. E. Oliveira, M. H. Braga, Rui D. M. Travasso
 CFP and Dep. of Eng. Physics, FEUP,

Lead free solder materials are under investigation for environmental reasons. Structural and mechanical properties are of great importance in what concerns solders, in particular for the amorphous ones. In order to study the mechanical properties of amorphous solders alloys, it is crucial to study the liquid phase.

In the phase separation occurring in the miscibility gap (in the spinodal region) of an alloy, a discrete symmetry is spontaneously broken and a domain wall network is formed. The Finite Element Method (FEM) is often used to simulate the dynamics of topological defects networks appearing in different physical contexts. In this work we focus on the dynamics of the two immiscible liquids appearing on the phase diagram of the Bi-Zn system, one of the basic systems of lead free solders. We use FEM to quantitatively simulate the dynamics of the two liquids separation (Liquid#1 and Liquid#2) in the Bi-Zn system (see Fig. 1), at different temperatures and for different concentrations. We obtain the miscibility gap curve using FEM and compare it with the experimental results. We also characterize the sample's domain morphologies as a function of time, temperature and component concentrations.



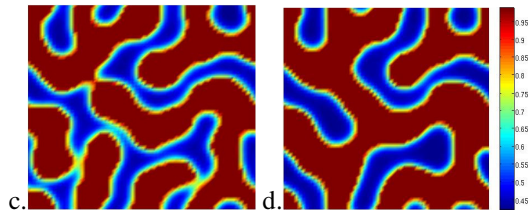


Fig. 1 (a. to d.) Diagrams showing the evolution of the two immiscible liquids in the Bi-Zn phase diagram for an alloy with $x(\text{Zn}) = 0.80$ at $450\text{ }^\circ\text{C}$ (723 K). $x(\text{Liquid}\#1, \text{Zn}) = 0.43$ and $x(\text{Liquid}\#2, \text{Zn}) = 0.99$

C-20

COMPOSITION AND NEAR SURFACE MECHANICAL PROPERTIES OF SILICATE GLASSES

Damir R. Tadjiev, Russell J. Hand

Ceramics and Composites Laboratory, Department of Engineering Materials

Sheffield University, Sheffield, S1 3JD, United Kingdom

The surfaces of silicate glasses undergo hydration in normal atmospheric conditions. The hydrated region will have different mechanical properties to the bulk glass and this work assesses the inter-relationships between composition and near surface mechanical properties of silicate glasses through the use of nanoindentation. The effect of glass composition and hydration on the near surface mechanical properties is considered for poorly durable and highly durable silicate glasses. With poorly durable glasses the hydration layer depth is much greater than the indentation depth and thus the results obtained on these glasses are used to help interpret the more complex results obtained on more durable glasses where the hydration layer is of smaller size to the indentation depth. Based on the results the application of nanoindentation technique for measuring the near surface mechanical properties and studying hydration as well as issues associated with it are discussed.

C-21

MICROSTRUCTURAL AND MAGNETIC CHARACTERISATION OF $\text{Nd}_2\text{Fe}_{17}$ BALL MILLED ALLOYS

P. Álvarez^a, J. L. Sánchez Llamazares^a, M. J. Pérez^a, B. Hernando^a, J. D. Santos^a, J. Sánchez-Marcos^{b,c}, J. A. Blanco^a, P. Gorria^a

^a *Departamento de Física, Universidad de Oviedo, Calvo Sotelo, s/n, 33007 Oviedo, Spain.*

^b *Institut Laue-Langevin, BP 156, 6, rue Jules Horowitz, 38042 Grenoble Cedex 9 France.*

^c *Instituto de Ciencia de Materiales de Aragón, C/ Pedro Cerbuna 12, 50009 Zaragoza Spain*

Fe-rich $\text{Nd}_2\text{Fe}_{17}$ compound crystallizes in the rhombohedral $\text{Th}_2\text{Zn}_{17}$ -type crystal structure ($R\bar{3}m$) [1], displaying

ferromagnetic order below $T_C = 330\text{ K}$ with a high value for the spontaneous magnetisation [2]. Moreover, this intermetallic compound exhibits strong magneto-volume effects below T_C , such as anomalous thermal expansion and a negative value for dT_C/dP [3], and a moderate magneto-caloric effect around room temperature [4]. In the present contribution we report the effect of a severe mechanical treatment on arc melted $\text{Nd}_2\text{Fe}_{17}$ bulk alloys performed via high energy ball milling. The main effects are observed on both the microstructure and magnetic properties. The milled powders were studied by means of x-ray and neutron powder diffraction, SEM, TEM, and magnetisation measurements. The most noticeable results are that although the average grain size has decreased down to 20 nm after 10 hours of milling, (i) the 2:17 crystal structure persists with almost unchanged values for the lattice parameters ($\Delta a, \Delta c < 0.1\%$), and (ii) the magneto-volume effects are still present, evidenced by neutron thermodiffraction experiments (nearly zero thermal expansion in the basal plane together with a contraction in the c axis, giving rise to a volume decrease of more than 0.1% between 5 K and 300 K). A good agreement was obtained between mean grain size determinations from the Rietveld analysis of the diffraction profiles and from TEM images. Furthermore, the low field $M(T)$ curve for the starting bulk alloys shows a well-defined and sharp decrease at $T_C = 330 \pm 2\text{ K}$, while for the milled samples the magnetic transition becomes broad not allowing an accurate determination of T_C ; in addition, this intrinsic parameter seems to be slightly shifted toward higher temperatures ($340 \pm 15\text{ K}$).

[1] Q. Johnson, *Acta Cryst.*, B25 (1969) 464.

[2] K.H.J. Buschow, *Rep. Prog. Phys.* 40 (1977) 1179.

[3] X.D. Zhang et al., *IEEE Trans. Mag.*, 31 (1995) 3713.

[4] A.M. Tishin & Y.I. Spichkin, « The magneto-caloric effect and its applications », IoP Publishing (2003).

C-22

EFFECT OF THERMAL TREATMENT ON HIGH-FREQUENCY MAGNETOIMPEDANCE IN FERROMAGNETIC/CU/FERROMAGNETIC TRILAYERS

F. Celegato, M. Coisson, P. Tiberto, F. Vinai

INRIM, Electromagnetism Division, Strada delle Cacce 91, I-10135 Torino (TO), Italy

Trilayers in the form FM/Cu/FM have been produced by sputtering on glass substrates, with thickness of each layer ranging in the interval $80\text{--}500\text{ nm}$. Co- and Fe-based amorphous ferromagnetic alloys have been employed as targets for sputtering the FM layers. The Cu interlayer is longer than the two FM layers and can thus be connected to a suitable strip line attached to a vector network analyzer covering the frequency interval $30\text{ kHz} - 6\text{ GHz}$. Giant Magneto-Impedance (GMI) curves are obtained by means of a double-measurement technique, exploiting open- and short-circuit terminations of the strip line, that allows the determination of the characteristic impedance of the line through a reflection parameter (S_{11}) measurement. The

variation of the characteristic impedance with a static magnetic field (up to 40 kA/m) defines GMI. The FM layers, in the as-prepared state, are characterized by an in-plane or out-of-plane anisotropy for Co- and Fe-based alloys respectively. Trilayers have been annealed in furnace, at temperatures below the Curie temperature of the FM materials, under the application of a static magnetic field, in order to induce a uniaxial anisotropy either along the direction of the field used for probing GMI (longitudinal annealing), or perpendicularly to it (transverse annealing).

The effect on GMI of the FM material composition, thickness and annealing conditions has been studied. In general, a reduction of GMI response is observed on annealed samples, together with a reduction of the field on longitudinally annealed specimens at which peak GMI response is detected.

C-23

OFF-DIAGONAL MAGNETOIMPEDANCE EFFECT IN FeB AMORPHOUS RIBBONS

M.L.Sánchez, T.Sánchez, I. Ribot, M.J.Pérez, J.D.Santos, J.L. Sánchez LL., V.M. Prida, B.Hernando, Ll. Escoda, J.J. Suñol
Departamento de Física, Universidad de Oviedo, Calvo Sotelo s/n, 33007-Oviedo, Spain

Universidad de Girona, Departament de Física. Campus de Montilivi, edifici PII. Lluís Santaló s/n. 17003-Girona, Spain

The Magnetoimpedance effect has been proved to be a valuable technique in order to give an insight of the magnetization processes that take place in a ferromagnetic sample when it is magnetized. It consists on the impedance change that occurs when a bias magnetic field is applied to the sample, and it carries an ac drive current. In this work we study the effect of two different quenching procedures in the off-diagonal components of impedance.

The Fe₈₀B₂₀ ribbons were produced by the roller quenching technique. Some of them were measured in the as quenched state (aq), and others were quenched while a transverse magnetic field of 0.07T was applied (field quenched samples, fq). The hysteresis loops, obtained by a conventional induction technique, show a very small improvement in the soft magnetic properties of the ribbon, after the field quenching procedure. Thermomagnetic curves provide a Curie temperature of 430°C for the aq-sample and 406°C for the fq-sample.

The off-diagonal components of impedance can be measured by means of a pick-up coil wounded around the ribbons [1, 2]. The samples are connected to the circuit using silver conductive paint. An ac current (100-1000kHz) of 8 mA rms is flowing through the sample and an axial magnetic field (0-100Oe) is applied to the ribbons. All parameters are controlled by a computer.

The impedance behaviour is different in each case. The responses are higher in the fq-samples, in all the studied frequencies. This can be related to the slightly higher transverse anisotropy, induced by the magnetic field applied during the quenching procedure.

- [1] T.Sánchez, P.Álvarez, J.Olivera, M.J.Pérez, F.J.Belzunce, J.D.Santos, J.L.Sánchez LL., M.L.Sánchez, P.Gorría, B.Hernando, J. Non-Cryst. Solids **353** (2007) 914
[2] J.D. Santos, J. Olivera, P. Álvarez, T. Sánchez, M.J. Pérez, M.L. Sánchez, P. Gorría, B. Hernando, J.Magn. Magn. Mater **316** (2007) e-915

C-24

SPECIFIC EFFECTS OF NANOMETER SCALE SIZE ON MAGNETIC ORDERING IN LA_{1-x}CA_xMNO₃ (X = 0.1, 0.3 AND 0.6) MANGANITES

E. Rozenberg,¹ M. Auslender,¹ A.I. Shames,¹ Ya. Mukovskii,² E. Sominski,³ and A. Gedanken³

¹ *Department of Physics BGU of the Negev, P.O.Box 653, Beer-Sheva 84105, Israel*

² *Moscow Steel and Alloys Institute, Leninskii prosp. 4, Moscow 119049, Russia*

³ *Department of Chemistry, Bar-Ilan University, Ramat-Gan 52900, Israel*

The mixed-valence La_{1-x}Ca_xMnO₃ (LCMO) manganite system demonstrates a rich phase diagram with a plethora of coexisting magnetic/electronic phases. It's intuitively clear that the samples' dimensions reduction down to nanometer sized scale is capable to influence magnetic ordering. Such influence was monitored on two hole-doped ($x = 0.1, 0.3$) and one electron-doped ($x = 0.6$) LCMO compounds. The powders of LCMO with the average size ranging from 15 to 25 nm were prepared by sonication-assisted coprecipitation. Their magnetic orderings were probed by electron magnetic resonance technique, comprising ferromagnetic and electron paramagnetic resonance. They were also confronted with these ones in bulk LCMO of the same compositions.

It appears that improved chemical homogeneity of $x = 0.1$ nano LCMO leads to suppression of mixed canted antiferromagnetic (AFM) + ferromagnetic (FM) order, characteristic for bulk. FM like state is observed below 90 K, while in interval 150-240 K a superparamagnetic magnetic state exists due to surface tunneling/magnetic ordering. A strong surface magnetic disorder, which leads to reduced local Curie-Weiss temperature as compared to bulk like core, is characteristic for $x = 0.3$ nano compound. It is shown that such core and surface regions/phases are coupled via AFM superexchange interaction, while both FM double exchange (DE) and inter-phases carriers' mobility are suppressed. At least, relatively stable charge and AFM ordered $x = 0.6$ nano LCMO demonstrates the FM like surface ordering on the background of partly suppressed CO/AFM state. The data obtained are discussed in the frame of suggested influence of size reduction via coupling between the spin subsystem and the lattice in LCMO, which results in confinement/band propagation of charge carriers responsible for FM DE in doped manganites.

C-25

GLASS FORMABILITY IN METALLIC MATERIALS

H.A.Davies, I.A.Figueroa and I.Todd

*Department of Engineering Materials, The University of Sheffield,
Mappin St., Sheffield S1 3JD, U.K.*

A renewed interest in the glass formability of metallic materials has been generated by the demonstration over the past 15 years that a much wider range of alloy systems are amenable to vitrification in thick sections, i.e. >300µm and often several mm thick, than was hitherto thought possible^[1,2].

The reduced glass temperature T_g/T_l , where T_g and T_l are the glass transition and equilibrium liquidus temperatures, respectively, initially proved useful as a figure of merit in correlating with the critical cooling rate for glass formation R_c ^[3,4]. However, with the advent of bulk alloy glass formers, the correlation is generally found to be rather unsatisfactory. The reasons for this will be discussed on the basis of the substantial uncertainties in the numerous factors that govern the kinetics of crystal nucleation and growth^[5]. The rôles of heterogeneous nucleants and of the relative importance of homogeneous and heterogeneous nucleation^[6] for 'conventional and bulk metallic glass formers will be highlighted.

Many of the easier glass forming alloys are based on the group IVA metals Ti, Zr and/or Hf^[1,2]. The possible rôle of these metals in governing the influence of heterogeneous nucleants will also be discussed, supported by the results of our recent investigations of the effects of small concentrations of various additional solute elements in substantially increasing the glass forming ability of Cu-Hf-Ti alloys^[7].

[1] A. Inoue, Bulk Amorphous Alloys- Preparation and Fundamental Characteristics,

(Trans Tech. Publications, Switzerland 1998)

[2] W.L. Johnson, Mater Sci. Forum Vol 225-227 (1996) p.35

[3] D. Turnbull, Contemp. Phys. Vol. 10 (1969) p.473

[4] H.A. Davies, Phys. Chem. Glasses Vol. 17 (1976) p.159

[5] H.A. Davies in "Nanostructured and Non-Crystalline Materials", eds. M Vazquez and A.Hernando, pp. 3-14, (World Scientific, Singapore 1995)

[6] B.G. Lewis and H.A. Davies in 'Liquid Metals 1976' Conf. Series No.30, eds. R Evans, D A Greenwood, pp. 274-82 (Inst. of Physics, Bristol & London 1977)

[7] I.A. Figueroa, I. Todd and H.A. Davies, to be published

C-26**FORMATION AND PROPERTIES OF THE NEW
Zr_{75-x}Al_xNi₁₀Cu₁₀Ag₅ BULK METALLIC GLASSES**

J. Latuch, A. Abramczyk, T. Kulik

*Faculty of Materials Science and Engineering, Warsaw University
of Technology**Wolowska 141, 02-507 Warsaw, Poland*

Zr – based bulk metallic glasses (BMGs) exhibit interesting mechanical properties since they combine high fracture stress, elastic strain (up to 2 %), significant fracture toughness and good corrosion resistance. Quaternary systems with general composition Zr-Al-Ni-Cu show wide composition ranges in which BMG can be obtain. The addition of the next element to the quaternary alloys often increases the glass forming ability (GFA). The aim of this work was to study the influence of aluminium content on the GFA and on the mechanical properties of the Zr-Ni-Cu-Ag alloys. Multicomponent Zr – based alloys were produced by melt spinning method obtaining ribbons, and by casting technique into a copper mould, manufacturing rod shape samples with maximum diameter of 2 mm. Structural characterizations were studied by x-ray diffraction. Calorimetric measurements were performed in order to check the stability of the amorphous phase, the presence of a glass transition temperature and the crystallization behavior. Mechanical properties of the investigated alloys were determined by means of Vickers microhardness test.

C-27**COMBINATORIAL ANALYSIS OF MG-BASED THIN
FILM METALLIC GLASSES**J.Rodriguez-Viejo, R.Domenech-Ferrer, Gemma Garcia,
M.T.Clavaguera-Mora*Grup de Nanomaterials i Microsistemes. Departament de Física.
Universitat Autònoma de Barcelona. Edifici Cc, 08193 Bellaterra.
Spain*

Mg-based bulk metallic glasses are attracting considerable attention because of their possible application as structural materials. Here, we present a new high-throughput thin film methodology that permits the growth of 24 independent compositions in a single run. This combinatorial procedure opens the way to the fast discovery of new quaternary or higher order glass former compounds with enhanced properties. Using this procedure, we have grown by a co-deposition process ternary and/or quaternary Mg-based metallic glasses containing Zr and/or Fe,Cu,Al and/or B as possible additional elements. The experimental set-up consists in a four gun dc-magnetron sputtering chamber equipped with two additional thermal evaporators to facilitate the incorporation of complex elements that can not be sputtered. We also show the potentiality of several high-throughput techniques to be used in the characterization of the glasses. The stoichiometry and amorphicity of the as-deposited libraries, as well as the crystallization temperature are determined by Energy Dispersive X-ray microanalysis and by X-ray microdiffraction, respectively. Hardness and Young modulus of each composition are determined by Nanoindentation measurements. Differential scanning calorimetry on selected compositions is also evaluated to analyze the glass forming ability of the alloys.

C-28

ASYMMETRY IN RESISTIVE SWITCHING IN MAGNETIC TUNNEL JUNCTIONS

J. Ventura¹, J. M. Teixeira¹, J. P. Araujo¹, J. B. Sousa¹, Z. Zhang², Y. Liu², P. P. Freitas²

¹IFIMUP and FCUP, R. Campo Alegre 678, 4169-007 Porto, Portugal

²INESC-MN and IST, R. Alves Redol 9-1, 1000-029 Lisbon, Portugal

Tunnel junctions (TJs) consisting of two ferromagnetic layers separated by an insulator are strong candidates for Magnetic Random Access Memories. Recently, reversible R-changes induced by an electrical current (I) were found in thin TJs and attributed to electromigration (EM) in nanoconstrictions in the insulating barrier; we thus obtain Current Induced Switching (CIS). Here we study the CIS effect on CoFe(80 Å)/AlO_x(7 Å)/CoFe(30 Å) TJs. In a CIS experiment the TJ resistance remains fairly constant in a high R-state when increasingly negative currents (from the top to the bottom lead) are applied. However, for I < -24 mA, a sharp R-decrease is observed, i.e. switching to a lower R-state. This indicates a sudden weakening of the oxide barrier, here associated with the migration of ions from the bottom metallic electrode (Co, Fe) into the insulator. Such migration should occur preferentially in hot-spots (nanoconstrictions where the barrier is thinner) and/or pinholes, and can be assisted both by intense electrical fields and local thermal effects. Upon reversing the electrical current direction, electromigration in the reverse sense is only observed for a sufficiently high positive current. If a CIS cycle is started with increasing positive currents, no R-switching is observed, indicating asymmetric electromigration between the FM/B (B=barrier) and B/FM interfaces. Since the top electrode is deposited onto a flat AlO_x surface, while the bottom one is deposited onto a rougher MnIr layer and its upper surface is covered with pure Al, subsequently oxidized, one expects the bottom electrode/insulating barrier to be more susceptible to atomic migration.

C-29

SYNTHESIS AND CHARACTERISATION OF 3C-SiC NANOWIRES

G. Attolini, F. Rossi, M. Bosi, B.E. Watts, G. Salvati

IMEM-CNR Institute, Parco Area delle Scienze 37A, 43010 Parma (Italy)

Recently, there have been many reports on the preparation and characterisation of one-dimensional nanostructures, such as nanowires of oxides, nitrides, carbides, III-V's, metals and silicon.

They present chemical, physical, electrical, optical, and mechanical properties superior to their bulk materials and offer opportunities for fundamental research as well as nano-technological applications.

Cubic silicon carbide (3C-SiC) is a wide band-gap semiconductor with high hardness, electron mobility, thermal conductivity and resistance to chemical attack.

3C-SiC nanowires (SiC-NWs) are interesting because their good physical and chemical properties make them a promising material for devices operating in harsh environments. Functionalized SiC-NWs have the potential to act as highly sensitive detector elements in bio-chemical field.

Here, we report a study on properties of cubic SiC-NWs. They have been prepared with carbon monoxide and nickel as the catalyst, in nitrogen or argon atmosphere at temperatures between 1050 and 1100°C in an open tube reaction. This method is based on carbothermal reduction of silica present on silicon substrate surface as native oxide.

The nanowires were characterized by X-ray diffraction and their morphology was studied by Scanning Electron Microscopy (SEM). Transmission Electron Microscope images and diffraction patterns of the structures will be presented. SEM studies of the nanowires show that wires have diameters less than 80 nm.

Open tube reactions are low cost and practical methods for fabricating nanostructures of refractory materials such as 3C-SiC. The method holds promise for applications on coated substrates and the functional single fibres.

C-30

DESIGN OF A DOUBLE CORE LINEAR MAGNETOMETER BASED ON ASYMMETRIC MAGNETOIMPEDANCE EFFECT IN NANOSTRUCTURED FINEMET RIBBONS

M. M. Tehranchi^{1,2}, M. Ghanaatshoar¹, S. M. Mohseni¹, H. Eftekhari¹

¹ Laser and plasma Research Institute, Shahid Beheshti University, Evin, 1983963113 Tehran, Iran

² Physics Department, Shahid Beheshti University, Evin, 1983963113 Tehran, Iran

Amorphous FeCuNbSiB (Finemet) had been heat treated at 560 °C for 1 hr to achieve the high magnetic permeability associated with the nanostructured state [1]. Subsequently, its magnetoimpedance (MI) response had been measured with a bias DC current in order to provide an asymmetric MI (AMI) behavior. We found out a linear MI behavior in a magnetic field interval including both ± directions. Samples were biased inversely, had linear response against applied magnetic field with contrary slope.

Fig. 1 demonstrates the AMI measured for both DC biased and inversely DC biased samples. A linear region can be observed in the MI curves which is suitable for sensor applications. The value of magnetic field can be obtained when sensor is immersed in a magnetic field between -P₁ or +P₂. In order to recognize the direction of applied field, the MI response of both samples is measured simultaneously and is compared with each other. Results of on-chip magnetometer are compared with laboratory equipment to calibrate the sensor response.

[1] M.E. McHenry, M.A. Willard, D.E. Laughlin, *Prog. Mater. Sci.* **44** (1999) 291.

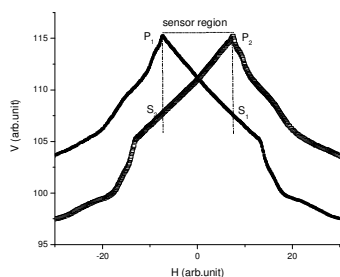


Fig.1. AMI response of samples against applied magnetic field.

C-31

STUDY OF HYPERFINE INTERACTIONS IN FE-CO NANOCOMPOSITE FILMS BY MÖSSBAUER SPECTROSCOPY AND NMR

Adriana Lancok^{1,2}, Frantisek Fendrych², Marcel Miglierini^{1,3}, and Jaroslav Kohout⁴

¹ Institute of Inorganic Chemistry AS CR, v.v.i., 250 68 Rez near Prague, Czech Republic

² Institute of Physics AS CR, v.v.i., Na Slovance 2, 182 21 Prague 8, Czech Republic

³ Slovak University of Technology, Ilkovicova 3, 812 19 Bratislava, Slovakia

⁴ Faculty of Math and Phys. Charles University, V Holesovickach 2, 180 00 Prague 8, Czech Republic

In the present work we investigate the magnetic properties of nanogranular ferromagnetic FeCoAlN films. The nanocomposite systems which consist of magnetic nanocrystals embedded in diamagnetic matrices were produced in an advanced UHV system combining the laser ablation, magnetron sputtering technique, hollow-cathode plasma jet and auxiliary ion/atom hybrid source. Plasma deposition process was performed by reactive sputtering of combined Fe₅₀Co₅₀+Al nozzle in Ar + N₂ working gas mixture flow on water-cooled Si, SiO₂/Si and glass substrates. The investigated films have thickness of about 600 nm.

Conversion electron Mössbauer spectra (CEMS) were obtained at ambient temperature using ⁵⁷Co/Rh source. The CEMS spectra of FeCoAlN film were decomposed into 3 sextets with hyperfine fields (B_{hf}) of about 32, 33.8, and 35 T and one doublet.

The nuclear magnetic resonance (NMR) spectra of ⁵⁷Fe and ⁵⁹Co nuclei have been measured by the spin-echo method using a phase-coherent spectrometer with an averaging technique and the Fourier transformation. The measurements have been performed in zero external magnetic field at the temperature of 4.2 K. The increase of average B_{hf} at ⁵⁹Co by ~3.5 T with respect to Co powder agrees with the effect of Fe atoms as nearest neighbours of resonating ⁵⁹Co nuclei. Similar effect is responsible for an increase of B_{hf} at ⁵⁷Fe nuclei due to Co nearest neighbours. High resolution transmission electron microscopy complemented the investigations of the current samples.

C-32

SYNTHESIS AND MAGNETIC PROPERTIES OF MONODISPERSE FE₃O₄ NANOPARTICLES WITH CONTROLLED SIZES

J. Salado, M. Insausti, I. Gil de Muro, L. Lezama and T. Rojo
Dpto. Química Inorgánica, U.P.V.-E.H.U., Apdo. 644, 48080, Bilbao, Spain

Magnetic iron oxide particles at the nanometer scale have attracted great interest due to their potential applications in storage devices, catalysis and biomedicine [1]. Biomedical applications, for instance, require producing magnetite nanoparticles with desired sizes and narrow size distribution without particle aggregation. Besides, dispersion of the particles in a liquid media for its use in the human body needs using a proper surface coating [2].

Taking these requirements into account, we have chemically synthesized monodisperse magnetite nanoparticles by the polyol method, which is based on heating a mixture of iron(III) acetylacetonate, 1,2-hexadecanediol, oleylamine, oleic acid and phenyl ether in an inert atmosphere [3]. By changing the synthetic conditions, nanoparticles coated with organic ligands with sizes ranging from 3.5 to 7.1 nm have been obtained. The characterization of the samples was performed by means of X-ray diffraction (XRD), transmission electron microscopy (TEM) and thermogravimetric analysis (TGA). Magnetic properties have been investigated using electron paramagnetic resonance spectroscopy (EPR) and SQUID magnetometer.

The organic content and the size of the particles have a remarkable influence on the magnetic behaviour. Nanoparticles present susceptibility plots which exhibit a cusp in the ZFC curve, which is not related to the blocking temperature, T_B. Above T_B, hysteresis loops with values of 30-130 Oe for H_c are observed, indicating a ferromagnetic behavior at room temperature. EPR measurements of these particles show a broad signal, which exhibits an orientational dependence of the ferromagnetic resonance. An exhaustive study with temperature and orientation has been performed.

[1] A.K. Gupta, M. Gupta, Biomaterials, **26** (2005) 3995.

[2] H. Lee, M.K. Yu, S. Park, S. Moon, J.J. Min, Y.Y. Jeong, H.-W. Kang, S.J. Jon, J. Am. Chem. Soc., **129**, (2007) 12739.

[3] S. Sun, H. Zeng, D.B. Robinson, S. Raoux, P.M. Rice, S.X. Wang, G. Li, J. Am. Chem. Soc., **126** (2004) 273.

C-33

ELECTRICAL AND OPTICAL PROPERTIES OF AMORPHOUS CR₂-XTIXO₃ THIN FILMS.

Conde-Gallardo¹, R. Escudero Derat², F. S. Aguirre-Tostado³
¹Departamento de Física, Centro de Investigación y de Estudios Avanzados del IPN Apdo. Postal 14-740, D.F. 07360, México.

²*Instituto de Investigación en Materiales. Universidad Nacional Autónoma de México. Apartado postal 70-360 D.F. México.*

³*Materials Science and Engineering, University of Texas, Dallas. Richardson, TX 75083.*

By employing chromium pentanedionate and titanium butoxide as precursors, $\text{Cr}_{2-x}\text{Ti}_x\text{O}_3$ thin films were grown by aerosol assisted chemical vapor deposition. When the films are deposited at substrate temperature $T_s < 550^\circ\text{C}$ they grow with an amorphous structure, and those deposited at $T_s \geq 550^\circ\text{C}$ grow in a crystalline structure that depends on the x values. There are great differences in the electrical and optical properties of the crystalline and amorphous films. While the crystalline ones are insulators with an optical band gap that depends on the titanium concentration, the amorphous are semiconductors, with an electrical conduction that strongly depends on the x -value and with a little change in the optical band gap. These differences between the crystalline and amorphous films can be explained by considering the different oxidation state that the titanium ions (Ti^{3+} or Ti^{4+}) obtain during their incorporation into the Cr_2O_3 matrix, as it is shown by the X-ray photoelectron spectroscopy. The electrical properties (resistance vs temperature and thermal assisted conductivity) of the amorphous films are explained by considering a variable range hopping model for magnetic semiconductors.

C-34

RELATIONSHIP BETWEEN NANOPARTICLE GROWTH AND MAGNETIC PROPERTIES OF MAGNETIC NANOCOMPOSITES

D. Ortega¹, J. S. Garitaonandía², M. Ramírez-del-Solar³,
C. Barrera-Solano³ and M. Domínguez³

¹*Dept. of Materials Science and Metallurgical Engineering and Inorganic Chemistry, Faculty of Science, University of Cádiz, E11510 Puerto Real, Spain*

²*Dept. of Applied Physics II, University of the Basque Country, P.O. Box 644, E48080 Bilbao, Spain*

³*Dept. of Condensed Matter Physics, Faculty of Science, University of Cádiz, E11510 Puerto Real, Spain*

In the present work, we report on the role of nanoparticle growth in the magnetic behaviour of iron oxide nanoparticles in silica matrix nanocomposites. Samples have been synthesized by means of the classic sol-gel method, by virtue of which a superparamagnetic regime for nanoparticles is expected to occur. Nevertheless, aggregation between nanoparticles may take place subject to the system composition and its processing conditions, giving rise to a more complex magnetic behaviour. The structural implications of heat treatment applied to the samples are also studied and correlated both with the evolution of initial iron precursors during processing and the distribution of iron oxide (III) phases. Samples taken at different stages of heat treatment have been studied by means of Analytical Electron Microscopy, observing the early iron distribution through the matrix and its subsequent

transformations into nanocrystals of two common iron oxide phases, i. e. maghemite and hematite. Magnetization curves of samples obtained before and after heat treatment are of importance when tracking the phase transitions; up to a treatment maximum temperature of 700°C ferrimagnetic behaviour is predominant, whereas at intermediate steps at lower temperatures (300 and 500°C), samples have been found to be paramagnetic.

On the basis of experimental results, a model for nanoparticle growth throughout heat treatment is proposed, taking into account two distinct aggregation mechanisms which depend on the mobility degree of nanoparticles and the high compressive forces generated inside the matrix structure during its policondensation.

C-35

SUPERPARAMAGNETIC BEHAVIOUR OF FE NANOPARTICLES EMBEDDED IN A COMMERCIAL POROUS CARBON

M. P. Fernández-García^a, M. Sevilla^b, A. B. Fuertes^b, A. Silva^c,
D. S. Schmooll^c, P. Gorria^a, J. A. Blanco^a.

^a*Departamento de Física, Universidad de Oviedo, Calvo Sotelo, s/n, 33007 Oviedo, Spain.*

^b*Instituto Nacional del Carbon (CSIC), Apartado 73, 33080 Oviedo, Spain.*

^c*IFIMUP and Departamento de Física, Universidade do Porto, Rua Campo Alegre 687, 4169 0071 Porto, Portugal.*

Physical properties of commercial porous carbon in which Fe nanoparticles are dispersed have been studied. The sample in powder form, with average grain sizes of several microns as SEM images revealed, contains around 17 wt.% of Fe. The XRD pattern collected at room temperature shows peaks corresponding to Bragg reflections of both BCC and FCC Fe phases. From the analysis of TEM images, it was found that Fe nanoparticles have diameters ranging from 5 to 50 nm, which are quite well described by a log-normal distribution giving an average value of ~ 15 nm with $\sigma = 6$ nm. The ZFC-FC curves measured at low applied magnetic fields (1 mT) suggest that all the nanoparticles are blocked below 50 K. Moreover, $M(H)$ curves exhibit hysteresis up to around 200 K with coercive field values of around 30 mT at 10K. For $T > 200$ K the $M(H)$ curves are reversible, thus suggesting that above this temperature almost all the system behaves as superparamagnetic. Besides that, exchange bias is observed for $T < 50\text{K}$, with maximum values $H_{\text{ex}} \approx 15$ mT at 2 K. Mössbauer spectra recorded at room temperature have been fitted using three different subspectra, a sextet associated to the ferromagnetic bcc Fe nanoparticles with $B_{\text{HF}} = 33$ T, an intense single peak that can be ascribed to the paramagnetic FCC-Fe phase, and a less intense doublet ($< 15\%$) that could come from an Fe oxide shell, which existence may be related to the observed low temperature exchange bias behaviour.

C-36

SYNTHESIS AND CHARACTERIZATION OF COFe₂O₄ – PVP NANOCOMPOSITES

Cintia Mateo Mateo,¹ Carlos Vázquez Vázquez,¹ María del Carmen Buján Núñez,¹

M. Arturo López Quintela,¹ David Serantes Abalo,² Daniel Baldomir Fernández,² José Rivas²

¹ *Facultade de Química, Departamento de Química Física, Universidade de Santiago de Compostela, Avenida das Ciencias, s/n; 15782 Santiago de Compostela (Spain)*

² *Facultade de Física, Departamento de Física Aplicada, Universidade de Santiago de Compostela, Campus Sur, s/n; 15782 Santiago de Compostela (Spain)*

Cobalt ferrite (CoFe₂O₄) nanoparticles were obtained by a non-aqueous procedure using acetophenone as reaction medium [1]. By selecting the reaction temperature (from 120 to 200°C), the particle size can be easily tuned from 2 to 15 nm.

In order to prepare stable dispersions of cobalt ferrite nanoparticles, they were capped with dimercapto succinic acid (DMSA). Then, several samples were prepared by mixing different amounts of the cobalt ferrite dispersion with a polyvinylpyrrolidone (PVP) solution. In this way, different nanoparticle concentrations were obtained.

The mixture was destabilized by adding acetone and washed several times. Then, it was dried at 70°C during several days to obtain the ferrite-PVP nanocomposites.

The nanocomposites were studied by dc-magnetization in order to determine the influence of dipolar interactions in their magnetic properties. For the smaller cobalt ferrite nanoparticles (average particle size ~ 4nm) a shift of the blocking temperature to lower temperatures is observed when the concentration is increased. For the larger nanoparticles a different behaviour was obtained: almost no shift is observed. These results are discussed taking into account the anisotropy constant of the nanoparticles and Monte Carlo simulations.

[1] C. Vázquez-Vázquez, and M. A. López-Quintela, J. Solid State. Chem. **129**, 3229 (2006).

C-37

MAGNETIC ANISOTROPY OF BATIO₃-COFE₂O₄ NANOGRANULAR COMPOSITE THIN FILMS

J. Barbosa¹, B.G. Almeida¹, J.A. Mendes¹, J.P. Araújo²

Departamento de Física, Universidade do Minho, Campus de Gualtar, 4710-057 Braga, Portugal

Dep. de Física and IFIMUP, Universidade do Porto, Rua Campo Alegre, 687, 4169-007 Porto, Portugal

Nanostructured materials presenting a coupling between the electric and magnetic degrees of freedom have been attracting much scientific and technological interest. By combining a piezoelectric ceramic and a magnetostrictive material the elastic interactions between the phases provide the coupling mechanism inducing a magnetoelectric behavior. Here, nanocomposites of cobalt ferrite (CoFe₂O₄-magnetostrictive) dispersed in a barium titanate (BaTiO₃-piezoelectric) matrix were prepared and the influence of the

stress on the magnetic properties was studied. The films were prepared by laser ablation with different cobalt ferrite concentrations (from 20% to 70% CoFe₂O₄), as well as pure barium titanate and cobalt ferrite thin films (end members). Their structure was studied by X-ray diffraction and the magnetic properties were measured in a SQUID magnetometer.

The films were polycrystalline with a slight (111) barium titanate phase orientation and (311) cobalt ferrite phase orientation. The lattice parameter of the CoFe₂O₄ phase varied from 8.26Å (x=20%) to 8.35Å (x=70%), and, comparing with bulk CoFe₂O₄, it was under compressive stress that relaxed as its concentration progressively increased. The magnetic measurements showed a decrease of the coercive field, from 6.6 kOe (x=20%) to 2.3 kOe (x=70%), with increasing cobalt ferrite. From the lattice parameter contraction of the CoFe₂O₄ phase, and using the bulk Co-ferrite magnetostriction and Young's modulus coefficients, the stress induced anisotropy was calculated and compared with the magnetocrystalline anisotropy of bulk CoFe₂O₄. The magnetic behavior of the films (anisotropy, coercivity) is discussed in terms of its correlation with the progressive relaxation of the stress in the films.

C-38

MAGNETIZATION PROCESSES IN ARRAYS OF ANTIDOTS LITHOGRAPHED ON AMORPHOUS FEB FILMS

J. Gutiérrez^a, R. Yanes^b, F. García-Sánchez^b, E. Paz^b, J. Haba^c, F. Cebollada^c, O. Chubykalo-Fesenko^b, F.J. Palomares^b and J.M. González^a

^a*Unidad Asociada ICMM/CSIC-IMA/UCM, Madrid, Spain*

^b*Instituto de Ciencia de Materiales de Madrid – CSIC, c/ Sor Juana Inés de la Cruz 3, 28049 Madrid, Spain*

^c*Departamento de Física Aplicada a las Telecomunicaciones, EUITT – UPM, Crtra. A-6 km XX.XX, 280YY Madrid, Spain*

It is known that an optimum anisotropy configuration for the sensing materials used on the implementation of magnetic field or magnetoelastic sensors is that corresponding to a homogeneous, reduced in effective magnitude, uniaxial anisotropy having an easy axis perpendicular to the measuring direction. In the present work, and following some previous results evidencing the occurrence in antidots arrays of highly inhomogeneous magnetization structures exhibiting constant reversible susceptibility, we explore the viability of those arrays to be used as sensing materials allowing the implementation of sensors adequate to measure in any direction contained in a plane. For that purpose, we have implemented micromagnetic simulations in order to obtain the magnetization distribution present in square arrays of antidots. From these simulations we have concluded that, for the amorphous FeB anisotropy, exchange and magnetization values, an square array of antidots having a diameter of 100 nm and a lattice parameter of 100 nm exhibits a continuously varying in direction moment

distribution. In order experimentally study these arrays we have i) deposited amorphous FeB films by means of a pulsed laser ablation set-up and ii) used focused ion beam lithography to engrave arrays of antidots having the geometry obtained from the micromagnetic simulations. The characterization of the samples was carried out by using a magneto-optic Kerr effect device and evidenced i) the occurrence in the array of a slight increase of coercivity with respect to that measured in the as-deposited film and ii) the induction through the lithographic process of an easy axis re-orientation.

C-39

ELECTROLYTE INFLUENCE ON THE ANODIC SYNTHESIS OF TiO₂ NANOTUBE ARRAYS

V. Vega¹, M. A. Cerdeira¹, V. M. Prida^{1*}, D. Alberts², N. Bordel¹, R. Pereiro², F. Mera³, S. García⁴, M. Hernández-Vélez^{4,5} and M. Vázquez⁴

¹Dept. Física, Universidad de Oviedo, Asturias, Spain

²Dept. Química-Física y Analítica, Universidad de Oviedo, Spain

³CENTA S.L.U., Pol. Industrial de Olloniego, Asturias, Spain

⁴ICM Madrid (CSIC), Cantoblanco, 28049, Madrid, Spain

⁵Dept. Física Aplicada UAM, Cantoblanco, 28049, Madrid, Spain

Titanium oxide is a well known semiconductor oxide which offers improved functional and sensing applications in many research fields as photocatalytic, spintronic or biocompatible material. It has been well established that the physical and chemical properties of the nanodimensional structures like nanotubes and nanoporous architectures, are strongly dependent on their geometrical features such as tube diameter, tube to tube interspacing, tube wall thickness and length, etc. A required specific architecture can be well controlled by varying the settings in the synthesis procedure [1]. In this work, structural, morphological and compositional features of self-aligned titanium oxide nanotube arrays grown by electrochemical anodization in different electrolytic media have been investigated [2]. The titanium oxide nanotube arrays were synthesized performing a single-step anodic oxidation of high purity Ti foils (Ti 99.6%) at several potentiostatic voltages ranging between 10-60 V_{dc}, by employing different aqueous solutions such as: HF, HF+H₂SO₄, or HF+H₃PO₄, as well as non aqueous solutions of NH₄F in ethylene glycol. The different characterizations have been carried out by means of Scanning Electron Microscopy, Transmission Electron Microscopy and radio-frequency Glow Discharge Optical

Emission Spectroscopy techniques. Varying the anodic voltage, Titanium oxide nanotube arrays have been grown with inner diameters ranging between 40 up to 100 nm, in a linear relationship. The results show an improvement in the self-alignment of the nanotube arrays, so as an increase of about 10,000% in the nanotubes length obtained by anodization with electrolytes containing NH₄F in ethylene glycol, respect to the ones obtained with the aqueous electrolytes.

[1] C.A.Grimes, *J. Mater. Chem.* 17, (2007) 1451.

[2] V. Vega et al, *Nanoscale Res. Lett.* 2, (2007) 355.

C-40

FINITE ELEMENT ANALYSIS OF THE HYPERELASTIC CONTACT PROBLEM IN DOOR AUTOMOTIVE SEALING

Ordieres-Meré J., Bello-García A., Muñoz-Munilla V., Del-Coz-Díaz JJ.

Mechanical Engineering Department University of la Rioja / Luis de Ulloa 2026004 LOGROÑO SPAIN

Specific problems regarding the sealing of doors and windows for the automotive industry will be considered in this work. Two main problems must be assessed for predicting sealing capabilities and close-up forces involved, firstly there is mandatory to identify chemical and mechanical properties for the rubber used on profiles. In addition, large deformation models with specific three dimensional constitutive equations are required for these problems.

The work carried out will present and implement such a constitutive model in order to evaluate the capability for predicting the final geometric configuration and for simulating the closing process for measuring the required force.

Specific efforts have been paid for evaluating the sensibility of forces against rubber's mechanical parameters. Specific three dimensional constitutive equations are formulated and implemented as they are more convenient. These studies are relevant as they will allow for producing valid sections even during preproduction stages and reducing additional costs for section rebuilding and also additional costs for line reconfiguration.

Finally real test results will be compared to simulated ones and specific conclusions will be formulated.

POSTER CONTRIBUTION

P-01

AMORPHOUS $\text{Ni}_{59}\text{Zr}_{20}\text{Ti}_{16}\text{M}_5$ (M = CU, AG) ALLOYS OBTAINED BY MELT SPINNING AND MECHANICAL ALLOYING

D. Oleszak, E. Zbrzeźniak, T. Kulik
Faculty of Materials Science and Engineering
Warsaw University of Technology
Wolaska Str. 141, PL – 02-507 Warsaw, Poland

Nowadays Ni-based bulk metallic glasses (BMG) are considered as potential engineering materials due to their good mechanical properties (high strength, relatively low Young's modulus and large elastic limit). Several Ni-based alloys have been reported to show the enhanced glass forming ability (GFA), enabling the preparation of BMG by Cu-mould injection casting. Another possibility of fabrication of amorphous powders is mechanical alloying (MA) method.

The main purpose of this work was to produce amorphous $\text{Ni}_{59}\text{Zr}_{20}\text{Ti}_{16}\text{M}_5$ (M = Cu, Ag) alloys by mechanical alloying of a mixture of the powders of pure crystalline elements. The studied alloys exhibit high GFA, however, the compositional ranges of amorphisation for MA and rapid quenching are usually different. Then, the thermal stability of all investigated amorphous alloys were studied and compared.

X-ray diffraction (XRD) and differential scanning calorimetry (DSC) were employed as the experimental techniques for samples characterization, both melt spun ribbons and MA powders at different stages of processing.

P-02

THE ROLE OF SURFACTANT IN SYNTHESIS OF MAGNETIC NANOCRYSTALLINE POWDER OF NiFe_2O_4 BY SOL-GEL AUTO-COMBUSTION METHOD

M. R. Barati^a, S.A. Seyyed Ebrahimi^a, A. Badi^b
^a*Center of Excellence in Magnetic Materials, School of Metallurgy and Materials, University of Tehran, Tehran, Iran*
^b*Faculty of Chemistry, University of Tehran, Tehran, Iran*

Soft ferrites are widely used in multilayer chip inductors, radar-absorbing coatings, electromagnetic wave absorber, magnetic resonance imaging contrast agents, ferro fluids and catalysts.

In this work a new sol-gel auto-combustion method has been performed to synthesize nickel ferrite nanocrystalline powders by using n-decyle trimethyl ammonium bromide, as a cationic surfactant. The gels were prepared from ferric, nickel and zinc nitrates and citric acid by various molar ratios of Surfactant / Ni. Ammonia was used as pH adjusting agent as well. The effects of surfactant on decreasing of after- combustion calcination and reduction

of crystallite size which affects the magnetic properties of the material were investigated by XRD, FTIR, DTA/TGA and SEM techniques.

The results showed that the ignition of the gels in air have a self-propagating behavior. Different Surf / Ni ratios in the starting solution affected the crystallite size of the synthesized powders and their phase constitution and the optimum molar ratio was evaluated as Surf / Ni = 0.2 with a crystallite size of about 31.2 nm. Another important result of this study was production of single phase ferrite directly after combustion while without surfactant the ferrite single phase was formed after a calcination process at 1000 °C.

P-03

BULK GLASS FORMABILITY FOR CU-HF-ZR-AG AND CU-ZR-AG-SI ALLOYS

A. Figueroa, H. Zhao¹, S. González², H. A. Davies and I. Todd.
Department of Engineering Materials, University of Sheffield,
Sheffield S1 3JD, UK

¹*Ningxia Orient Tantalum Industry Co., Ltd, Shizuishan, Ningxia, China, 753000*

²*National Centre for Metallurgical Research, CSIC, Avda. Gregorio del Amo 8, 28040, Madrid, Spain*

The bulk glassy Cu-Zr and Cu-Hf binary alloys form the basis of a number of easy glass forming compositions, e.g. the addition of Ti[1], Ag[2], Al[3] to these binary alloys substantially enhance the glass formability (GFA) up to rod diameters of 4 mm, 6mm and 10mm, respectively. In this paper, we report and discuss the effects of the gradual substitution of Hf by Zr on glass formability and thermal stability in the $\text{Cu}_{45}\text{Hf}_x\text{Zr}_{45-x}\text{Ag}_{10}$ alloys and the effect of the small additions of Si on glass formability in the $\text{Cu}_{45}\text{Zr}_{45}\text{Ag}_{10}$ alloy. The samples were prepared as ribbons of thickness in the range 25-200 μm by melt spinning and as conical bulk shapes, with a length of 50 mm and cone base diameters in the range 2-10 mm, by suction die casting. The alloy $\text{Cu}_{45}\text{Zr}_{45}\text{Ag}_{10}$ had a dc of 3.5mm but substitution of 1.5 and 3.5 at. % Zr by Hf resulted in substantial increases to 5.5 and 4.5mm, respectively. However, for x in the range 5-40 at.%, dc was reduced to <1mm. The small addition of Si proved to be beneficial to the GFA, increasing dc up to 5.5 mm with 0.5 at.% Si. The chemical similarity of Hf and Zr does not guarantee the possibility of forming bulk glasses on substituting large proportions of Zr by Hf though small substitutions of Hf and Si are beneficial to the GFA.

[1] A. Inoue, W. Zhang, T. Zhang, K. Kurosaka, J. Mater. Res., 16 (2001), p.2836.

[2] W. Zhang and A. Inoue, J. Mater. Res., 21, (2006), p. 234.

[3] P. Jia, H. Guo, Y. Li, J. Xu, E. Ma, Scripta Mater., 54 (2006), p. 2165.

P-04

RAPID THERMAL PROCESSING OF ZNO NANOCRYSTALLINE FILMS FOR APPLICATION IN DYE-SENSITIZED SOLAR CELLS

M. C. Kao¹, H. Z. Chen², S. L. Young², and C. H. Lin²¹Department of Electronic Engineering, Hsiuping Institute of Technology, Taichung, Taiwan²Department of Electrical Engineering, Hsiuping Institute of Technology, Taichung, Taiwan

The nanocrystalline anatase ZnO thin films were prepared by the sol-gel method and crystallized by conventional (CTA) and rapid thermal annealing (RTA) process for application as the work electrode for the dye-sensitized solar cells (DSSC). The electrode of DSSC fabricated with ZnO thin films were characterized by X-ray diffraction (XRD) and scanning electron microscopic (SEM) Brunauer-emmett-Teller (BET) analysis. The photoelectric performance of DSSC were studied by I-V curve and photo-to-electric conversion efficiency, the influence of pore size and surface area of ZnO thin films on the performance of DSSC was also discussed. Based on the results, the highly (002)-oriented nanocrystalline anatase ZnO thin film crystallized by the RTA process presented better crystallization than CTA-derived films. In addition, the increase in pore size and surface area of ZnO films crystallized by the RTA process contributed to the improvement on the absorption of dye onto the films and the short-circuit photocurrent (J_{sc}) and open-circuit voltage (V_{oc}) of DSSC. The optimum efficiency (η) of 2.8 % with J_{sc} and V_{oc} of 6.2 mA/cm² and 0.65 V, respectively, was obtained by the ZnO film crystallized by the RTA process.

P-05

ANODIZATION PROCESS OF SELF-ORDERING NANOPOROUS ALUMINA MEMBRANES IN PHOSPHORIC ACID

M.P. Proenca, C.T. Sousa, D.C. Leitao, J. Ventura, F. Carpinteiro, J.B. Sousa, J.P. Araujo

Dep. Física and IFIMUP, Rua do Campo Alegre 687, Porto

Nanoporous alumina membranes are an easy-made product that has attracted much interest in these last years. They can be used as templates for well ordered growth of nanowires, nanotubes, nanorods and nanodots, thus providing a wide range of applications in areas such as medicine (biosensors, photocatalyses), electronics (ultrahigh-density magnetic memories, optoelectronic devices), energy storage (solar cells).

The fabrication of these membranes follows a simple two step anodization process [1]. Depending on the electrolyte type, concentration, temperature and applied anodizing potential, different pore sizes and interpore distances can be obtained. Membranes with pore diameters ranging from 2 to 900 nm and interpore distances from 35 to 980 nm, have already been produced using inorganic (sulphuric,

phosphoric) and organic acids (oxalic, glycolic, tartaric, malic, citric) [2]. However, in the particular case of anodization using phosphoric acid, optimization of the process is required.

In this work we will describe the pore formation mechanism for anodizations in phosphoric acid (pore diameters ~ 100 nm) [3]. Since high anodizing potentials (160-195V) and consequently high electric field densities are required, a pre-anodization process in oxalic acid was made or a ramp potential applied, to avoid the aluminium rupture. The current density transients during the first anodization process allowed us to identify four major regimes, similar to those obtained in sulphuric and oxalic acids. A detailed study of these different regimes using Scanning Electron Microscopy (SEM) will be presented and compared with the results obtained in sulphuric and oxalic acids.

[1] H. Masuda and K. Fukuda, *Science*, **1995**, 268, 1466.[2] S. Z. Chu, K. Wada, S. Inoue, M. Isogai, Y. Katsuta and A. Yasumori, *J. Electrochem. Soc.* **2006**, 153, B384[3] W. Lee, R. Ji, U. Gosele and K. Nielsch, *Nature Materials*. **2006**, 5, 741

P-06

THE CRYSTALLINITY OF SiC GROWN FROM THE VAPOUR PHASE

B.E. Watts¹, G. Attolini¹, M. Bosi¹, G. Salviati¹ and O. Martinez²¹IMEM/CNR, Parco Area delle Scienze 37A. 43010 FONTANINI (Parma), Italy²Física de la Materia Condensada, ETSII, Universidad de Valladolid, 47011 VALLADOLID, Spain

Although crystalline silicon carbide is being studied intensely for its mechanical, electrical and thermal properties, amorphous SiC possesses high reflectance at ultraviolet wavelengths and so finds application in UV optics. This work presents a study of the crystalline, morphological and optical properties of SiC grown by metal-organic vapour phase epitaxy (MOCVD) using silane and propane as reagents.

The films were grown on silicon (001) substrates at different growth chamber temperatures, pressures and propane:silane ratios. Prior to growth, a nucleation treatment (carburisation) that involved treating the substrate in propane only was applied.

X ray diffraction analysis shows that low growth temperatures led to less well crystallised SiC, however, the carbon silicon ratios of the reactor gas and the carburisation process is critical to the texture and crystallinity. Raman spectroscopy suggests that different polytypes of SiC are present, both hexagonal and cubic.

The crystalline quality of SiC films, grown by MOCVD, can be modified, not only by controlling the growth temperature but also the carbon:silicon ratio used and the carburisation step.

P-07

INVESTIGATION OF THE EFFECTIVE PARAMETERS ON THE SYNTHESIS OF NI FERRITE NANOPOWDERS BY COPRECIPITATION METHOD

R. Dehghan, S.A. Seyyed Ebrahimi, A. Badieli

Center of Excellence in Magnetic Materials, School of Metallurgy & Materials, University of Tehran, Tehran, Iran

NiFe₂O₄ is largely used in electronic and telecommunication applications, electric and electronic devices, ferro-fluids, magneto-caloric refrigeration, and catalysts.

In this work, synthesis of nanostructured NiFe₂O₄ powders by coprecipitation of novel precursors, followed by calcination was investigated for the first time. Ni-ferrite powder was synthesized by dissolving Fe and Ni chlorides and ammonium ferrous sulfate in deionized water. After stirring, the precipitating agent of NaOH was added to the solution and after 1 hour of aging, the resultant precipitate was washed with deionized water and acetone. Then the powder was characterized and the effects of different parameters such as molarity of precipitant, calcination temperature, ratio of Ni²⁺ ion to Fe²⁺ and Fe³⁺ ions, the effect of degassing and washing and the effect of aging time and temperature were studied by different techniques such as XRD, DTA/TGA, TEM and SEM.

It is concluded that an increase in molarity of precipitant can decrease the calcination temperature and the best conditions to obtain a single phase Ni ferrite are using of 2 molar NaOH as precipitant solution, calcination temperature of 900°C and the same ratio of one for Ni²⁺ ion to Fe²⁺ and Fe³⁺ ions. The crystallite size of resulting ferrites is in the range of 20-50 nm.

P-08

EPITAXY AND SURFACE MORPHOLOGY OF ZNO THIN FILMS GROWN BY RF-MAGNETRON SPUTTERING ON SAPPHIRE

A.C. Lourenço¹, S. Pereira¹, M. Peres², T. Monteiro², M.R. Correia², S. Magalhães³, E. Alves³

¹*Departamento de Física and CICECO, Univ. de Aveiro, Portugal*

²*Departamento de Física and I3N, Univ. de Aveiro, Portugal*

³*Instituto Tecnológico e Nuclear, Sacavém, Portugal*

A custom/home made UHV rf-sputtering system was developed to deposit complex oxide thin layers and it has been successfully used to grow ZnO thin films on Al₂O₃ (0001). The films were analyzed in terms of their crystalline structure by high-resolution XRD and RBS, optical properties using Photoluminescence and Raman techniques, and surface morphology using SEM and AFM. A very accurate control of deposition parameters, such as growth temperature, oxygen and argon partial pressures, RF power/DC_bias and target to substrate distance, is essential to optimize the growth conditions.

Structural and optical characterization shows that the developed system is able to reproducibly provide high

quality epitaxial thin films of ZnO on various substrates. The crystalline quality figures of merit obtained by XRD and RBS indicate high quality thin films: ZnO (0002) diffraction peak FWHM is 0.15° and RBS minimum yield is 3%-4%. Furthermore, the crystalline quality of the grown samples was corroborated using Raman spectroscopy. With above band gap excitation the low temperature photoluminescence spectra is typically dominated by the presence of the near band edge and orange deep level recombination. Surface morphology is assessed using SEM and AFM microscopy.

P-09

THE EVOLUTION OF BOND STRUCTURE IN GE₃₃AS₁₂SE₅₅ FILMS UPON THERMAL ANNEALING

R.P. Wang, D.Y. Choi, A.V. Rode, S. Madden and B. Luther-Davies

Centre for Ultra-high-bandwidth Devices for Optical Systems,

Laser Physics Centre, Research School of Physical Sciences &

Engineering, The Australian National University, Canberra,

ACT0200, Australia

Ge₃₃As₁₂Se₅₅ films deposited by ultrafast pulse laser deposition were annealed at various temperatures and pressures, and the evolution of the bond structure and the surface oxidation under various processing conditions were investigated by x-ray photoelectron spectroscopy (XPS). It was found that, the as-grown film contains a large number of Se-rich structures which may coalesce with As and Ge after annealing at high temperatures. In addition, both Ge and As 3d spectra show the presence of oxides, which could deteriorate the optical transmission of the films in the infrared region. Whilst the Ge oxidation increases with increasing annealing temperature, As oxidation is almost unaffected by annealing. The difference could be due to their different electronegativities. The oxygen distribution exponentially decays along the normal direction of the films regardless of different processing conditions. The critical thickness of the oxidized layer was 6.5 nm, 11 nm, 48 nm and 98 nm, respectively, for the as-grown, 250°C annealing sample for 4 hours under 1×10⁻⁶ Torr of the oxygen, and 150°C and 250°C annealing samples for 15 hours under 20 mTorr.

P-10

PRIMARY CRYSTALLIZATION IN FE₆₅NB₁₀B₂₅ METALLIC GLASS

M.T. Clavaguera-Mora, J. Torrens-Serra, J. Rodriguez-Viejo
Grup de Nanomaterials i Microsistemes. Departament de Física.
Universitat Autònoma de Barcelona. 08193 Bellaterra. Spain

The kinetic analysis of primary crystallization under heat treatment of Fe₆₅Nb₁₀B₂₅ metallic glass is obtained from quantitative microstructural data in combination with calorimetric data. The mathematical description is grounded

on the Kolmogorov-Johnson-Mehl-Avrami model generalized to account for the compositional changes of the parent phase, responsible for the decreasing of both the nucleation frequency and the growth rate of the primary grains. The coupling of isothermal and continuous heating calorimetric data is performed to take into account that the transformed fraction is very sensitive to the temperature dependence of the thermodynamic and kinetic quantities under continuous heating conditions, whereas the time evolution under isothermal treatment of the transformed fraction is very sensitive to the mechanisms that control the transformation process.

In the present analysis, soft nucleation is introduced to deal with the consequences of the compositional changes of the matrix in the nucleation frequency whereas soft growth is used to designate the consequences of these compositional changes in the growth mechanism. Both effects are included in the mean-field approximation presented and discussed.

The modeling and calculation of the transformation rate has been performed to determine the optimum range of values of the viscosity, driving force for crystallization and interfacial energy, leading to a reasonable agreement with the experimental kinetic data. It is shown that the indicated modeling procedure is quite suitable to obtain an indirect evaluation of the interfacial energy between the Fe_{23}B_6 -type nanocrystals embedded in a disordered matrix with global $\text{Fe}_{65}\text{Nb}_{10}\text{B}_{25}$ composition.

P-11

EPR STUDY OF CRYSTALLINE AND GLASSY ETHANOL

Marina Kveder, Dalibor Merunka, Milan Jokić, and Boris Rakvin
Ruder Bošković Institute, Bijenička 54, 10000 Zagreb, Croatia

X-band electron paramagnetic resonance (EPR) spectroscopy was applied in studying molecular dynamics in two different solid ethanol matrices. Nitroxyl radicals as paramagnetic reporter groups were embedded in crystalline and glassy ethanol and their spectral properties investigated by continuous wave (CW) and pulsed EPR techniques. Different anisotropy of molecular packing was evidenced by larger nitroxide maximal hyperfine splitting characterizing crystalline ethanol than ethanol glass. This phenomenon is a consequence of larger anisotropy of interactions in the crystalline matrix due to the orientational/positional ordering. [M. Kveder *et al.*, Chem. Phys. Lett. **419**, 91 (2006)] The mechanisms that affect spin dynamics were addressed by measuring phase memory time, T_m , and spin-lattice relaxation time, T_1 , of the reporter groups probing different local environments. The relaxation rate data showed differences in two ethanol matrices and the respective temperature dependencies were analyzed in terms of the contribution from spectral diffusion and slow-motional isotropic diffusion (T_m) as well as in terms of energy exchange between the spin system and the lattice (T_1). [M. Kveder *et al.*, Phys. Rev. B *in press*]

P-12

STRUCTURES OF LANTHANUM AND YTTRIUM ALUMINOSILICATE GLASSES

I. Pozdnyakova¹, L. Hennem¹, N. Sadiki², V. Cristiglio^{1,3}, A. Bytchkov⁴, G. Cuello³, J. P. Coutures² and D. L. Price¹

¹ CNRS-CRMHT, 1d avenue de la Recherche Scientifique, 45071 Orléans cedex 2, France

² PROMES, Rambla de la Thermodynamique, Tecnosud, 66100 Perpignan, France

³ ILL, 6 rue Jules Horowitz, BP 156, 38042 Grenoble, France

⁴ ESRF, 6 rue Jules Horowitz, BP 220, 38043 Grenoble, France

Aluminosilicate glasses containing rare-earth element cations such as Y^{3+} and La^{3+} are interesting for a variety of technological applications, as well as for elucidating general principles of glass formation and structure. These glasses have unusually high glass transition temperatures ($\sim 900^\circ\text{C}$), high hardness (~ 8 GPa) and elastic modulus (~ 100 GPa), and good chemical durability.

Rare earth aluminosilicate based glasses have been successfully used as a laser ion hosts, optical lenses, seals, and as in vivo radiation delivery vehicles. Also these glasses, with or without small amounts of alkali modifiers, can be considered as model systems for the study of a potential matrix for the storage of long-lived actinides.

The physical properties of a glass are closely related to its atomic structure. Despite their industrial importance, the information about the structure of Y^{3+} and La^{3+} contained aluminosilicate glasses is not complete.

The combination of neutron and x-ray diffraction can provide structural information at the partial level in glasses and we will present measurements of the local structure in these two systems of glasses using the two techniques. In particular, it was possible to extract detailed structural information including interatomic distances and coordination numbers. The results obtained are in good agreement with previous NMR studies performed on the same compositions.

P-13

THERMAL AND MAGNETIC BEHAVIOR OF COBALT-BASED ALLOYS

A. Rosales-Rivera, M. Gómez-Hermida and P. Pineda-Gómez
Laboratorio de Magnetismo y Materiales Avanzados, Facultad de Ciencias Exactas y Naturales, Universidad Nacional de Colombia, A.A. 127, Manizales, Colombia

A systematic study of the thermal and magnetic behavior of the amorphous $\text{Co}_{80-x}\text{Fe}_x\text{B}_{10}\text{Si}_{10}$ alloy ribbons is presented. The experiments were performed on samples of $\text{Co}_{80-x}\text{Fe}_x\text{B}_{10}\text{Si}_{10}$ with $x = 6, 8$ and 10 , prepared by the melt spinning technique. The thermal behavior was studied using differential scanning calorimetric (DSC) and thermogravimetric analysis (TGA). Six samples of appropriate weight of each of the ribbons were used for thermal analysis. The DSC and TGA runs were performed at various heat rates, $r = 2, 5, 7, 10, 15$ and 20°C , in nitrogen

flow. The structure of the as-cast ribbons was analysed by XRD monochromatized Cu K α radiation, $\lambda = 1.5406\text{\AA}$, in a Rigaku diffractometer. The field (H) dependence of the magnetization, M , of the samples was measured, from -1 to 1 KOe at room temperature, with a vibrating sample magnetometer. The XRD patterns indicate that the as-cast ribbons are amorphous at room temperature. The crystallization kinetics was studied using the *Avrami* model [1]: $\ln(r/T_{\text{per}}) = (E_a/hRT_{\text{per}}) + \text{constant}$, where T_{per} is the primary crystallization temperature, E_a is the activation energy, n is the *Avrami* exponent and R is the ideal gas constant. A value of E_a has been determined for the different samples and it decreases as x increases changing from 3.44 to 3.28 eV. The TGA results confirm the development of the primary and secondary crystallization process of the nanocrystalline phase in $\text{Co}_{80-x}\text{Fe}_x\text{B}_{10}\text{Si}_{10}$ alloy ribbons observed in the DSC experiments. The M vs. H curves exhibit soft magnetic behavior.

[1] M. Avrami, J. Chem. Phys. 7 (1939) 1103; J. Chem. Phys. 9 (1941) 177.

P-14

DIFFUSION PHENOMENA IN NON-CRYSTALLINE OBSIDIAN SAMPLES AND APPLICATIONS IN THE DATING OF ANCIENT OBSIDIAN TOOLS BY SIMS AND FT-IR.

Th. Ganetsos¹, B. Kotsos¹, I. Liritzis², M. Novak³ and N. Laskaris²
¹ Department of Electronics, Techn. Educ. Institute of Lamia, 35100 Lamia, Greece
² Laboratory of Archaeometry, University of Aegean, Dept. of Mediterranean Studies, Rhodes 85100, Greece
³ Evans Analytical, USA

The measurement and use of the hydrating surface layer of obsidian as a chronometric tool in archaeology has gone through a number of improvements over the past two decades. [1,2] The Secondary Ion Mass Spectroscopy is now well established as a surface technique which provides depth profiling, mapping or imaging to be carried out. In this paper we represent a novel software programme, using MATLAB, incorporating all numerical parameters developed for the nuclear dating of hydrated obsidians. SIMS measures the H⁺ concentration (C), versus hydration depth profile. The modelling of this diffusion process is essentially based on the idea that a saturated surface (SS) layer is encountered near the exterior [3]. Examples are given for several archaeological obsidians. Comparison of SIMS-SS method with indirectly dating of similar cultural phases by radiocarbon (¹⁴C) is excellent.

A secondary calibration has also been developed using Infrared Spectroscopy. Total diffused molecular water in the hydration layer used the FT-IR absorbance band at 1630 cm^{-1} and correlated with the concentration-depth H⁺ profile of SIMS. A novel relationship between

SIMS and IR-PAS data provides a linear trend useful in the future dating of obsidian.

- [1] Abrajano, T., Bates, J. and Mazer, J., Journal of Non-Crystalline Solids, **8**, 269-288 (1989).
 [2] C. Stevenson, I. Abdelrehim and S. W. Novak, J. Archaeol. Sci., **28**, 109 (2001)
 [3] Liritzis I., Ganetsos Th. and Laskaris ., Mediterranean Archaeology and Archaeometry, **5**, 1, (2005)

P-15

CRYSTALLIZATION OF KNBO₃ IN A B₂O₃ GLASS NETWORK

R. C. C. Figueira, M. P. F. Graça, L. C. Costa, M. A. Valente
 Physics Department, University of Aveiro, Portugal
 I3N, University of Aveiro, 3810-193 Aveiro, Portugal

Potassium niobate (KNbO₃) is one of the most known ferroelectric crystals. This crystal shows a large number of exceptional electronic and optic properties. It presents high electro-optic and nonlinear optical coefficients and it has been used in optical waveguides, frequency doublers and holographic storage systems. Due to the high preparation difficulties and costs of the single crystals, and associated with their main technological applications, a considerable interest in the preparation of glass-ceramics with the KNbO₃ crystal phase and consequent analysis of their structure, optic and electric properties exist.

In this work we present the preparation of the transparent glass with the molar composition $0.4\text{B}_2\text{O}_3\text{-}0.4\text{K}_2\text{O-}0.2\text{Nb}_2\text{O}_5$ and of the glass-ceramics obtained through controlled heat treatments. The samples microstructures were analyzed using X-ray power diffraction (XRD), Scanning Electron Microscopy (SEM) and Raman spectroscopy. The dc conductivity (σ_{dc}) and ac conductivity (σ_{ac}) measurements, as a function of the temperature were made and discussed.

The heat treatment of the glass at 500°C promotes the crystallization of KNbO₃ single phase. For treatment temperatures above 500°C , others niobate phases are present. The 500°C treated sample shows the larger σ_{dc} which was related with the crystalline particles dispersed in the glass network. The conductivity behaviour depends on the number of charge carriers which are associated with the number of the ions structurally inserted in the glass network. The rise of volume ration between the KNbO₃ particles and the glass matrix was associated to the decrease of the dielectric constant.

P-16

STRUCTURAL STUDY OF UNDOPED AND (MN, IN) DOPED SNO₂ THIN FILMS GROWN BY RF SPUTTERING.

A. Espinosa¹, N. Menéndez², J. Rubio-Zuazo^{1,3}, C. Prieto¹ and A. de Andrés¹

¹*Instituto de Ciencia de Materiales de Madrid, Consejo Superior de Investigaciones Científicas, Cantoblanco, E-28049 Madrid, Spain.*

²*Departamento de Química-Física Aplicada, Universidad Autónoma de Madrid, Cantoblanco, E-28049 Madrid, Spain.*

³*SpLine, European Synchrotron Radiation Facilities, F-38043 Grenoble, France.*

Diluted magnetic semiconducting oxides have been intensively studied in last years because of their potential use in spintronics. However, the origin of ferromagnetism is still unclear and the formation of clusters or secondary phases has not been ruled out yet. In this frame, a structural study is essential in order to understand the mechanisms present in these materials.

We have grown undoped and 5% (Mn,In)-doped SnO₂ thin films deposited onto Si(100) by RF magnetron sputtering. The (Mn,In):SnO₂ and SnO₂ layers were grown at different deposition power (10-90 W), sputtering gas mixture (Ar/O₂ proportion) and substrate temperature (RT and 550°C). X-ray reflectivity was used to determine the films thickness (between 10 and 130nm) and roughness (~5nm). Grazing incidence high-angle X-ray diffraction measurements showed, in doped and undoped films grown at low power and temperature, broad diffraction bands that cannot be originated by nanocrystalline SnO₂ but could be due to small SnO clusters. In order to further investigate the nature of the films, a Mössbauer study of the Sn signal in undoped films evidenced the presence of Sn⁴⁺ in an amorphous environment for as-grown sample and in crystalline SnO₂ for annealed films. As the deposition power, substrate temperature or O₂ proportion are increased, the incipient formation of SnO₂ nanocrystals is detected by diffraction. Nevertheless, transmission electronic microscopy (TEM) images reveal an increase in inhomogeneity with increasing power. No secondary phases or segregation of dopants were detected. The homogeneity of the deposited films grown at low power seem to be relevant regarding magnetic properties.

P-17

STRUCTURAL AND OPTICAL SPECTROSCOPY OF LINBO₃:TM NANOCRYSTALS EMBEDDED IN A SiO₂ GLASS MATRIX

M.P.F. Graça*, M.A. Valente, T. Monteiro, A.J. Neves, M. Peres.
*Physics Department (I3N), Aveiro University,
Campus Universitário de Santiago 3800-193 Aveiro, Portugal*

In this paper we present the preparation, by the sol-gel method, of a transparent SiO₂:Li₂O:Nb₂O₅ gel doped with Tm³⁺. The dried gel was heat treated in air at temperatures between 500°C and 800°C.

The glasses and glass-ceramics were studied by differential thermal analysis (DTA), X-ray powder diffraction (XRD), scanning electron microscopy (SEM). Furthermore, optical studies using photoluminescence (PL), excitation

luminescence (PLE) and Raman spectroscopy's was performed.

X-ray diffraction patterns and Raman spectroscopy show that SiO₂ and LiNbO₃ crystal phases are present in the samples treated at temperatures above 650°C. Besides the SiO₂ and LiNbO₃, NbTmO₄ crystal phase was detected in the sample treated above 750°C. Blue (¹G₄→³F₄), red (¹G₄→³F₄) and near infrared (³H₄→³H₆) intra-4f¹² transitions due to Tm³⁺ ion in the matrix are observed for temperatures above 650°C. The XRD and SEM analysis show that the particles size and number increases with the rise of the HT temperature.

P-18

ASYMMETRIC MAGNETIZATION REVERSAL OF PARTIALLY DEVITRIFIED CO₆₆SI₁₅B₁₄FE₄NI₁ AMORPHOUS ALLOYS.

J. C. Martínez-García, J. A. García, M. Rivas
Departamento de Física de la Universidad de Oviedo, c/ Calvo Sotelo s/n, 33007 Oviedo

Anomalous hysteresis has been observed in annealed Co₆₆Si₁₅B₁₄Fe₄Ni₁ amorphous ribbons consisting of asymmetrically distorted and horizontally shifted loops. Although the magnetic hysteresis loops present remarkable similarities with those produced by exchange bias uniaxial anisotropy, this is discarded as being present in these samples, so the comprehension of the origin of these characteristics is an interesting topic of research. Transmission Electron Microscopy, Selected Area Diffraction and X-Ray Diffraction experiments have been carried out in order to investigate the structural properties of the samples. A very low dilution of nanocrystallites, with sizes of about 20 nm, has been detected coexisting with some bigger crystals around 0.4-0.8 μm. The hysteretical particularities and their evolution with different magnetic treatments is then analyzed as a consequence of the dipolar interaction between the crystalline particles and the residual amorphous matrix.

[1] M. Rivas, J. A. García, M. Tejedor, E. Bertrán and J. G. Céspedes, *J. Appl. Phys.*, *J. Appl. Phys.*, 97 (2005) 023903.

P-19

NANOCRYSTALLIZATION AND FRACTURE CHARACTERISTICS IN CO-BASED RIBBONS

J. A. García^a, J. A. Riba^b, R. Quintana^a and L. Elbaile^a
^a*Depto. de Física, Universidad de Oviedo, c/ Calvo Sotelo s/n, 33007 Oviedo, Spain*
^b*Depto. de Ciencias de los Materiales, Universidad de Oviedo, c/ Independencia 13, 33004 Oviedo, Spain*

Although there are a lot of studies devoted to study the mechanical properties of amorphous materials, the situation is completely different for nanocrystalline materials. In the latest case the research has been mainly focused to study

the hardness and yield strength of these materials but few results have been reported on their fracture behaviour. Recently, some of the authors of this work have made a study about the relaxation and fracture characteristics in Co-based amorphous alloys [1], in which it has been reported a decrease of the plastic flow involved in the fracture when the material is relaxed.

In this work a study of the fracture characteristics of nanocrystalline materials obtained from the amorphous precursor $\text{Co}_{66}\text{Si}_{16}\text{B}_{12}\text{Fe}_4\text{Mo}_2$ by thermal treatments at two different temperatures (slight and well below the crystallization temperature) is presented.

The results show that the nanocrystalline materials obtained at a temperature slight below the crystallization one are very brittle and the plastic flow involved in the fracture process practically disappears. The embrittlement of these nanocrystalline materials are related with the relaxation of the sample due to the thermal annealing and the appearance of Co_2Si , Co_2B and Co_3B phases. In addition, an interesting nanolamellar structure has been observed in this sample.

[1] M. Tejedor, J. A. García, L. Elbaile, J.A. Riba, L. García-Gancedo and R. Quintana, *J. Non-Cryst. Solids* 352 (2006) 5122

P-20

STRUCTURAL EVOLUTION OF METALLIC GLASSES DURING ANNEALING THROUGH IN-SITU SYNCHROTRON X-RAY DIFFRACTION

Eloi Pineda¹, Pere Bruna², Trinitat Pradell¹, Jorge Serrano², Ana Labrador³ and Daniel Crespo²

¹*Departament de Física i Enginyeria Nuclear, ESAB, Universitat Politècnica de Catalunya, Avda. del Canal Olímpic 15, 08860 Castelldefels, Spain*

²*Departament de Física Aplicada, EPSC, Universitat Politècnica de Catalunya, Avda. del Canal Olímpic 15, 08860 Castelldefels, Spain*

³*LLS - BM16, ESRF, 38043-Grenoble, France*

Metallic glasses are promising materials both for fundamental research on the glass transition and crystallization phenomena and for technological applications. The properties of these materials are largely affected by their unstable or metastable structure; different fracture, magnetic or elastic behaviors are observed in the same material as a function of the degree of relaxation of the glassy state or the extent of nanocrystallization. In this work we present a study of the structural evolution in three metallic glass compositions (Al-Fe-Nd, Fe-Zr-B, Fe-B-Nb-Cu). The samples were obtained as ribbons by melt-spinning, their glass stability and crystallization were analyzed by DSC and dilatometry, and their structural changes were recorded by in-situ synchrotron X-ray throughout glass transition and crystallization. The structure factor and the corresponding total radial distribution function were obtained from the X-ray measurements.

The computed total radial distribution functions show no appreciable changes along the different structural changes. . On the contrary, the analysis of the main diffraction peak position allows us to detect structural relaxation, differences in free volume content and the onset of crystallization. The synchrotron results are compared to calorimetric and dilatometric measurements and the structural changes occurred during annealing are determined and described for each alloy. Finally, the sensibility of the experimental data obtained from different sources to detect the onset of the different phenomena is discussed.

P-21

DETECTION OF THE CURIE TRANSITION ON CO-BASED AMORPHOUS ALLOYS BY MEANS OF MICROWAVE ABSORPTION.

H. Montiel¹, G. Alvarez², J. M. Saniger¹ and R. Valenzuela²

¹*Centro de Ciencias Aplicadas y Desarrollo Tecnológico de la Universidad Nacional Autónoma de México, México, D. F. 04510, México.*

²*Instituto de Investigaciones en Materiales de la Universidad Nacional Autónoma de México, México, D. F. 04510, México.*

Microwave power absorption measurements were carried out on as-spun amorphous alloys of nominal composition $\text{Co}_{66}\text{Fe}_{4}\text{B}_{12}\text{Si}_{13}\text{Nb}_{4}\text{Cu}$, prepared by melt-spinning. The Curie temperature (T_c) was investigated by means microwave absorption measurements in an Electron Paramagnetic Resonance (EPR) spectrometer, at frequency of 9.4 GHz (X-Band) and DC magnetic fields (HDC) in the -0.01 to 0.5 T range. The Curie transition temperature was confirmed by magnetometry and permeability measurements. The measuring temperature was varied about T_c in the 300-500 K temperature interval. Two absorptions were observed: a low field absorption (LFA) around zero magnetic field and another one at high dc magnetic field corresponding to ferromagnetic resonance (FMR). The Curie transition was followed by means of the two absorptions. The peak-to-peak linewidth, ΔH_{pp} , of FMR signal exhibited a maximum in the Curie temperature, while LFA signal disappeared at $T > T_c$ when the long-range magnetic order is completely lost. The appearance of LFA signal has been widely accepted as a signature of microwave absorption processes closely related to the magnetization processes leading to saturation [1]. LFA is therefore a sensitive detector of magnetic transitions. This behavior has been observed in a number of magnetic materials. The combination of resonant and non-resonant microwave absorption processes can become a powerful method for characterization of magnetic materials.

[1] H. Montiel, G. Alvarez, M.P. Gutiérrez, R. Zamorano and R. Valenzuela, *J. Alloys Comp.* 369, 141 (2004).

P-22

INFLUENCE OF MN ALLOYING ON THE DEVITRIFICATION PROCESS OF COFEMNNBB ALLOYS

M. Millán, J.S. Blázquez, C.F. Conde, A. Conde
*Dpto. Física de la Materia Condensada, ICMSE-CSIC,
 Universidad de Sevilla, P.O. Box 1065, 41080, Sevilla, Spain.*

Effects of Mn addition on the devitrification process and resulting microstructure of CoFeNbB HITPERM-type alloys are reported. As cast and heat treated samples (at different crystallization stages) were studied by different experimental techniques and results are correlated. The amorphous character of as cast alloys, produced by planar flow casting, was checked by X-ray diffraction and transmission electron microscopy. Calorimetric data show that the devitrification process takes place in three stages. The first stage, corresponding to a primary crystallization, gives place to a nanocrystalline microstructure where bcc α -FeCo type nanocrystals, about 5 nm in size, are embedded in a residual amorphous matrix. The crystalline fraction reaches ~50-60 % at the end of this transformation. Kinetics of this nanocrystallization process can be described by an isokinetic approach. After the second calorimetric transformation, related to the formation of intermetallic phases, the alloys became fully crystallized. Mn addition does not significantly affect the thermal stability of the amorphous but reduces that of the nanocrystalline alloy and changes the subsequent transformation stages.

Mössbauer spectra were taken at room temperature. For amorphous alloys the spectra are quite similar. A bimodal distribution of the magnetic hyperfine field can be observed and characterized by two overlapped peaks. For nanocrystalline samples, hyperfine parameters of the crystalline phase remain almost constant for different crystalline fractions. Therefore, the composition of the nanocrystals is expected to be constant along the nanocrystallization process. The influence of the Mn addition in these alloys seems to be influenced by their high Co content.

P-23

ANALYSIS OF THE MECHANICALLY ALLOYED FE85-NB5-B10 POWDER USING A NON UNIQUE LATTICE PARAMETER

J.J. Ipus¹, J.S. Blázquez¹, A. Conde*¹, M. Krasnowski², T. Kulik²
¹*Dpto. Física de la Materia Condensada, ICMSE-CSIC,
 Universidad de Sevilla, P.O. Box 1065, 41080, Sevilla, Spain.*
²*Faculty of Materials Science and Engineering, Warsaw
 University of Technology, ul. Woloska 141, 02-507, Warsaw,
 Poland.*

Nanostructured Fe₈₅Nb₅B₁₀ alloy was prepared by mechanical alloying from elemental powders. The evolution of the milled material against milling time was studied by X-ray diffraction (XRD), Mössbauer spectrometry (MS), differential scanning calorimetry

(DSC), scanning electron microscopy (SEM) and energy dispersive X-ray analysis (EDX). After milling process, a supersaturated bcc Fe(Nb,B) solid solution was found and no amorphous phase was detected. Due to the asymmetry of the diffraction maxima and the non homogeneous composition of the powder particles observed by EDX, a distribution of bcc Fe lattice parameter (from 0.2866 to 0.2896 nm) was proposed to fit the diffraction patterns using whole powder pattern decomposition procedure (Pawley method). The crystal size, *D*, of the pure α -Fe contribution was always found larger than 12 nm, whereas contributions with a larger lattice parameter correspond to smaller than 15 nm. The Average value of *D* decreased with milling time from 29 down to 7 nm. For each milling time studied, there are no significant changes between the microstrain of the different bcc Fe contribution and the maximum value calculated from assigning the experimental width only to the microstrain of a single contribution. The asymmetry of MS absorption lines and the appearance of hyperfine magnetic field contributions below 33 T confirm the progressive incorporation of Nb and B impurities into the bcc Fe lattice.

P-24

WITHDRAWN

P-25

TRANSPORT PROPERTIES NEAR THE MAGNETO/STRUCTURAL TRANSITION OF Tb₅Si₂Ge₂

A.M.Pereira¹, M.E. Braga¹, P.A. Algarabel², L.Morellon^{2,3}, C. Magen⁴, R. Fermento¹, M.R.Ibarra^{2,3}, J.P. Araújo¹ and J.B. Sousa¹,
¹*IFIMUP unit and Physics Department of FCUP, University of
 Porto, R. Campo Alegre 687, 4169-007 Porto, Portugal;*
²*Instituto de Ciencia de Materiales de Aragón, Universidad de
 Zaragoza and Consejo Superior de Investigaciones Científicas,
 50009 Zaragoza, Spain*
³*Instituto de Nanociencia de Aragón, Universidad de Zaragoza,
 50009 Zaragoza, Spain*
⁴*Oak Ridge Natl Lab, High Temp Mat Lab, Oak Ridge, TN 37831
 USA*

The R₅(Si_xGe_{1-x})₄ (with R=Rare earth) is under intensive studies due to their interesting magnetic effects, namely the Giant Magnetocaloric Effect (MCE), Colossal Magnetostriction (MS) and Large Magnetoresistance (MR) [1].

These effects are related with a magneto-structural transition usually fully coupled with a 1st-order structural transition (martensitic-like transformation) from an orthorhombic O(I) to a monoclinic (M) phase, coupled to a magnetic transition from ferromagnetic (FM) to paramagnetic (PM).

In the Tb₅Si₂Ge₂ compounds an incomplete coupling between structural and magnetic transition was observed, occurring first the magnetic transition followed a few degrees later (on cooling) by the structural transition. Note

that both transitions can be coupled when pressure is applied [2].

The temperature (T) dependence of the electrical resistivity $\rho(T)$ and thermopower $S(T)$ will be here analysed in the context of existing s-f scattering models. Information is obtained on parameters such as the s-f exchange constant, the Fermi level energy EF, and the effect of spin disorder and phonon scattering on the transport properties. Experiments suggest the possible existence of an extra contribution in Tb5Si2Ge2, besides that arising from s-f scattering, with origin on the structural transition [Si(Ge)-Si(Ge) covalent bond]. Finally, the critical behaviour of dS/dT and $d\rho/dT$ near the Curie point and the structural point will be investigated in detail on Tb5Si2Ge2.

[1] V.K. Pecharsky and K.A. Gschneidner Jr., Adv. Mater. 13, 683 (2001).

[2] L. Morellon, Z. Arnold, C. Magen, C. Ritter, O. Prokhnenko, Y. Skorokhod, P. A. Algarabel, M. R. Ibarra, and J. Kamarad, Phys. Rev. Lett. 13, 93 (2004)

P-26

QUANTUM SPIN-RESONANT TUNNELING IN MAGNETIC JUNCTIONS WITH A DOUBLE-SPACER STRUCTURE

H. Silva^{1,2}, Y. Pogorelov¹

¹IFIMUP-IN, Universidade do Porto, Porto 4169-007, Portugal

²CEOT, Universidade do Algarve, Faro 8005-139, Portugal

We study the quantum-coherent conduction in a junction with thin nonmagnetic (NM) metallic layer between insulating (I) barrier and ferromagnetic (FM) electrode, FM₁/NM/I/FM₂ [1,2], using the tight-binding model. In the simplest 1D single-band approach, the system is seen as a combined atomic chain, whose quantum state with energy ϵ and spin σ is $|\psi_{\epsilon,\sigma}\rangle = \sum_{l=-\infty}^{\infty} \psi_l^\sigma |l, \sigma\rangle$. Here $|l, \sigma\rangle$ is l th atomic state, and amplitudes obey equations of motion $(\epsilon - \epsilon_l^\sigma) \psi_l^\sigma = t_{l,l+1} \psi_{l+1}^\sigma + t_{l,l-1} \psi_{l-1}^\sigma$. The on-site energies and hopping parameters are defined within finite NM elements, the gate (g) and barrier (b), as: $\epsilon_l^\sigma \equiv \epsilon_g$, $t_{l,l+1} \equiv t_g$ ($l = 1, \dots, n - 1$) and $\epsilon_l^\sigma \equiv \epsilon_b$, $t_{l,l+1} \equiv t_b$ ($l = n, \dots, n + m - 1$), and within semi-infinite FM elements, the source (s) and drain (d), as: $\epsilon_l^\sigma \equiv \epsilon_s + \sigma\Delta$, $t_{l,l+1} \equiv t_s$ (at $-l = 0, 1, \dots$) and $\epsilon_l^\sigma \equiv \epsilon_d$, $t_{l,l+1} \equiv t_d$ ($l = n + m + 1, \dots$). The interface hoppings are $t_{0,1} \equiv t_{sg}$, $t_{n,n+1} \equiv t_{gb}$, $t_{n+m, n+m+1} \equiv t_{bd}$. Then the spin-dependent transmission coefficient:

$$T_{\sigma,\sigma}(\epsilon) = \frac{2i(t_{sg}t_{gb}t_{bd}/t_d)\sin q_\sigma^s}{t_g t_b (u_m^b - u_{m-1}^b \gamma_\sigma^{db}) (u_n^s - u_{n-1}^s \gamma_\sigma^{sg}) - t_{gb}^2 (u_{m-1}^b - u_{m-2}^b \gamma_\sigma^{db}) (u_{n-1}^s - u_{n-2}^s \gamma_\sigma^{sg})} \quad (1)$$

with $u_l^i = \sin(l+1)q_i/\sin q_i$, $\gamma_\sigma^{ij} = \exp(iq_i^\sigma) t_{ij}^2 / (t_i t_j)$, and $\cos q_i^\sigma = (\epsilon - \epsilon_i^\sigma) / 2t_i$, reveals n strong resonances in ϵ when ϵ_g is set only slightly below the Fermi energy in FM elements. This suggests that, instead of common choice of

copper for NM gate layer, an optimum material should be rather sought among semiconductors (Ge, Si) or semimetals (Sb, As).

[1] J. S. Moodera *et al.*, Phys. Rev. B **40**, 11980 (1989).

[2] J. J. Sun and P. P. Freitas, J. Appl. Phys. **85**, 5264 (1999).

P-27

MAGNETOCALORIC EFFECT IN NANO- AND POLYCRYSTALLINE LA_{0.8}SR_{0.2}MNO₃ MANGANITES

M. Pękała¹, V. Drozd^{1,2,3}

¹Department of Chemistry, Warsaw University, Al. Zwirki i Wigury 101, 02-089 Warsaw, Poland

²Department of Chemistry, Kiev National Taras Shevchenko University, 60 Volodymyrska st, Kiev, 01033 Ukraine

³Center for Study Materials at Extreme Conditions, Florida International University, Miami, USA

La_{0.8}Sr_{0.2}MnO₃ samples were prepared by two wet-chemistry methods. Sol-gel method [1] started from La₂O₃, Sr(NO₃)₂ and MnCO₃ reagents which were dissolved in diluted nitric acid at continuous stirring and moderated heating. Gelation agent, monohydrate of citric acid, was added together with ethylene glycol. The molar ration metals: citric acid: ethylene glycol was 1:10:10. The obtained solution was evaporated on a hot plate till homogeneous gel-like product was formed which was decomposed at 300oC in air.

Nanocrystalline La_{0.8}Sr_{0.2}MnO₃ powder (LSM-nano) was produced by calcination of sol-gel precursor at 600oC for 12h in air atmosphere. Sintering of this precursor at 1100oC for 48 h with intermediate grinding lead to polycrystalline La_{0.8}Sr_{0.2}MnO₃ sample (LSM-1100oC). Another polycrystalline sample (LSM-1250oC) was prepared by coprecipitated carbonate precursor method at 1250oC. The polycrystalline as well as the nanocrystalline samples of La_{0.75}Ca_{0.25}MnO₃ manganites are single phase and have the rhombohedral perovskite crystal structure.

The temperature dependence of the AC magnetic susceptibility was measured at 1 mT amplitude. The temperature variation of the field-cooled (FC) and zero-field-cooled (ZFC) magnetization was registered at magnetic fields of 0.01 and 0.03 T. The DC magnetization isotherms were recorded in magnetic fields up to 2 T.

The magnetocaloric effect in this nanocrystalline manganite is spread over a broader temperature interval than in the polycrystalline case. The relative cooling power of the poly- and nanocrystalline manganites is used to evaluate a possible application for magnetic cooling below room temperature. The structural and magnetocaloric results are compared to similar systems.

P-28

MAGNETIC PROPERTIES OF COMPACTED CAMNO_{3,8} NANOPARTICLES

V. Markovich¹, I. Fita^{2,3}, R. Puzniak², A. Wisniewski², D. Mogilyansky¹, L. Titelman¹, L. Vradman¹, M. Herskowitz⁴ and G. Gorodetsky¹

¹Department of Physics & Department of Chemical Engineering, Ben-Gurion University of the Negev, 84105 Beer-Sheva, Israel

²Inst. of Physics, Polish Academy of Sciences, Warsaw, Poland

³Donetsk Institute for Physics & Technology, National Academy of Sciences, 83114 Donetsk, Ukraine

⁴Blechner Center for Industrial Catalysis & Process Development, Department of Chemical Engineering, Ben-Gurion University of the Negev, 84105 Beer-Sheva, Israel

Magnetic properties of compacted 50 nm CaMnO₃ nanoparticles, prepared by citrate method, have been investigated in temperature range 5 – 320 K, magnetic field up to 90 kOe and under quasi-hydrostatic pressures up to 11 kbar. Measurements of ac-susceptibility exhibit upon cooling two magnetic transitions: at $T \sim 270$ K accompanied by a small spontaneous magnetic moment and a para-antiferromagnetic (AFM) transition at $T_N \sim 120$ K, observed previously in bulk CMO. It was found that an applied pressure enhances T_N with a pressure coefficient of $dT_N/dP \approx 0.5$ K/kbar, in similarity with results for the bulk [1]. Asymmetric magnetization hysteresis loops observed at applied magnetic fields $H \leq 90$ kOe are attributed to an exchange coupling between AFM core and the ferromagnetic (FM) shell of the CMO nanoparticles. An examination of these hysteresis loops reveals the existence of a large effective anisotropy, as indicated by a large coercive field H_C (~ 15 kOe at $T = 5$ K) and a very large irreversibility field ($H_{irr} \sim 70$ kOe at 5 K), below which the decreasing and increasing branches of the magnetization loop separate. A very high H_{irr} may be attributed to the spin-glass like phase. This work provides a verification for exchange bias effect in manganite nanoparticles with inverted AFM-core/FM-shell structure, as compared to the typical FM-core/AFM-shell. Effects of surface magnetism and exchange anisotropy are also discussed.

[1] V. Markovich et al., Phys. Rev. B 70, 024403 (2004).

P-29

THE EFFECT OF CHEMICAL DISTRIBUTION ON ESTIMATING THE MAGNETOCALORIC EFFECT FROM MAGNETIC MEASUREMENTS

J.S. Amaral¹, N.J.O. Silva¹ and V.S. Amaral¹

¹Departamento de Física da Universidade de Aveiro and CICECO, Aveiro, Portugal

The magnetocaloric effect is a property common to all magnetic materials and can be directly measured in adiabatic conditions, by the change of temperature of the magnetic sample by variations on applied field, ΔT_{ad} . Alternatively, the indirect estimation of the isothermal magnetic entropy change ΔS_M can be made either from specific heat or magnetization measurements [1]. The

estimation of ΔS_M from magnetization measurements, from the integration of a Maxwell relation has been questioned for the case of 1st-order transition materials [2],[3]. In this work we discuss the effect of chemical inhomogeneity on estimating the magnetocaloric effect from magnetic measurements, by results from the molecular mean-field model and estimating ΔS_M from either the inverse-Brillouin function [4] or the typical Maxwell relation integration, in the case of 2nd and 1st-order (in mixed and non mixed-phase conditions) phase transitions.

[1] Pecharsky, V.K. and K.A. Gschneidner, J. Appl. Phys., 1999. **86**(1): p. 565-575.

[2] Giguere, A., et al., Phys. Rev. Lett, 1999. **83**(11): p. 2262-2265.

[3] Liu, G.J., et al., Appl. Phys. Lett. 2007. **90**(3): p. 032507-1-032507-3.

[4] Amaral, J.S., N.J.O. Silva, and V.S. Amaral, Appl. Phys. Lett., 2007. **91** (17): p. 172503-172506.

P-30

MAGNETIC AND MECHANICAL PROPERTIES FECONBB AMORPHOUS RIBBONS

I. Betancourt and R. Landa

Departamento de Materiales Metalicos y Ceramicos, Instituto de Investigaciones en Materiales, Universidad Nacional Autonoma de Mexico, Mexico D.F. 04510, Mexico.

Fe-M-B-type amorphous alloys (M=Nb, Zr, Hf; commercially known as Nanoperm © TM) have been subject of research since their discovery during the mid 90's [1], due to their excellent combination of soft magnetic properties, such as large magnetic permeability and saturation magnetization values, together with small magnetostriction coefficients [1]. For these alloys, significant boron increments (up to 30 at%) has shown to be effective in increasing their Curie temperature as well as their glass forming ability [2]. In this work, we present the effect of cobalt addition on the mechanical and on the magnetic properties of FeNbB-base amorphous ribbons.

The alloy series Fe52-xCo10+xNb8B30 (x= 0,12, 24,36) was prepared by means of melt spinning technique with a roll speed of 30 m/s. The amorphous state for all the alloy samples was confirmed by XRD. The alloys Vickers microhardness showed high values (between 1539-1644) for the whole composition series. On the other hand, the saturation magnetization decreased monotonically from 125 emu/g to 50 emu/g with increasing Co concentration, as well as the Curie temperature, with a marked reduction from 362oC to 177oC. High initial ac permeability values (between 1500 and 7500) were observed for the alloy series, together with relaxation frequencies within the range 2-7 kHz, which were associated to reversible bulging of magnetic domain walls. In addition, a low frequency magnetoimpedance effect ($\sim 5\%$) was also detected for the whole alloy series, thus rendering these alloys as a potential material candidate for sensor applications under wear conditions at intermediate temperatures.

- [1] M.E. McHenry, M.A. Willard, D.E. Laughlin, Prog. Mater.Sci. 44 (1999) 291
 [2] T.Gloriant, S. Suriñach, M.D. Baro, J.Non-Cryst. Sol. 333 (2004) 320

P-31

DIELECTRIC, MORPHOLOGICAL AND THERMIC PROPERTIES OF TERNARY MELT-BLEND PROCESSING

C. R. Martins¹, C. P. L. Rubinger², L. C. Costa^{2,3}, R.M. Rubinger^{2,4}

¹ Chemistry Engineer Department, University of São Paulo 05424-970, SP, Brazil

² Physics Department, University of Aveiro, Portugal

³ I3N, University of Aveiro, 3810-193 Aveiro, Portugal

⁴ Physics and Chemistry Department, Institute of Science, Federal University of Itajubá, CP 50, 37500-903 Itajubá, MG, Brazil

Conductive ternary blends of polystyrene (PS), styrene-butadiene-styrene (SBS) block copolymer and doped polyaniline (PAni) were prepared in an internal mixer. The doping agents of PAni were dodecylbenzene sulfonic acid (DBSA) and polystyrene sulfonic acid (PSS). We prepared a series of PS/SBS/PAni blends with the different PAni content as 30, 40 and 50 %. The content of SBS for the studies samples was 6%. We investigated dielectric properties by impedance spectroscopy in the frequency range from 10 Hz to 100 kHz. At low frequency, the real part of impedance is reduced from 26 M Ω to 2 M Ω with the increasing of PAni concentration (Figure 1). From the impedance spectroscopy fittings we obtained the relaxation strength, the depression angle and the relaxation time. The morphological characteristics of the materials were studied by scanning electron microscopy (SEM), which suggests that the presence of SBS improves the compatibility and homogeneity of the blends. The miscibility of the blends components were evaluated by differential scanning calorimetry (DSC) and the degradation by termogravimetry (TGA). We observed that the PS/SBS/PAni blends presented the same weight loss, independent of the doped-PAni concentration.

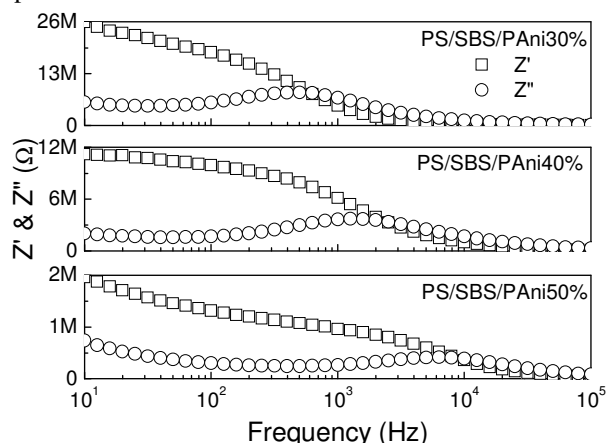


Figure 1- Impedance spectroscopy for different samples.

P-32

THE STABILITY OF THE MAGNETIC DOMAINS INSIDE THE CORE OF AMORPHOUS METAL WIRE.

A.A Gavriiliuk^a, A.Yu. Mokhovikov^a, A.V. Semirov^b, A.L. Semenov^a, N.V. Turik^a, V.O. Kudrewcev^b

^aIrkutsk State University, Irkutsk, Russia

^bIrkutsk State Teacher's Training University, Irkutsk, Russia

It was estimated the size of the stable domain inside the core of amorphous metal wire without applying magnetic field. The wire diameter is about 100-150 μm . The size of the stable domain inside the core was calculated by the means the minimum of the sum of the energy of domain walls, energy of transition region between the core and shell of the wire, magnetostatic domain energy and energy of domain collapse. The following possible forms of the domain were considered: domain, which consisted of two cones; domain, which had the cylindrical shape without tops; domain, which consisted of the cylindrical region and two conical domains tops; domain, similar to ellipsoid of rotation. It was shown that the least sizes inside the wire core have the domain, similar to the ellipsoid of rotation. It has 30-60 μm radii. The domain, which consisted of two cones, is the most energetically unprofitable case. The stable radii of these domains exceed the wire's radii. It has 100-300 μm . The size of the stable domain was determined by the coercitivity of the domain walls and domain demagnetization factor as well. Analysis results according to the experimentally viewed domain structure of the core of amorphous metal wire. According to the received results, it was explained the decreasing of the residual induction due to decreasing of wire length.

P-33

MAGNETIC AND TRANSPORT STUDIES OF THE α - σ TRANSFORMATION IN AN $\text{Fe}_{50}\text{V}_{50}$ ALLOY

B.F.O. Costa¹, V.S. Amaral², G. Le Caër³, M.E.Braga⁴, M.M. Amado⁴, and J.B. Sousa⁴

¹ CEMDRX, Department of Physics, University of Coimbra, P-3004-516 Coimbra, Portugal

² Departamento de Física, Campus de Santiago, Universidade de Aveiro, P-3810-193 Aveiro, Portugal

³ Institut de Physique de Rennes, UMR URI-CNRS 6251, Université de Rennes I, Campus de Beaulieu, Bâtiment 11A, F-35042 Rennes Cedex, France

⁴ IFIMUP and DFUP, Rua do Campo Alegre, 687, P-4169-007 Porto, Portugal

The hard and brittle sigma phase forms at elevated temperature in various alloy systems involving transition elements. The sigma phase forms in FeV alloys in wide temperature and composition ranges. At high temperature, the equiatomic FeV alloy may transform into a metastable ordered phase having a B2 type structure prior to the

formation of the sigma phase. In previous studies [1], the decrease of the electrical resistivity in a Fe₅₀V₅₀ alloy with holding temperatures at 1015K and 1115K was attributed to the ordering of the alpha phase, namely the formation of a transient B2 structure, in agreement with literature results [2-4]. However, it was suggested that an electrical resistivity of the sigma phase lower than that of the alpha phase at high temperature might contribute to or even account for the observed decrease of resistivity.

In the present work, the resistivity of the sigma phase was measured during a heating-cooling cycle (up to 1000K). The resistivity decreases when heating but remains essentially constant when cooling down to room-temperature (RT).

Magnetization measurements from RT down to 50K were performed for samples previously heated and cooled in cycles up to 1015K and 1115K, in order to find out whether these phenomena are associated to an ordering of the alpha phase or to an ordering of the sigma phase.

[1] B.F.O. Costa, M.E. Braga, M.M. Amado, J.B. Sousa, G. Le Caër and V.S. Amaral, IV International Materials Symposium, Porto, Portugal, Abril de 2007, (abstract book, pp. 180).

[2] R.J. Chandross and D.P. Shoemaker, J. Phys. Soc. Japan, **17** supp B-III (1962) 16-20.

[3] M. Daire, Compt. Rend., **259** (1964) 2640-2646.

[4] J. Seki, M. Hagiwara and T. Suzuki, J. Mater. Sci., **14** (1979) 2404-2411; J.M. Sanchez, M.C. Cadeville, V. Pierron-Bohnes and G. Inden, Phys. Rev. B, **54** (1996) 8958-8961; T. Ziller, G. Le Caër, O. Isnard, P. Cénédès and B. Fultz, Phys. Rev. B, **65** (2002) 024204

P-34

CALCULATING GIANT MAGNETOIMPEDANCE IN ARBITRARY SHAPES

S. Sarkarati, M. H. Khaksaran, M. M. Tehranchi and S. M. Mohseni

Laser Research Institute, Shahid Beheshti Univ., Tehran, Iran

A fast algorithm for calculating magnetoimpedance ratio is introduced. It is based on solving reduced Maxwell equation and Landau-Lifshitz equation simultaneously. The skin effect in this method is considered by finding current distribution. The algorithm is applied on 2D and 3D shapes. A good advantage with experimental results is obtained.

P-35

ROOM TEMPERATURE FERROMAGNETISM WITH GIANT MAGNETIC MOMENT IN FE:ZNO

L.M.C. Pereira^{1,2,4}, J.P. Araújo^{1,2}, U. Wahl^{3,4}, J.G. Correia^{3,4,5}

¹Faculdade de Ciências da Universidade do Porto, Portugal

²Instituto de Física de Materiais da Universidade do Porto, Portugal

³Centro de Física Nuclear da Universidade de Lisboa, Portugal

⁴Instituto Tecnológico e Nuclear, Portugal

⁵CERN-PH, Switzerland

Dilute Magnetic Semiconductors (DMS) are seen as strong candidates to make use of the spin of carriers in spintronic devices. In this respect, experimental results and theoretical calculations have been drawing interest towards 3d transition metal doped oxide semiconductors. The room temperature ferromagnetism (FM) observed in some of these systems is however far from being completely understood.

Some preliminary results on magnetic characterization by SQUID magnetometry are presented, which unambiguously evidence a ferromagnetic state of Fe ion-implanted ZnO ($5 \times 10^{15} \text{ cm}^{-2}$ at 60keV and 800°C post-annealed) over the 5-300K investigated range. Moreover, the ferromagnetic hysteresis shows a giant (saturation) moment of $\sim 7.5 \mu\text{B}$ per implanted Fe (higher than the spin-only value). This behaviour has recently been observed in other DMS systems and is generally attributed to unquenched orbital contributions and/or to magnetic polarization of the (non-magnetic) matrix atoms. While both these hypothesis remain proven, we propose the alternative explanation that the magnetic moments of some point defects (massively produced during implantation) and those of the magnetic impurities couple ferromagnetically when sitting close to each other. Such a mechanism may not only explain the observed giant moment but also the stabilization of the FM state by means of percolation chains. The formation of such magnetically coupled impurity-defect complexes is further supported by the electron emission channelling (EC) results, as the co-implanted radioactive ⁵⁹Fe was located not in the perfectly substitutional Zn site but displaced by a few tenths of Å towards the *nn* and *nmn* Zn sites.

The proposed defect-related magnetic order is an attractive hypothesis also for an explanation of ferromagnetism under other preparation conditions of ZnO based DMSs as well as in others and it challenges present concepts for a theoretical modelling of room temperature ferromagnetism.

P-36

ANGULAR DEPENDENCE OF FERROMAGNETIC RESONANCE IN AMORPHOUS CO-RICH RIBBONS

E. M. Mata-Zamora¹, H. Montiel¹, G. Alvarez², J. Saniger¹, and R. Valenzuela²

¹Centro de Ciencias Aplicadas y Desarrollo Tecnológico UNAM, ²Instituto de Investigaciones en Materiales UNAM, 04510 México D. F., México.

Ferromagnetic resonance was investigated in as-cast amorphous ribbons of Vitrovac 6025, at microwave frequency of 9.46 GHz (X-band) in two orientations. When varying the angle θ , between the ribbon plane and the dc magnetic field (orientation 1), the resonance field (H_{res}) and the peak-to-peak linewidth (H_{pp}) showing a large increment when increasing θ from 0° to 180°. On the orientation 2 varying the angle ϕ in ribbon plane, the H_{res}

exhibited only very small variations as a function of the angle between the dc field and the ribbon axis. These results showed the difference between shape anisotropy (the energy needed to move the magnetization out of the plane) and induced anisotropy (creation of an in-plane easy axis perpendicular to the ribbon axis).

P-37

PHOTO AND ELECTROLUMINESCENCE BEHAVIOR OF TB(ACAC)₃PHEN COMPLEX USED AS EMISSIVE LAYER ON ORGANIC LIGHT EMITTING DIODES

L. Rino¹, W. Simões¹, G. Santos², F.J. Fonseca², A.M. Andrade³, V.A.F. Deichmann⁴, L. Akcelrud⁴, L. Pereira¹

¹Departamento de Física e I3N – Instituto de Nanoestruturas, Nanofabricação e Nanomodulação, Univ. de Aveiro, Portugal

²Laboratório de Microeletrônica, Departamento de Engenharia de Sistemas Eletrônicos, Escola Politécnica da Universidade de São Paulo, Av. Prof. Luciano Gualberto, trav. 3, n° 380, CEP 05508-900, São Paulo – SP, Brasil

³Instituto de Eletrotécnica e Energia – Universidade de São Paulo, 05508-900 São Paulo, Brasil

⁴Laboratório de Polímeros Paulo Scarpa, Departamento de Química, Centro Politécnico da UFPR – Universidade Federal do Paraná, CP 19081, CEP 81531-900 Curitiba, Paraná – PR, Brasil

Electroluminescence devices of organic materials are promising candidates for the next generation flat panel displays (OLED's). A good device implies a material with high photoluminescence efficiency. Rare earths complexes are actually good candidates, in special those based on europium and terbium. Although the photoluminescence properties of those lanthanide complexes have been discussed, some questions remain unclear, in special those related to the influence of the organic ligands in the energy transfer. This question is one of the most important to be addressed when that materials are used develop electroluminescence devices. In this work, the temperature a photoluminescence property of Tb(ACAC)₃phen is studied. The results shows clearly the ⁵D₄ → ⁷F_{3,4,5,6} transitions with no influence of any ligand emission. The photoluminescence excitation spectrum in the near-UV and visible region, exhibits differences with temperature, that are tentatively attributed to the ion and ligands absorption. With these results, multilayered OLEDs was made by thermal evaporation (total thickness of 100 nm) using TPD and Alq₃ as hole and electron transport layers, respectively. The light emission reproduces the photoluminescence spectrum of the terbium complex at room temperature, with x,y CIE color coordinates of (0.28, 0.55). No presence of any bands from the ligands was observed. The potential use of this compound in efficient devices is discussed.

P-38

MICROWAVE POWER ABSORPTION ANALYSIS OF THE DEVITRIFICATION PROCESS OF CO-BASED AMORPHOUS RIBBONS

R. Valenzuela^a, H. Montiel^b, R. Zamorano^c and G. Alvarez^a
^aDepartamento de Metálicos y Cerámicos, Instituto de Investigaciones en Materiales, Universidad Nacional Autónoma de México, México, D. F. 04510, México.

^bCentro de Ciencias Aplicadas y Desarrollo Tecnológico, Universidad Nacional Autónoma de México, D. F. 04510, México.

^cEscuela Superior de Física y Matemáticas del Instituto Politécnico Nacional, México, D. F. 07738, México.

Melt-spun Co₆₆Fe₄B₁₂Si₁₃Nb₄Cu soft magnetic ribbons were devitrified at low annealing temperatures (623 K), for annealing times, t_{ann} , of 5,10, 15 and 20 minutes. Microwave power absorption measurements at 9.4 GHz were carried out in two orientations. In both cases, the ribbon plane was parallel to DC magnetic field. In orientation 1, the ribbon plane was oriented parallel to the AC magnetic field. For orientation 2, the ribbon plane was normal to the AC magnetic field. In orientation 1, for all the samples, a single FMR spectrum was observed with small shifts in resonant field as a function of t_{ann} . For orientation 2, in the as-cast sample, a single FMR was observed. In contrast, for all the annealed samples, a new resonant absorption to a slightly lower magnetic field was superimposed to the original resonance. This result indicated that the FMR spectra are due to the combination of two different magnetic phases. Deconvolution calculations were carried out on FMR spectra to separate the contributions of these two phases, which can be attributed to the nanocrystallites and the amorphous matrix, respectively. Finally, the differences in microwave absorption for both orientations, which depend essentially on the cross-section of ribbon exposed to the AC field, can be explained by differences in the electromagnetic wave propagation volume.

P-39

THE INFLUENCE OF LASER ANNEALING IN THE PRESENCE OF LONGITUDINAL WEAK MAGNETIC FIELD ON ASYMETRICAL MAGNETOIMPEDANCE RESPONSE OF COFESIB AMORPHOUS RIBBONS

M. Ghanaatshoar¹, N. Nabipour¹, M. M. Tehranchi^{1,2}, S. M. Hamidi¹, S. M. Mohseni¹

1. Laser and plasma Research Institute, Shahid Beheshti University, Evin, 1983963113 Tehran, Iran

2. Physics Department, Shahid Beheshti University, Evin, 1983963113 Tehran, Iran

Asymmetrical magnetoimpedance (AMI) is very important to further improve micromagnetic sensor performance in terms of linearity and sensitivity. This behavior was investigated for Co_{68.15}Fe_{4.35}Si_{12.5}B₁₅ amorphous ribbons irradiated by a 1064 nm Nd:YAG pulsed laser in air and in the presence of 3 Oe longitudinal magnetic field with alternating pulse repetition rates. Each pulse after passing through BK7 cylindrical lens, illuminated two third of middle part of the ribbons. Results indicate that for

different pulse repetition rates, various types of AMI profiles appear. This diversity is particularly related to peaks number. For samples annealed in the presence of longitudinal field, because of induced anisotropy, more peaks in the magnetoimpedance profile occur and changing in asymmetry factor takes place (we defined the asymmetry factor as the difference between peaks value of impedance at right and left side of external magnetic field axis). The asymmetry factor of the sample annealed at repetition rate of 10 Hz is lower than that of samples annealed at 1 and 5 Hz. According to figure 1, appearance of dense protrusions on the surface of sample annealed at 10 Hz repetition rate, can be responsible for the perpendicular anisotropy which leads to a decreasing in asymmetry factor. Variation of MI_{max} and field sensitivity after field annealing can also be observed.

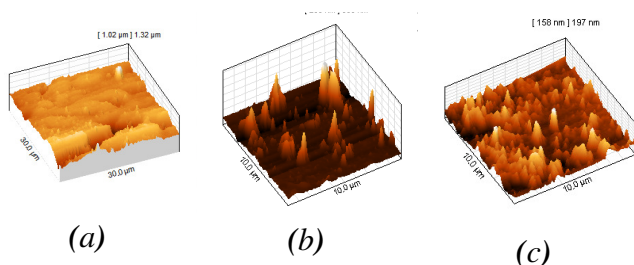


Fig. 1: Topography of the annealed samples at repetition rates: (a) 1 Hz, (b) 5 Hz and (c) 10 Hz.

P-40

MAGNETO-OPTICAL KERR EFFECT IN GLASS/CU/COFESIB/SNO₂ THIN FILMS

M. Ghanaatshoar¹, M. Moradi¹, M. M. Tehrani^{1,2}, S. M. Hamidi¹

1. Laser and plasma Research Institute, Shahid Beheshti University, Evin, 1983963113 Tehran, Iran
2. Physics Department, Shahid Beheshti University, Evin, 1983963113 Tehran, Iran

The magneto-optic Kerr effect (MOKE) is of interest for the development of magnetic recording media [1]. MOKE is also very important in the magnetic semiconductors [2]. It combines the magnetic and optical properties of the materials together, which will extend the application areas of the magnetic semiconductors. In this work, we report the Kerr signal (KS) enhancement due to the capping effect of SnO₂ on the CoFeSiB amorphous ferromagnetic layer. Thin films and multilayers of magnetic alloys are suitable for miniaturized magnetic sensors due to their integrability with microelectronic components. SnO₂ is a wide band gap semiconductor with excellent optical transmission in the visible and ultraviolet regions.

CoFeSiB layers were prepared by pulsed laser deposition. Targets of CoFeSiB ferromagnetic amorphous ribbons were ablated in evacuated condition by Nd:YAG laser pulses. X-ray diffraction patterns confirmed the amorphous nature of studied films. Then SnO₂ layers with various thicknesses

were deposited by electron beam evaporation on magnetic layers. All samples were deposited onto coated glass substrate with Cu buffer layer. The magnetic behavior of the samples was investigated by polar and longitudinal magneto-optical Kerr effect at room temperature. As the SnO₂ thickness increases up to about 70 nm, the KS increases and then decreases. The results were analyzed using the formalism based on the matrix method.

[1] B.M. Lairson, B.M. Clemens, *Appl. Phys. Lett.* 63 (1993) 1438.

[2] N. Akdogan and et al, *J. Magn. Magn. Mater.*, 300 (2006) e4–e7.

P-41

ANOMALOUS MAGNETIC PROPERTIES IN Fe₇₈Si₉B₁₃ THIN FILMS

S. M. Hamidi¹, M. M. Tehrani^{1,2}, M. Ghanaatshoar¹, M. Moradi¹, S. M. Mohseni¹

1. Laser and plasma Research Institute, Shahid Beheshti University, Evin, 1983963113 Tehran, Iran
2. Physics Department, Shahid Beheshti University, Evin, 1983963113 Tehran, Iran

In this paper, nano-layered Fe₇₈Si₉B₁₃ are prepared by pulsed laser deposition (PLD). Targets of Fe₇₈Si₉B₁₃ ferromagnetic amorphous ribbons are ablated in evacuated condition (10⁻⁵ mbar) by Nd:YAG laser pulses. Composition of thin films is investigated by the aid of Rutherford backscattering spectroscopy which its results indicate that the film composition is not changed in compare to its target composition. Droplets formation in the film is confirmed by an optical microscope.

Magnetic field dependence of electrical properties of the sample is studied by fixing it in the Hall measurement setup. Fig. 1 represents the measured signal as a function of applied magnetic field. After the electrical measurements, number of droplet islands decreases whereas the size of them grows up. According to deformation of the droplets, the behavior of the transverse voltage versus applied magnetic field changes. Magnetic properties of the samples are studied by the magneto-optical Kerr effect. Fig. 2 shows the longitudinal and polar Kerr hysteresis curves for samples before and after the droplet deformation.

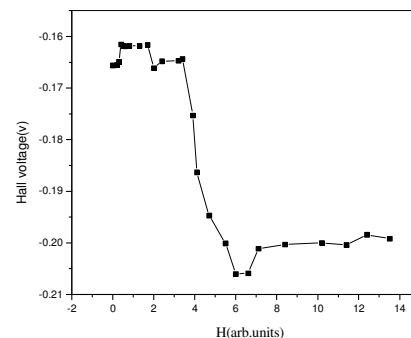


Fig.1: dependence of transverse voltage on external magnetic field.

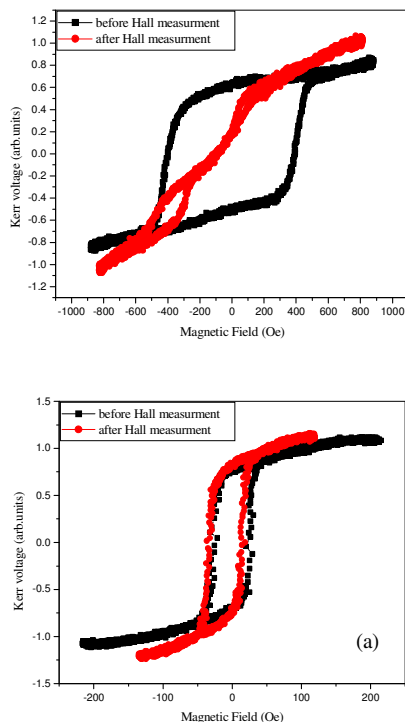


Fig.2: Magneto-optical Kerr hysteresis for thin films before and after electrical measurements.

P-42

PECULIARITIES OF THE TRANSPORT AND MAGNETIC PROPERTIES OF THE CATION-SUBSTITUTED MANGANESE SULPHIDES

O.B. Romanova and L.I. Ryabinkina

*L.V. Kirensky Institute of Physics, Siberian Branch of the Russian Academy of Sciences,
660036, Krasnoyarsk, Russia;*

We present the results of the investigations of transport and magnetic properties of the $\text{Me}_x\text{Mn}_{1-x}\text{S}$ (Me = Fe, Cr, Co) sulfide compounds synthesized on the basis of α -MnS. According to the electrical measurements data with increasing of X in $\text{Me}_x\text{Mn}_{1-x}\text{S}$ systems the semiconductor – semimetal transitions at concentrations of $X_c = 0.4$ (Me=Fe; Co) and $X_c = 0.67$ (Me=Cr) are observed. These transitions are accompanied by changes of the magnetic state of compounds. The concentration transition from an antiferromagnetic (AFM) to a ferromagnetic (FM) state for $\text{Fe}_x\text{Mn}_{1-x}\text{S}$ system is observed in the concentration range $0.25 < X < 0.3$, for $\text{Cr}_x\text{Mn}_{1-x}\text{S}$ at $X=0.5$ and for $\text{Co}_x\text{Mn}_{1-x}\text{S}$ at $X=0.3$. Colossal negative magnetoresistance (CMR) $\delta_H \sim -450\%$ at 50K in magnetic field 30 kOe has been found in the $\text{Fe}_x\text{Mn}_{1-x}\text{S}$ sample with concentration of $X=0.29$. For $\text{Cr}_{0.5}\text{Mn}_{0.5}\text{S}$ compound $\delta_H \sim -25\%$ at 4.2 K in magnetic field 30 kOe. For $\text{Co}_{0.35}\text{Mn}_{0.65}\text{S}$ compound $\delta_H \sim -27\%$ at 140 K in magnetic field 10 kOe. It may be assumed that the possible CMR mechanism in the

cation-substituted of $\text{Me}_x\text{Mn}_{1-x}\text{S}$ manganese sulphides is the magnetic and electron phase separation, namely, the formation of a system in which the regions of antiferromagnetic semiconductor and ferromagnetic metal coexist. The observed behavior of the magnetic and electric properties of these compounds shows that its would be promising to study materials based on α -MnS.

P-43

MAGNETIC BEHAVIOR AND MAGNETO IMPEDANCE EFFECT IN COBALT BASED RIBBONS

A. Rosales-Rivera¹, M. Gómez-Hermida¹, A. A. Velásquez¹,
D. Muraca², H. Sirkin²

¹Laboratorio de Magnetismo y Materiales Avanzados, Facultad de Ciencias Exactas y Naturales, Universidad Nacional de Colombia, A.A. 127, Manizales, Colombia

²Laboratorio de Sólidos Amorfos, Departamento de Física, Universidad de Buenos Aires, Argentina

The amorphous alloy ribbons $\text{Co}_{80-x}\text{Fe}_x\text{B}_{10}\text{Si}_{10}$ with $x = 6, 8$ and 10, are studied at room temperature by magnetization, ac susceptibility and magnetoimpedance measurements, under finite dc applied fields (H). The experiments were performed on samples of as-cast ribbons $\text{Co}_{80-x}\text{Fe}_x\text{B}_{10}\text{Si}_{10}$, prepared by the melt spinning technique. The dc field dependence (H) of the magnetization, M , of the samples was measured, from -1 to 1 KOe, with a vibrating sample magnetometer. The ac susceptibility of the samples was measured for dc applied magnetic field (H) from -60 to 60 Oe, using the standard ac inductance method. The frequency of the ac modulating field was applied in the range 10 to 10^4 Hz, while its amplitude was maintained at $H_{ac} \sim 1$ Oe. The complex impedance in the samples was measured for dc applied magnetic field (H) from -80 to 80 Oe, via the so-called four-probe technique. The M vs. H curves exhibit soft magnetic behavior, i.e., the loop is square shaped, having low coercivity. The real χ'_{ac} part of the susceptibility show a peak at $H = \pm H_0 \neq 0$ which could be associated with the transverse anisotropy field. The amplitude of these peaks increases with increasing frequency, which could be related with the soft magnetic character of the samples. The ribbons exhibit ultrasoft magnetic behavior, especially giant magneto-impedance effect, GMI. This behavior is consistent with the field dependences of the magnetization and ac susceptibility.

P-44

A GRAPHICAL APPROACH FOR HAMILTONIAN OF T-J MODEL

C.R.Ou¹, S.L.Young¹, Chung-Ming Ou²

¹Department of Electrical Engineering, Hsiuping Institute of Technology, Taichung, Taiwan ROC

²Department of Information Management, Kainan University, Taoyuan, Taiwan ROC

The calculation on the Hamiltonian is the center dogma for exploring the properties of the solid materials. This article reports a novel methodology to calculate the evolution of the Hamiltonian in a graphical way. The T-J Model for superconductivities is taken as an example for the demonstration of this novel approach. Though this graphical representation, renormalization and the related fluctuation of the ensemble can be visualized. It is of interesting to note that the pictorial images for exchange and double exchange mechanism in the TJ model can give the information on the evolution of the system dynamics toward to the superconductivities. Appropriate analysis techniques like, Fourier transform, can be implemented to explore some unique features during the phase change process of the solid. Since the long range and the short range interactions will lead to different dynamics behaviors of the Hamiltonian, it will reflect these phenomena on the frequency domain of the pictorial images. Through this graphical process approach, a dimensionless number can be defined to indicate the criterions for certain dynamics regions of the whole system.

P-45

LASER ACTION IN 1D AND 2D PHOTONIC CRYSTAL STRUCTURES WITH ACTIVATED GLASSES

Olga N. Kozina¹, Leonid A. Melnikov²

¹ *Saratov Division of the Institute of Radio-Engineering and Electronics of Russian Academy of Science, Zelyonaya 38, Saratov 410019, Russia,*

² *Saratov State University, Saratov 410026, Astrakhanskaya 83, Russia.*

We present the results of calculations of laser action in 1D and 2D PC with air/glass-doped layers. The model of active medium corresponds to Nd³⁺ doped glass. For the calculations of the 1D PC structures we used the transfer matrix formalism. Reflection and transmission coefficients, field distribution, threshold conditions, which correspond to infinity reflection coefficient, and the angular spectrum of radiation from such laser system are investigated for two cases: axial and off-axial propagation for TE and TM modes. We have shown the noticeable enhancement of the transmission at wavelength near 1.06 μm occurs, when unsaturated gain is about 10 cm⁻¹. The results of calculation, accounting nonlinear deformation of the field distribution along the structure due to gain and refraction index saturation, were presented too. We used iteration method for estimate saturation influence on field deformation. We have shown that at real gain parameters the field deformation is negligible. Using this approximation the results of calculations of laser power and laser frequency are presented on the dependence from gain, angle of propagation θ, gain bandwidth, refraction index and others parameters for the both case axial and off-axial propagation of radiation. The spatial distributing of electromagnetic field in such structures will present too.

For 2D case we use plane wave expansion method for calculations of reflection and transmission coefficients of

finite-thickness PC slab having regular placed air holes in doped glass medium. Both in-plane and out of plane propagation are investigated. Threshold conditions and laser characteristics are presented for 2D case.

P-46

MÖSSBAUER STUDY OF MULTIPHASE IRON OXIDE COMPOSITES

D. Ortega¹, M. Dominguez¹, C. Barrera-Solano¹ and J.S. Garitaonandia²

Dpto. de Física de la Materia Condensada, Universidad de Cádiz, Av. República Saharaui s/n 11510 Puerto Real (Spain).

Fisika Aplikatua II saila, Euskal Heriko Unibertsitatea (UPV/EHU), 644 p, 48080 Bilbao (Spain).

Systems composed by ferrimagnetic γ -Fe₂O₃ nanoparticles grown in semitransparent silica xerogels stand as the optimum component in several magneto-optic devices. A current priority aim is to improve the chemical procedure in order to obtain samples of high purity and thermal stability. However, although great advances has been performed in the synthesis, non-negligible quantities of stable antiferromagnetic α -Fe₂O₃ phase coexist with the desired metastable γ -Fe₂O₃ nanoparticles in the final product. This coexistence generates different interparticle interactions and transitions which can alter the magnetic response of the system with the temperature. A representative sample of this system with final estimated weighed fractions of ~ 10% for the α -Fe₂O₃ phase and ~ 90% for the γ -Fe₂O₃ one has been prepared by the sol-gel method. The magnetic behaviour with respect to the temperature has been followed by Mössbauer spectroscopy. The changes of the hyperfine parameters of the different subspectral components have been compared with macroscopic magnetic measurements. This comparison has allowed us to identify the phase involved in each transition and to estimate approximately the quantity of effective magnetic phase with respect to the temperature. Three different magnetic transitions are discussed. Two of them involve, in one hand, the blocking temperatures of the smallest fraction of both phases and, in the other hand, the corresponding of γ -Fe₂O₃ bigger fraction. The third one is related to the continue decrease of the intensity of the magnetic subspectral components, and the consequent increase of the superparamagnetic one, with respect to the temperature. This transition is discussed in terms of the particle size distribution and interphase interactions.

P-47

SURFACE AND BULK MAGNETIC PROPERTIES OF AMORPHOUS AND NANOCRYSTALLINE NI-SUBSTITUTED FINEMET SAMPLES

L. Elbaile^{a,*}, M^a R. D. Crespo^a, A. R. Pierna^b and J. A. García^a

^a *Depto. de Física, Universidad de Oviedo, Spain*

^b *Depto. Ingeniería Química y Medio Ambiente, EUPSS, UPV/EHU, San Sebastián, Spain*

It is known that the substitution of a small number of Fe atoms by Ni leads to an improvement of the soft magnetic properties of Finemet alloy [1]. Until now there has not been a study of the oxidation in these samples. In this work a study of the variation of the bulk and surface magnetic properties with oxidation in the Ni-substituted Finemet ribbons in the as-quenched and nanocrystalline state is presented.

Ingots of $\text{Fe}_{73.5-x}\text{Ni}_x\text{Cu}_1\text{Nb}_3\text{Si}_{13.5}\text{B}_9$ alloy with $x=0, 8, 10, 20$ were prepared by arc melting in a water-cooled copper crucible in He atmosphere. From these ingots, amorphous ribbons of 1 mm width and 25 μm thickness were obtained by the melt spinning technique. Thermal treatments to obtain the nanocrystallized samples were performed using a furnace with argon atmosphere. To study the variation of surface magnetization of the samples with oxidation, some of as-quenched and nanocrystallized samples were treated with consecutive potential cycles in a highly alkaline solution.

Bulk and surface hysteresis loops were obtained at room temperature using a low frequency induction method and the transverse magneto-optical Kerr effect, respectively.

The results indicate that the as-quenched samples show a similar behaviour in the bulk as in the surface, reaching a minimum coercivity for $x=10$. The surface coercive values are approximately one order of magnitude higher than the obtained in the bulk measurements. Besides, the coercive values in oxidized samples show practically the same values than in non-oxidized ones except for $x=10$ that increases a 40%.

[1] P. Agudo and M. Vázquez, J. Appl. Phys. 97 (2005) 023901.

P-48

CAPPING LIGAND EFFECTS ON THE SIZE-DEPENDENT AMORPHOUS-TO-CRYSTALLINE TRANSITION OF CDSE NANOPARTICLES

Mauro Epifani¹, Eva Pellicer², Jordi Arbiol,^{2,3} Joan R. Morante²

¹Consiglio Nazionale delle Ricerche - Istituto per la

Microelettronica ed i Microsistemi (C.N.R.-I.M.M.), Lecce, Italy

²EME/CeRMAE/IN²UB, Departament d'Electrònica, Universitat de Barcelona, 08028 Barcelona, CAT, Spain

³TEM-MAT, Serveis Científicotècnics, Universitat de Barcelona, 08028 Barcelona, CAT, Spain;

Amorphous CdSe nanoparticles were prepared by a base-catalyzed room temperature reaction between cadmium nitrate and selenourea, by using dodecanethiol as a capping ligand. The mean particle size could be controlled from 1.7 nm to 3.5 nm by increasing the water concentration in the reaction. When the particles were heated in a pyridine suspension, excitonic peaks appeared in the initially featureless optical absorption spectra, with larger particles requiring higher heating temperatures. By changing the suspensions solvent, the capping ligand and its concentration, it was shown that the dynamic surface

exchange between the ligand and pyridine controls the crystallization process. This phenomenon was interpreted as a surface rigidity effect imposed by the ligand, whose importance was separately evidenced on the dried nanoparticles by the evolution of X-ray diffraction patterns carried out with in-situ heating. The results showed that crystallization occurs in the same temperature range resulting in ligand desorption. The surface effect was directly visualized by high-resolution transmission electron microscopy observations on the amorphous particles, where crystallization under the electron beam was observed to start by the formation of a crystalline nucleus in the nanoparticle interior and then extends to the whole structure.

P-49

ANGULAR DEPENDENCE OF MICROWAVE ABSORPTION IN MULTILAYER FILMS

¹G. Alvarez, ²H. Montiel, ³D. de Cos, ³A. García-Arribas,

⁴R. Zamorano, ³J.M. Barandiarán, and ¹R. Valenzuela

¹Departamento de Materiales Metálicos y Cerámicos, Instituto de Investigaciones en Materiales de la UNAM, 04510, D.F. Mexico.

²Centro de Ciencias Aplicadas y Desarrollo Tecnológico de la Universidad Nacional Autónoma de México, 04510, D.F. Mexico.

³Departamento de Electricidad y Electrónica, Universidad del País Vasco, Apartado 644, 48080 Bilbao, Spain.

⁴Departamento de Física, ESFM-IPN, 07738, D.F. Mexico.

Microwave absorption measurements on a NiFe/Au/NiFe multilayer film were carried out using a JEOL JES-RES 3X spectrometer operating in the X-band (8.8–9.8 GHz). The angular dependence of microwave absorption, both in ferromagnetic resonance (FMR) and low-field microwave absorption (LFA), was investigated from $\theta=0^\circ$ to 180° in two orientations. In both cases the film plane was orientated parallel to the AC field. In longitudinal orientation, the film axis was parallel to the DC magnetic field. In transverse orientation, it was perpendicular to the DC magnetic field. For the longitudinal orientation, FMR spectra suggested a compound absorption mode that can be interpreted as the combination of two different magnetic phases. Additionally, these measurements showed an increased in the resonance field as a function of the angle, which can be explained in terms of the contribution of the shape anisotropy. For this orientation, the LFA spectra exhibited a compound antisymmetric shape around zero with two peaks, which we associated again with each one of the magnetic phases as observed by FMR. The separation of these peaks increased as a function of the angle between the DC field and the multilayer film axis, suggesting that the shape anisotropy field can be observed in the angular dependence of LFA signals. In the transverse orientation, we observed a similar effect of shape anisotropy in FMR measurements. The LFA measurements have differences with the longitudinal orientation that can be associated with the induced transverse anisotropy during the deposition and thermal treatment.

P-50

DIELECTRIC PROPERTIES OF POLYSTYRENE-CCTO COMPOSITE

F. Amaral ^a, C. P. L. Rubinger ^a, F. Henry ^b, L. C. Costa ^{a,c}, M. A. Valente ^{a,c}

^a Physics Department, University of Aveiro, Portugal

^b Laboratoire de Recherche en Polymères, C. N. R. S., France

^c I3N, 3810-193 Aveiro, Portugal

The control of the dielectric properties in polymer composites is a relevant tool to synthesize a material to a specific industrial application.

Polystyrene (PS) is a suitable host because it is readily available, and is easy to cast into desired forms, maintaining the mechanical integrity of the matrix. CaCu₃Ti₄O₁₂ (CCTO) is a well known high dielectric constant material, very useful for capacitors and memory devices.

In this work, we studied the dielectric properties of the composite PS-CCTO, in the frequency range 10 Hz to 100 kHz, for CaCu₃Ti₄O₁₂ grains concentrations up to 64%.

Different mixture laws were used to fit the data: Hanai, Wiener, Maxwell-Wagner, Kraszewsky, Looyenga and Generalized Looyenga. The last one presents the best results. The calculated exponent of this law expression was then correlated with the shape particles observed by Scanning Electron Microscopy.

Finally, using Generalized Looyenga law, we can carefully select the adequate CCTO concentration in order to tailor the desired behaviour, producing interesting composites for potential applications.

P-51

ON THE ENHANCEMENT OF METHANOL AND CO ELECTRO-OXIDATION BY AMORPHOUS (NiNb)PTSNRU ALLOYS VERSUS BIFUNCTIONAL PTRU AND PTSN ALLOYS.

A. R. Pierna, J. Barranco, F. F. Marzo, A. Lorenzo, B. Cartón, M. M. Antxustegi, and F. Lopez.

Dpto de Ingeniería Química y Del Medio Ambiente. Universidad del País Vasco. Plaza de Europa 1. 20018 San Sebastián. Spain

It has been observed in this work and previous works [1-2] that (NiNb)PtSn alloys surfaces are very effective catalyst for CO electro-oxidation, but not for methanol electro-oxidation. On the contrary, (NiNb)PtRu alloys seems to be a very effective catalyst for methanol, but not for CO, electro-oxidation. Since CO_{ads} is postulated to be a by-product in methanol electro-oxidation on Pt alloy surfaces, the lack of inactivity of (NiNb)PtSn amorphous alloys appears paradoxical. In this work we present the behaviour of a trifunctional amorphous alloy, in methanol and CO_{ads} electro-oxidation in an attend to enhance the methanol and CO oxidation mechanisms of the Sn and Ru containing alloys, respectively. It has been observed that the specific activity for (NiNb)PtSnRu for methanol electro-oxidation,

is enhanced around 50-80 % with respect the bifunctional alloys, at low methanol concentration, whereas at high methanol concentrations, PtRu catalysts seems to be more effective. The enhanced in the CO_{ads}, is observed by the lower rate of poisoning of such alloy compare with the bifunctional ones. The onset of CO_{ads} oxidation, appear to shift 0.2 V towards negative values of potentials, with respect (NiNb)PtSn electrodes.

[1] J. Barranco and A. R. Pierna, J. of Non Crystalline Solids, 353/ 8-9, (2007) 851.

[2] J. Barranco and A. R. Pierna. J. of Power Sources, 166/1, (2007) 157.

P-52

ELECTROCATALYTIC ACTIVITY OF ORR AT AMORPHOUS Ni₅₉Nb₄₀Pt_xM_{1-x} ELECTRODES IN ACID MEDIUM.

G. Ramos-Sánchez¹, O. Solorza-Feria¹ and A. R. Pierna²

¹CINVESTAV-IPN. Depto de Química. México.

²Dpto. Ingeniería Química y del Medio Ambiente, Universidad del País Vasco. Plaza Europa 1, 20018 San Sebastián, Spain.

The oxygen reduction reaction, ORR, on amorphous Ni₅₉Nb₄₀Pt₁, Ni₅₉Nb₄₀Pt_{0.6}Ru_{0.4} and Ni₅₉Nb₄₀Pt_{0.6}Sn_{0.4} was analyzed by cyclic voltammetry, CV; rotating disk electrode, RDE and chronoamperometry polarization curves in 0.5M H₂SO₄. The amount of platinum and the incorporation of transition metals in the amorphous catalyst were found to have significant effect on the kinetic parameters of the oxygen reaction. Table 1 summarizes parameters deduced from Tafel slope after mass transfer corrected currents of RDE data at 25°C. The three amorphous catalysts present stability after 30 min of electrochemical activation. The performance towards the cathodic reaction reveals that small amount of the Pt content in the catalyst can be envisaged for the fabrication of good amorphous electrocatalytic materials with possible applications as cathode electrodes in polymer electrolyte fuel cells.

Table 1. Kinetic parameters deduced from RDE data of ORR in 0.5M H₂SO₄.

	$E_{CA} /$ V	$-b /$ mVdec ⁻¹	A	$i_0 /$ mAcm ⁻²
Ni ₅₉ Nb ₄₀ Pt ₁	0.936	88	0.67	8.099E-06
Ni ₅₉ Nb ₄₀ Pt _{0.6} Ru _{0.4}	0.906	97	0.60	5.405E-06
Ni ₅₉ Nb ₄₀ Pt _{0.6} Sn _{0.4}	0.911	69	0.85	1.611E-07

P-53

SIMULATIONS ON THE REFRIGERATION OF INTEGRATED CIRCUITS USING MICRO-CHANNELS

A. M. Pereira, J. C. R. E. Oliveira, J. C. Soares,
J. Ventura, J. B. Sousa and J. P. Araújo

IFIMUP - Physics Department of FCUP, University of Porto,

The number of components in an integrated circuit (IC) chip continues to increase at a very fast speed. One consequence of the naturally higher power consumption is the increase of the device operating temperature, which may in turn degrade its performance and reliability. Heat generation and thermal management are then becoming obstacles for the decrease of the IC components' size. Consequently, there has been an increase of the demand for localized cooling and temperature stabilization of micro- and opto-electronic devices. Micro Electro Mechanical Systems (MEMS), namely integrated solid-state micro-coolers, are an attractive way to achieve compact localized cooling, with the thermoelectric refrigerators being the most studied cooling system. However, magnetic refrigeration has recently become an alternative to the thermoelectric refrigerators. A magnetic micro-cooler system is constituted by a magnetic material on a silicon wafer containing micro-channels where a flowing fluid serves as a heat exchanger. However, this is a scarcely studied subject, so that numerical simulations can provide a valuable first step to validate the use of magnetic materials for refrigeration.

The magnetic material used in the simulations is the $Gd_5Si_2Ge_2$ compound, because it exhibits a giant magnetocaloric effect, with a magnetic entropy of $\Delta S_m \sim 18$ J/(kg.K) and a temperature variation of $\Delta T_{ad} \sim 15.3$ K for an applied magnetic field of 5 T. At room temperature, this compound presents a specific heat of $C_p \sim 50$ J/(Kg.K), a thermal conductivity of $K \sim 5$ W/(m.K) and density of 7516 kg/m³. We numerically simulate water fluid cooling in silicon micro-channels using the Incompressible Navier Stokes equations with the finite elements method for an adiabatic system. Different initial conditions will be considered, namely the influence of the magnetic material thickness, the micro-channels shape and size and the distance between them, aiming to increase the performance of the micro-cooler device.

P-54

DETERMINATION OF TRACE METAL RELEASE DURING CORROSION CHARACTERIZATION OF FECO-BASED AMORPHOUS METALLIC MATERIALS BY STRIPPING VOLTAMMETRY. NEW MATERIALS FOR GMI BIOSENSORS

F. F. Marzo^a, A. R. Pierna^a, J. Barranco^a, A. Lorenzo^a,
J. Barroso^a, J. A. García^b and A. Pérez^c

^a*Chemical Engineering and Environment Dept., University of the Basque Country, Plaza de Europa, 20018 San Sebastian, Spain.*

^b*Dept. of Physics, University of Oviedo, c/ Calvo Sotelo s/n, 33007, Oviedo, Spain.*

^c*Graphical Expression and Engineering Projects Dept., University of the Basque Country, UPV-EHU, La Casilla, nº 3, 48012, Bilbao, Spain.*

The Giant Magnetoimpedance (GMI) effect was recently considered to create a new type of biosensor for molecular recognition systems and selective detection [1, 2]. Some requirements of this new generation of biosensors are high sensitivity, small size, low power consumption, stability of operation parameters, quick response and resistance to aggressive medium. The purpose of this work was to study the corrosion susceptibility of $Fe_{2.5}Co_{64.5}Cr_3Si_{15}B_{15}$, $Fe_3Co_{67}Cr_3Si_{15}B_{12}$ and $Fe_5Co_{70}Si_{15}B_{10}$ biosensor prototype amorphous materials in biological medium.

The corrosion behaviour of these materials has been studied in phosphate buffered saline solutions (PBS, artificial biological solutions) at pH 7.4 at different temperatures. The electrochemical characterization of alloys has been made by means of dc and ac electrochemical techniques. From the cyclic anodic polarization curves, the pitting potential, protection potential, and the perfect and imperfect passivity regions were obtained [3]. The electrolytes were no de-aerated. Electrochemical impedance spectroscopy (EIS) experiments were performed with a Solartron model SI 1255 Frequency Response Analyzer attached to a Princeton Applied Research (PARC-273) potentiostat-galvanostat. Impedance spectra were carried out potentiostatically from 60 kHz to 1 mHz, superimposing an a.c. voltage of 10 mV over the stabilization potential of each alloy, obtained previously from anodic polarization curves. The metal concentrations (Fe, Co, Cr, B) in the various solutions used in the electrochemical tests, were analyzed by voltammetric stripping analysis [4] with a Metrohm 797 VA Computrace. The experimental results of amorphous alloys obtained from different electrochemical techniques were compared and discussed in order to study their corrosion behaviour in artificial biological solutions, and thus, determine their possible use as GMI-biosensor prototype materials.

[1] Galina Kurlyandskaya and Vladimir Levit, *Biosens. Bioelectron.*, 20 (2005) 1611.

[2] G. V. Kurlyandskaya, M. L. Sánchez, B. Hernando, V. M. Prida, P. Gorria and M. Tejedor. *Appl. Phys. Lett.*, Vol. 82 No. 18, (2003) 3053.

[3] *Portugaliae Electrochimica Acta* 25 (2007) 131-137.

[4] Tanaka, Tatsuhiko; Nishu, Kumi; Nabekawa, Hidenori; Hayashi, Hideo. *ISIJ International* (2006), 46(9), 1318-1323.

P-55

PRESSURE-INDUCED SUPPRESSION OF FERROMAGNETIC PHASE IN $LaCoO_3$ NANOPARTICLES

I. Fita^{1,2}, D. Mogilyansky¹, V. Markovich¹, R. Puzniak³, A. Wisniewski³, L. Titelman⁴, L. Vradman⁴, M. Herskowitz⁴, V. N. Varyukhin² and G. Gorodetsky¹

¹Department of Physics & Department of Chemical Engineering, Ben-Gurion University of the Negev, 84105 Beer-Sheva, Israel

²Donetsk Institute for Physics & Technology, National Academy of Sciences, 83114 Donetsk, Ukraine

³Institute of Physics, Polish Academy of Sciences, Warsaw, Poland

⁴Blechner Center for Industrial Catalysis & Process Development, Department of Chemical Engineering, Ben-Gurion University of the Negev, 84105 Beer-Sheva, Israel

Magnetic properties of nanocrystalline LaCoO₃ with particle size ranging from 25 to 38 nm, prepared by the citrate method, were investigated in temperature range 2 – 320 K, magnetic field up to 50 kOe and under hydrostatic pressure up to 10.5 kbar. All nanoparticles exhibit ferromagnetism below $T_C \approx 85$ K, in agreement with recent observation [1,2]. It was found that with decreasing particle size, the unit-cell volume increases monotonically and ferromagnetic (FM) moment increases simultaneously with lattice expansion as well, while T_C remains nearly unchanged. It appears that both magnetic and structural properties of LaCoO₃ nanoparticles are size-dependent due to the surface effect. Contrary to the effect of downsizing, an applied pressure suppresses strongly the FM phase leading to a full disappearance of the FM order at 10 kbar. Remarkably, the T_C does not change visibly under pressure until FM phase exists in the sample.

The observed correlation between the FM phase and lattice parameters suggests that the ferromagnetism of LaCoO₃ is likely related to the Co³⁺ ions with intermediate-spin (IS) state, induced by an expansion of the Co-O bonds. Our data reveal therefore that the ferromagnetism in LaCoO₃ nanoparticles is simply controlled by unit-cell volume. Within this scenario, the FM coupled IS Co³⁺ ions appear/disappear with expanding/compressing the lattice and/or Co-O bonds.

[1] J.-Q. Yan, J.-S. Zhou, and J. B. Goodenough, Phys. Rev. B 70, 014402 (2004).

[2] A. Harada et al., Phys. Rev. B 75, 184426 (2007).

P-56

MAGNETIC CHARACTERIZATION OF FE, NI, CO NANOPARTICLES, DISPERSED IN PHYLLOSILICATE TYPE SILICON OXIDE .

V. Sagredo¹, O. Peña², A. Loaiza-Gil³, Marlin Villarroel³, María La Cruz³ and José Balbuena³.

¹Laboratorio de Magnetismo, Departamento de Física, Facultad de Ciencias, Universidad de Los Andes, Mérida, Venezuela.

²Sciences Chimiques de Rennes, Université de Rennes, Francia.

³Laboratorio de Cinética y Catálisis, Departamento de Química, Facultad de Ciencias, Universidad de Los Andes, Venezuela.

Nanosized particles of ferromagnetic metals as Fe, Ni, and Co have attracted great interest because of their physical properties and potential applications as catalyst. Many methods have been tried to develop composites in which

the metallic nanoparticles are dispersed in a silica matrix. (1) In the present study, M/Si oxides (M: Fe, Ni, Co) catalyst, phyllosilicate type, ranging 20–120 nm have been prepared by coprecipitation method. The method basically consist of contacting silica aerosil 200 with a solution of M(NO₃)₃.nH₂O to which ammonia solution was added.

The magnetic properties of the nanopowders were characterized by ZFC-FC magnetization measurements in applied field of 500 Oe and hysteresis cycles within the 2 – 300 K range under magnetic fields ranging from ± 5 T. Their structural characteristics were studied by XRD and SEM microscopy. The obtained structures were previously found on silica support cobalt catalysts synthesized with the same method. (2) Magnetic characterizations at 2K indicate that samples exhibit superparamagnetic behavior above the blocking temperature TB between 11K and 8 K for the Fe, Ni and Co nanoparticles. It is important to notice that above TB the reciprocal susceptibility is closed to linear with temperature. These behaviors agree quite well for particles previously studied (3,4). The hysteresis loops measured at $T < TB$ suggest that the metallic nanoparticles are free from an oxide layer because the hysteresis loops presents a symmetrical shape.

[1] C.B.Murray, S.Sun, H.Doyle, T.Betley, MRS.Bull. 26 (2001) 985

[2] C.Clauso, M.Kenmarec, L.Bonneviot, F.Villain, M.Che, J.Amer. Chem.Soc. 114 (1992) 4709

[3] A.S.Ferlauto, F.Alvarez, F.C.Fonseca, G.F.Goya, R.F.Jardim, J. Met. and N. Mat. 20-2 (2004) 700

[4] J.Chen, C.Sorensen, K.Klabunde, C.Hadjiapanayis, Phys. Rev. 51, (1995) 11527

P-57

CARBON NANOCONES: A VARIETY OF NON-CRYSTALLINE GRAPHITE

H. Heiberg-Andersen¹, A.T. Skjeltorp¹, and Klaus Sattler²
¹Institute for Energy Technology, Physics Department, 2027 Kjeller, Norway

²University of Hawaii at Manoa, Department of Physics and Astronomy, 2505 Correa Road, Honolulu, Hawaii 96822, USA

Previously known graphitic structures of conic shape - whiskers and helical cones - consist of a single sheet wrapped around itself, which gives a rather amorphous tip structure. Carbon nanocones, on the other hand are near perfect graphite sheets, curved by 1 to 5 pentagonal rings in the otherwise hexagonal network of carbon atoms. The resulting loss of periodicity implies electronic properties quite different from flat graphite and nanotubes. As for fullerenes, it can be shown that the pentagonal rings promote heterogeneous distribution of the total π -charge, and the resulting enhanced reactivity is confirmed by oxidation experiments. However, we have found theoretical evidence [1] that a large fraction of the cones are stable to Jahn-Teller distortions, while there are very few known fullerenes with this property outside the so-called leapfrog series.

A decade ago, mesoscopic cones with all the five possible apex angles were synthesized [2] during an accidental modification of Kvaerner's Carbon-Black & Hydrogen Process [3] for pyrolysis of heavy oil. The nucleation process remains a mystery, and it has been correspondingly difficult to replicate the thermodynamic conditions for cone production. Restricted access to sample material has therefore delayed experimental studies until recently. Yet it has been confirmed by independent Norwegian laboratories that the cones release adsorbed H₂ at room temperature [4]. Together with the light weight and low cost of carbon, this property makes the cones a promising hydrogen storage material for fuel-cell driven vehicles. Some results achieved by the EC project HYCONES [5] initiated to explore this potential will be discussed.

- [1] H. Heiberg-Andersen and A.T. Skjeltorp, *J. Math. Chem.* 38, 589 (2005)
 [2] A. Krishnan, E. Dujardin, M.M.J. Treacy, J. Hugdahl, S. Lynam and T.W. Ebbesen, *Nature* 388, 45 (1997)
 [3] Kvaerner's patent no PCT/NO98/00093 for production of micro domain particles by use of a plasma process
 [4] Norwegian patent No. 307986 (2000), US patent No. 6,290,753 (2001), EPO Patent No. 1051530 (2004), "Hydrogen storage in carbon material"
 [5] <http://www.hycones.eu/>

P-58

SYNTHESIS AND CHARACTERIZATION OF NANOCRYSTALLINE Fe₆₀X₂₀P₁₀B₁₀ (X = CO, NI) ALLOYS

M. Pilar¹, J.J. Suñol¹, L. Escoda¹, J. Saurina¹, B. Arcondo²
¹Univ. Girona, EPS, Campus Montilivi s/n, Girona, 17071 Spain
²Univ Buenos Aires, Fac Ingn, Lab Sólidos Amorfos, Buenos Aires, DF RA-1063 Argentina

Mechanical alloying (MA) represents a non-expensive versatile route able to produce equilibrium as well as non-equilibrium materials including amorphous, nanostructured, composites, and extended solid solution systems. In this work, two nanocrystalline alloys, Fe₆₀Ni₂₀P₁₀B₁₀ and Fe₆₀Co₂₀P₁₀B₁₀, were produced by mechanical alloying at different milling times until 100 hours. It is known that the substitution of small amounts of Co or Ni for Fe in Fe-based magnetic materials generally results in an increase of saturation magnetization. Furthermore, Ni favors the development of metastable structures at low milling times. Structural properties were determined by X-ray diffraction and transmission Mössbauer spectroscopy. The 100 hours as milled alloys consisted primarily of metastable bcc Fe(Ni,Co) nanocrystals (8-12 nm) with different Fe-rich environments. Differential scanning calorimetry measurements were performed in order to compare thermal behavior of the nanocrystalline phase front crystalline growth. Co favors the thermal stability. The apparent activation energy values of the main crystallization process are 2.1 ± 0.1 eV and 2.4 ± 0.1 eV and can reasonably be associated with a grain growth process. At high temperatures, P presence favors the phosphide formation.

P-59

PECULIARITIES OF MAGNETIC PROPERTIES OF HETEROGENEOUS NANOCRYSTALLINE MAGNETIC MATERIALS

E.E. Shalyguina, V.V. Molokanov, M.A. Komarova,
 V.A. Melnikov, A.N. Shalygin
Faculty of Physics, Moscow State University, Moscow, Russia

Results on the investigation of the magnetic properties of nanocrystalline Co/Ni/Fe, Fe-Zr-N thin-film systems and Fe_{80.5}Nb₇B_{12.5} ribbon are presented. The nanocrystalline Co/Ni/Fe and Fe-Zr-N samples were prepared by magnetron sputtering technique under a base pressure of less than 10⁻⁸ Torr. The ribbons were obtained by a planar flow casting method from the melt. The Fe-Zr-N films and ribbon samples were annealed in vacuum for 1h at temperature $T = 200-700$ and $380-650$ °C, respectively. The annealed the Fe-Zr-N films and ribbon samples were found to have inhomogeneous microstructure along their thickness. The study of the near-surface and bulk magnetic properties of the above samples was carried out employing magneto-optical micromagnetometer with a surface sensitivity of about 20 nm of the thickness depth and vibrating magnetometer.

The examined samples were revealed to exhibit near-surface hysteresis loops of a complicated form (very similar to partially inverted hysteresis loops). This fact was explained by using theoretical calculations, performed in [1]. According to [1], the hysteresis loops of the complicated shape can observe for heterogeneous multilayer magnetic systems. In this case, the stray fields, created by neighbouring layers, influence on the magneto-field behaviour of the every layer. The orientations of these fields are opposite to the external magnetic field. So, due to the magnetostatic interaction between the layers, the strong modification of the hysteresis loops (up to the appearance of the partially and completely inverted hysteresis loops) is possible.

- [1] A. Aharoni. *J. Appl. Phys.* 76 (1994) 6977.

P-60

INTERPLAY BETWEEN THE MAGNETIC FIELD AND THE DIPOLAR INTERACTION ON THE BLOCKING TEMPERATURE OF A MAGNETIC NANOPARTICLE SYSTEM: A MONTE CARLO STUDY

D. Serantes^{1,2}, D. Baldomir^{1,2}, M. Pereiro^{1,2}, J.E. Arias¹, C. Mateo-Mateo³, M.C. Buján-Núñez³, C. Vázquez-Vázquez³, and J. Rivas²
¹Instituto de Investigaciones Tecnológicas, Universidad de Santiago de Compostela, Galiza, Spain
²Departamento de Física Aplicada, Universidad de Santiago de Compostela, E-15782 Santiago de Compostela, Galiza, Spain
³Departamento de Química Física, Universidad de Santiago de Compostela, E-15782 Santiago de Compostela, Galiza, Spain

We have studied the influence of the applied magnetic field on the blocking temperature (T_B) of a fine magnetic particle system. By means of a Monte Carlo technique we have simulated zero field cooling (ZFC) curves under different applied fields, obtaining the respective T_B as a function of H . We have focused our study on the limit $H \rightarrow H_K$ (where H_K is the anisotropy field), since the results found in the literature usually lack a detailed study of this range. The simulations were done at different sample concentration of the nanoparticles, with the purpose of observing how the dipolar interaction affects the field dependence of T_B . The classical expression predicts T_B to disappear for $H \geq H_K$, independently of the dipolar interaction strength. Our simulations show an intriguing behavior: at weak interacting conditions T_B disappears for values of H larger than $\sim 0.7 H_K$, while at strong interacting conditions T_B persists even for fields $H > H_K$.

P-61

INFLUENCE OF NANOPARTICLE SIZE ON BLOCKING TEMPERATURE OF INTERACTING SYSTEM: MONTE CARLO SIMULATIONS

M.C. Buján Núñez¹, N. Fontaiña-Troitiño¹, C. Vázquez-Vázquez¹, M.A. López Quintela¹, Y. Piñeiro², D. Serantes², D. Baldomir² and J. Rivas²

Departamento de Química-Física¹ y Física Aplicada², Universidad de Santiago de Compostela, Spain.

Ensembles of single domain magnetic nanoparticles are very important in a wide range of applications. These systems form a superparamagnetic state at high temperature [1]. On lowering the temperature, the particles become blocked at a specific temperature that depends on the size of particles. In this work we study using Monte Carlo simulations of ZFC curves [2] the influence of nanoparticles concentration, c/c_0 , on the rate of increase of the blocking temperature, T_B , with the nanoparticles size, v/v_0 . All simulations were performed using the same value of the external field, h/h_0 , (in units of the anisotropy field h_0). Results show that for all nanoparticles concentrations the blocking temperature increases linearly with the nanoparticles size. The rate of increase of the blocking temperature is bigger as larger is the nanoparticles concentration, although it tends to a constant value for very large interactions between particles.

[1] L. Dormann, D. Forani, E. Tronc, *J. Magn. Magn. Mater.*, **292**, 251 (1999)

[2] D. Baldomir, J. Rivas, D. Serantes, M. Pereiro, J.E. Arias, M.C. Buján Núñez and C. Vázquez, *Vazquez, J. of non-Crystalline Solids*, **353**, 793 (2007)

P-62

HIGH PULSED MAGNETIC FIELD MAGNETORESISTANCE IN COFe(T)/AL₂O₃ DISCONTINUOUS MULTILAYERS

J. M. Moreira, H. Silva, J. P. Araújo, Y. G. Pogorelov, A. M. Pereira and J. B. Sousa
IFIMUP - Physics Department of FCUP, University of Porto, R. do Campo Alegre 687, 4169-007 Porto, Portugal.
 P. P. Freitas, S. Cardoso
INESC-MN, Rua Alves Redol, 9-1, 1000-029 Lisbon, Portugal
 B. Raquet, H. Rakoto
Lab Natl Champs Magnet Pulses, F-31432 Toulouse, France

Nanogranular magnetic systems can be conveniently prepared in the form of discontinuous metal-insulator magnetic multilayers (DMIM) displaying large tunnel-magnetoresistance (TMR). One example is [CoFe(t)/Al₂O₃(s)]_n which, upon variation of the nominal thickness of the magnetic layer (t), exhibits a series of magnetic phases with different TMR and magnetic responses.

A series of [Co₈₀Fe₂₀(t)/Al₂O₃(30Å)]₁₀ multilayers was formerly prepared [1] from t=7Å (well separated magnetic granules) up to 18Å (almost continuous magnetic film), progressively exhibiting, at room temperature, superparamagnetism (t<13Å), superferromagnetism (SFM; t>13Å, magnetic percolation) and the common exchange ferromagnetism (FM; t>18Å) preceding the electrical/structural percolation [1].

Here we concentrate near the SFM/FM critical boundary (t=16, 17 and 18Å), where the ferromagnetism evolves from mixed (exchange/dipolar) to fully exchange-dominated and the magnetic layer structure evolves from mixed (coalescent magnetic islands and amorphous Al₂O₃ regions) to wards a polycrystalline continuous magnetic layer.

Due to the rapid change in short-range order in this thickness region one expects important fluctuation effects, both magnetic and structural. We then performed a detailed study of magnetoresistance (MR; 77-300K) under magnetic field pulses up to 35T ($\Delta t \sim 0.5s$), with H both parallel and perpendicular to the electrical current.

For t=16Å and 17Å the MR is larger and negative (-MR~1.8% and 1.0% respectively), with only a small anisotropy between the two H-configurations (0.1% and 0.04% respectively). This shows virtual absence of AMR-magnetoresistance (characteristic of conduction in s-d band structure), so the magnetic layer still has considerable structural discontinuities. The negative MR is then associated with a significant spin disorder effect on tunnel resistance at H=0. The observed anomalous MR(T) dependence may be also explained by this conduction mechanism.

For t=18Å quite different MR(H) curves appear for H(∥) and H(⊥), namely a large anisotropy (1.1%) indicating a significant AMR contribution (electron band related), and so almost continuous magnetic layers. This also fits with the change from tunnel (t=16 and 17Å) to metallic (t=18Å) conduction observed in R(T). However the negative values of total MR still indicate considerable spin-disorder at H=0.

[1] G.N. Kakazei *et al.*, in Handbook of Advanced Magnetic Materials-III, Springer, chap.3 (2004)

P-63

**TIME-RESOLVED SYNCHROTRON RADIATION
INVESTIGATION OF MAGNETITE GRAIN-GROWTH
DURING MICROWAVE HEATING**

M. Stir¹, R. Nicula¹, B. Schmitt², J.-M. Catala-Civera³, and S. Vaucher¹

1 EMPA, Swiss Federal Laboratories for Materials Testing and Research, Feuerwerkerstrasse 39, CH-3602 Thun, Switzerland

2 Swiss Light Source, Paul Scherrer Institute, Switzerland

3 Polytechnical University of Valencia, School of Telecommunication, Camino de Vera s/n E-46022 Valencia, Spain

Microwave heating is a versatile materials processing technology, particularly suited for manufacturing bulk nanostructured solids and composites. The use of microwaves in the processing of new nanomaterials strongly benefits from the development of new experimental techniques for the detailed characterization of the microwave field – materials interaction. The time-resolved synchrotron radiation powder diffraction method was recently used in conjunction with in situ microwave heating to obtain information on structural and microstructural changes of materials with a time resolution of only a few seconds [1]. The thermal stability and grain-growth kinetics of magnetite was here investigated using the above technique, in view of the potential use of magnetite as internal susceptor material for the microwave-assisted synthesis of nanocomposites.

[1] S. Vaucher, R. Nicula, J.-M. Catala-Civera, B. Schmitt, B. Patterson, In situ synchrotron radiation monitoring of phase transitions during microwave heating of Al-Cu-Fe alloys, *J. Mater. Res.* 23(1) (2008) 170-175.

P-64

**BROAD UHF FERROMAGNETIC RESONANCE OF IRON
RICH-ALUMINIUM PULSED LASER DEPOSITED THIN
FILMS**

V. Madurga, J. Vergara, C. Favieres

Laboratory of Magnetism, Physics Department, Public University of Navarre, Campus Arrosadia, E31006 Pamplona, Spain

The magnetic susceptibility of Fe-Al pulsed laser deposited, PLD, thin films was measured at ultra high frequencies, UHF. Different films with different composition, $\text{Fe}_{1-x}\text{Al}_x$ from pure Fe to $x=0.3$ Al, were prepared using a cylindrical target formed by two sectors of pure Fe and Al. A fine dispersion of Al nano-grains in the nano-structured Fe matrix was expected. The films were ≈ 40 nm thick and non crystalline peaks were detected in the x-ray diffractometry studies. The magnetization of the films remained between 2.0 and 1.8 T for composition bellow to $\approx 20\%$ Al. A magnetic anisotropy, from $H_u \approx 18$ Oe for pure Fe to $H_u \approx 150$ Oe for 20% Al, was measured for samples deposited at 52° off-normal angle. These samples exhibited a well defined ferromagnetic resonance at frequencies

between ≈ 1.0 GHz and 2.4 GHz depending on the composition. The broad resonance peaks had a width, at half maximum, w_h , in the interval from 2.8 GHz to 4.1 GHz depending on Al content. These values were 4-6 times wider than that corresponding to, for example, a sharp ferromagnetic resonance peak, $w_h \approx 0.7$ GHz of a pure Co PLD film. To explain this broad ferromagnetic resonance of these $\text{Fe}_{1-x}\text{Al}_x$ films with high magnetization values, we used their resistivity values in the Landau-Lifshitz-Gilbert equation and a superposition of different solutions corresponding to different values of the magnetic anisotropy.

P-65

**A PROTECTIVE LAYER ON As_2S_3 FILM FOR PHOTO-
RESIST PATTERNING**

*Duk-Yong Choi, Steve Madden, Andrei Rode, Rongping Wang,
Barry Luther-Davies*

*Centre for Ultrahigh bandwidth Devices for Optical Systems,
Laser Physics Centre*

*Research School of Physical Science and Engineering, The
Australian National University Canberra, ACT0200, Australia*

Arsenic tri-sulphide (As_2S_3) glass is a good candidate for non-linear optic devices due to its high non-linearity and low optical loss. Fabricating planar As_2S_3 waveguides, however, is not straightforward. Like most other chalcogenides (ChGs), As_2S_3 is dissolved in alkalis such as photo-resist developer; thus this makes standard photolithography of this material difficult. To protect the film from the solvent we had applied several materials as a protective layer before photo-resist coating; these included thin photo-resist (PR), SiO_2 coating, and Ge-As-Se based ChG which is quite inert in alkaline solutions. Even though PR patterns could be satisfactorily formed on the films using any of these coatings, complexity in the process was unavoidable.

In this study we present the application of bottom anti-reflective coat (BARC) as a protective layer and the development of the dry etching process of this layer. BARC was spin-coated on the film and thermally cured. The conformal coverage of the coat even on the surface defects kept the film from contacting the developer so that no damage of the film was observed during PR patterning. Before As_2S_3 film etching, the BARC layer was etched in oxygen-based plasma. Small amount of CHF_3 were added in order to etch the As_2S_3 film very slightly, otherwise surface defects of As-O compound were generated. Moreover, the etch rates of BARC and PR were almost the same, therefore under- or over-cutting of BARC did not occur, which is a prerequisite to obtain smooth etched sidewall and vertical profile.

P-66

**STRUCTURAL PROPERTIES OF EXCHANGE BIASING
MNPT AND MNNI ANTIFERROMAGNETIC MATERIALS
FOR SPINTRONIC**

J. Ventura¹, J. M. Teixeira¹, J. P. Araujo¹, J. B. Sousa¹, V. Amaral², B. Negulescu³, M. Rickart³, P. P. Freitas³
¹*IFIMUP and FCUP, R. Campo Alegre 678, Porto, Portugal*
²*CICECO Aveiro, Portugal*
³*INESC-MN and IST, R. Alves Redol 9-1, Lisbon, Portugal*

The field of spintronics is continuously seeking new ways to improve device performance. Two such devices are constituted by two ferromagnetic (FM) layers separated by a metallic (spin valves) or insulator (tunnel junctions) spacer. Their electrical resistance depends on the relative orientation of the FM magnetizations. To obtain well separated resistance states, an antiferromagnetic (AFM) layer is deposited adjacent to one of the FM layers. Due to an exchange interaction at the interface, such FM-magnetization reverses only at very high magnetic fields. New AFM materials with improved exchange coupling are then intensively researched, including MnPt and MnNi, where exchange bias is linked with the corresponding microstructure. As-deposited MnPt and MnNi have a non-magnetic fcc phase and an annealing is necessary to induce the AFM fct phase.

We present a study of the structural properties of MnPt (as a function of thickness) and MnNi (for different annealing procedures) materials, obtained by X-ray diffraction (XRD) measurements. For MnPt (5 to 20 nm thick; annealed at $T = 310^\circ\text{C}$), we observe only the fct phase. The average out-of-plane MnPt grain size calculated from the XRD spectra increases with layer thickness, as does the exchange bias. Different thermal annealings were used to induce exchange bias in MnNi: i) rapid thermal annealing at 180°C for 5 min; ii) standard annealing at 260°C ; iii) annealing at 280°C . X-ray diffraction measurements show only partial transformation to the fct phase for all annealing procedures. The measured values of exchange bias are correlated with the degree of phase transformation.

P-67

STRUCTURAL, MAGNETIC AND TRANSPORT PROPERTIES OF ION BEAM DEPOSITED NiFe THIN FILMS

J. Ventura¹, R. Fermento¹, D. Leitao¹, J. M. Teixeira¹, A. M. Pereira¹, J. P. Araujo¹, J. B. Sousa¹
¹*IFIMUP and FCUP, R. Campo Alegre 678, Porto, Portugal*

Developments in thin film deposition techniques opened a huge new field both for technological applications and fundamental research. It is now possible to deposit smooth films with thicknesses as low as a few Å, and we master the ability to accurately fabricate nanostructures (multilayers, spin valves, tunnel junctions or nanocontacts) displaying new and interesting physical phenomena. A great variety of applications based on such nanostructures are already commercially available, while others are in accelerated development. It is essential to control the properties of such nanostructures to be able to enhance in a reproducible way device performance.

Here we present a study of the structural, magnetic and transport properties of NiFe thin films deposited by ion beam sputtering under an applied magnetic field (250 Oe) to induce a magnetic easy axis. We studied the influence of the buffer layer material (Ta, Cu or Ru) and thickness (10-100 Å) on the structural properties of NiFe thin films using X-ray diffraction (XRD) measurements. The average out-of-plane NiFe grain size (D) calculated from the XRD spectra was also obtained as a function of the buffer layer thickness. The magnetic properties (coercive and saturation fields) of the same NiFe thin films were obtained using magneto-optical Kerr effect (MOKE) measurements, both for the easy and hard axis. Finally, the electrical resistivity of our NiFe thin films (on the Ta buffer) was obtained as a function of NiFe thickness. The obtained results will be correlated with the influence of surface effects on the transport properties.

P-68

PY ANTIDOT THIN FILMS: A TRANSPORT AND MAGNETIC CHARACTERIZATION AS A FUNCTION OF TEMPERATURE

D. C. Leitao¹, C. T. Sousa¹, J. Ventura¹, F. Carpinteiro¹, K.R. Pirola², M. Vazquez², J. B. Sousa¹, J. P. Araújo¹
¹*IFIMUP, Rua do Campo Alegre 687, 4169-007 Porto*
²*Instituto de Ciencia de Materiales de Madrid, CSIC, Spain*

Nanopatterned media, and in particular arrays of magnetic dots and antidots, have gained increased attention in the last years. Antidots are particularly interesting because, since there is no isolated magnetic volume, the superparamagnetic limit below which thermal fluctuations erase the average magnetization [1], does not occur. In this way, they are strong candidates to be used as ultra-high density recording media. However, to achieve the desired submicron features, expensive, time consuming lithographic techniques, like e-beam or focused ion beam lithographies are usually required. An alternative route may be the use of easily fabricated nanoporous alumina as templates for the subsequent growth of a thin magnetic layer on top [1].

Nanoporous alumina templates (average pore diameter of ~35 nm, separation of ~100 nm) were obtained by a two-step [2] anodization of high-purity (>99.997%) aluminum foils. First anodizations were performed at 40 V for 2 hours, in 0.3M oxalic acid, at a temperature between 2-6°C; the second anodization was carried out using the same conditions. Permalloy thin films were then deposited on top of nanoporous alumina substrates with an Ion Beam Deposition (IBD) system.

As expected, antidot matrices exhibit properties very different from those of continuous films. The holes introduce shape anisotropies and act as major nucleation sites for magnetic domains. Changes in the macroscopic magnetic properties, can also be observed, such as magnetic anisotropy, coercive field and magnetoresistance. We will present a detailed study of temperature dependence of

electrical resistivity and magnetoresistance as a function of pore diameter.

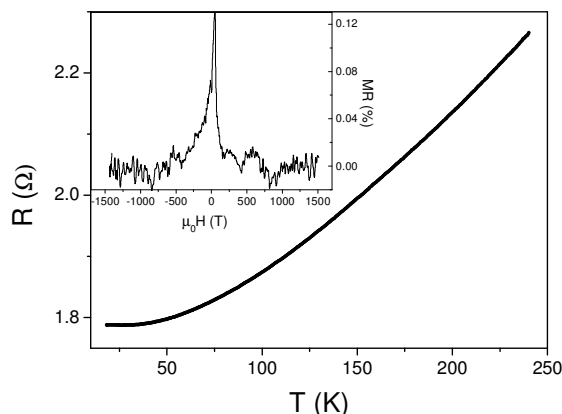


Fig. 1: $R(T)$ for Py(33nm) over nanoporous alumina. Inset: $MR(T=70K)$ for the same sample.

[1] Z. L. Xiao et al., *Appl. Phys. Lett.*, vol. 81, (2002) pp. 2869-2871.

[2] H. Masuda et al., *Science*, vol. 268, (1995) pp. 1466-1468.

P-69

STRUCTURAL AND MAGNETIC EVOLUTION OF MECHANICALLY ALLOYED $Fe_{30}Cr_{70}$ ALLOYS STUDIED BY NEUTRON THERMO-DIFFRACTOMETRY AND X-RAY ABSORPTION SPECTROSCOPY

A. Fernandez-Martinez^a, D. Martinez-Blanco^b, M. J. Perez^c, G. J. Cuello^a, G. Castro^d, J. A. Blanco^c, P. Gorria^c

^a Institut Laue-Langevin, BP 156, 6 rue Jules Horowitz, 38042 Grenoble Cedex 9 France.

^b Unidad de Magnetometría, SCT's, Universidad de Oviedo, Julián Clavería 8, 33006 Oviedo, Spain

^c Departamento de Física, Universidad de Oviedo, Calvo Sotelo, s/n, 33007 Oviedo, Spain.

^d European Synchrotron Radiation Facility, B.P. 220, Grenoble, 38043, France

Binary Fe_xCr_{100-x} solid solutions have a body centred cubic (bcc) crystal structure at room temperature in the whole compositional range, with a lattice parameter close to those of Fe and Cr (around 2.87 Å). These alloys display a complex magnetic phase diagram especially in the Cr-rich compositional range where coexistence of spin glass, re-entrant spin glass, ferro- or antiferromagnetism can occur [1]. The use of mechanical alloying allows synthesizing single phase Fe_xCr_{100-x} compounds with either a bcc nanometer grain size or amorphous structures [2]. The magnetic behaviour of these mechanically alloyed systems can be largely influenced by the paramagnetic disordered intergranular zone [3]. High-energy ball milling $Fe_{30}Cr_{70}$ powders are paramagnetic at room temperature, as expected from previous studies [4]. In this contribution we present magnetisation vs. temperature, $M(T)$, measurements in heating-cooling cycles between 10 K and 1100 K together

with *in situ* neutron powder thermo-diffraction experiments from 300 K to 1100 K. On heating the as-milled powders, the $M(T)$ curve does not coincide with that corresponding to the cooling from 1100 K. However, further heating-cooling cycles give rise to overlapping $M(T)$ curves, suggesting that structural changes take place during the first heating. From the Rietveld analysis of the neutron thermo-diffraction patterns, the temperature-induced microstructural relaxation (grain growth and decrease of internal microstrain) can be monitored, as well as the structural changes during heating-cooling processes, which could explain the anomalous $M(T)$ behaviour. In addition, EXAFS experiments at the Fe K-edge have revealed an important decrease in the coordination number of the Fe atoms in the as-milled samples, going down from 8(6) first (second) neighbours (theoretical values) to 4.7 ± 0.7 (3.5 ± 0.9). This fact may have a marked influence in the control of the magnetization.

[1] A.T. Aldred, *Phys. Rev. B*, 14 (1976) 219; A.T. Aldred et al., *Phys. Rev. B*, 14 (1976) 228.

[2] T. Koyano et al., *J. Appl. Phys.*, 73 (1993) 429.

[3] A. Fnidiki et al., *Physica B*, 357 (2005) 319.

[4] M. Murugesan et al., *IEEE Trans. Mag.*, 35 (1999) 3499.

P-70

THEORETICAL STUDY OF MAGNETODYNAMICS IN FERROMAGNETIC NANOPARTICLES

N. Sousa¹, H. Kachkachi², D. S. Schmool¹

¹IFIMUP and Departamento de Física, Universidade do Porto, Rua do Campo Alegre 687, 4169-007 Porto, Portugal

²Groupe d'Etude de la Matière Condensée, Université de Versailles St. Quentin, CNRS UMR 8634, 45 Avenue des Etats-Unis, 78035 Versailles, France

The theory of magnetodynamics is a well established area of magnetism and is based on the Landau-Lifshitz equation of motion. This dynamical theory forms the basis of the formalism of ferromagnetic resonance (FMR) and spin wave resonance (SWR). The classical theory has been adapted to many magnetic systems, from bulk samples to magnetic thin films and multilayers. Low dimensional systems such as the latter require additional considerations of the surface or boundary conditions which permit the evaluation of the allowed standing spin wave mode wave vectors. In the case of thin films and multilayers the problem can be reduced to one dimension, i.e. in the direction perpendicular to the film plane. Other low dimensional systems, such as nanowires, nanorods and nanostructured materials will be more complex since we must take into account the three dimensional nature of the problem. In recent years, with interest in nanometric systems increasing enormously, attention has been directed to these ends. Of particular concern is the manner in which the surface spins should be treated, since for such small structures the number of surface spins, with reduced magnetic coordination compared to bulk spins, will be a

significant number of the total. As such surface magnetic properties in these systems can dominate, thus allowing us to manipulate magnetic properties via a control of particle size.

In this paper we present the formalism for obtaining the excitation spectrum, and in particular, the FMR resonance characteristics, of a nanoparticle using a many-spin approach. This method takes the environment of each spin into account and in particular its positional specific resonance condition. We have made numerical simulations of the FMR spectra for iron nanoparticles with different external parameters (such as anisotropy, direction of the applied magnetic field, etc.) and we compare the results with the corresponding analytical treatment.

P-71

MEASURING MAGNETIC PROPERTIES IN EXCHANGE SPRING SYSTEMS USING FERROMAGNETIC RESONANCE

A. Apolinário¹, F. Casoli², L. Nasi², F. Albertini² and D. S. Schmol¹

¹Departamento de Física and IFIMUP, Universidade do Porto, Rua do Campo Alegre 687, 4169 007, Porto, Portugal

²Istituto IMEM - CNR, Parco Area delle Scienze, Parma, Italy

The magnetic interaction between hard and soft magnetic materials is of current technological interest due to their potential for applications in magnetic storage devices. Such systems are referred to as “exchange springs”. We have studied the magnetic bilayer system which consists of Fe (soft ferromagnet) layer exchange coupled with FePt (hard ferromagnet) which have been deposited on an MgO substrate. The coupled magnetic system forms part of a discontinuous trilayer structure: Ag(2 nm)/Fe (2nm and 3.5 nm)/FePt(10 nm), where the Ag overlayer serves as protection against oxidation. The epitaxial FePt layers were prepared by RF sputtering with various substrate temperatures and post growth annealing in order to obtain different morphologies. All FePt layers were epitaxial as evidenced from x-ray diffraction. Atomic force microscopy (AFM) of the FePt layers reveals a granular morphology, with typical diameters of around 40 – 50 nm. Angular ferromagnetic resonance (FMR) measurements were made (0 - 360 degrees), in the plane which includes the in-plane and out of film plane directions, to study the magnetic anisotropies and the exchange coupling mechanism.

For the sample with 3.5 nm Fe, we observe several components, in the FMR spectra which display uniaxial symmetries. In particular the spectra were divided into two groups of resonances, where we note uniaxial components, which are related to the magnetic anisotropies of the layers and the exchange coupling between the magnetic layers. The sample with 2.0 nm Fe displays significantly different spectra where one contribution is absent. We therefore assign these resonances to the bottom part of the (soft) Fe layer, which show very similar features in both samples. Thus the other component only present in the 3.5 sample is due to the top part layer of Fe. The spectra of 3.5 sample

revealed differences in the fitting procedure, which arises from magnetic inhomogeneities. These spectra display resonances which show that the resonance field appears to arise from a uniaxial symmetry while the line intensities appear to have a unidirectional component.

P-72

CHARACTERIZATION OF ELECTRODEPOSITED Ni AND Ni₈₀Fe₂₀ NANOWIRES

D. C. Leitao¹, C. T. Sousa¹, J. Ventura¹, J. Amaral¹, F. Carpinteiro¹, K.R. Pirota², M. Vazquez², J. B. Sousa¹, J. P. Araújo¹

¹IFIMUP, Rua do Campo Alegre 687, 4169-007 Porto

²Instituto de Ciencia de Materiales de Madrid, CSIC, Spain

During the past years, a huge effort is being made on the development of arrays of highly ordered nanostructures due to the potential applications in a wide range of areas as semiconductors, magneto-optics, biomedical applications, and various sensor devices or magnetic storing.

In this work we use nanoporous alumina substrates, with an average pore diameter of ~35 nm and pore separation of ~100 nm, as templates for the growth of Ni and NiFe nanowires. Our membranes were obtained by a two-step anodization process of high-purity (>99.997%) aluminum foils: first anodizations were performed at 40 V for 20 hours in 0.3M oxalic acid, at 2–6°C; the second anodization was carried out using the same conditions but for only 2 hours, giving pore lengths of ~5 μm. After the second anodization, the existent barrier-layer (~60 nm thick) at the pores bottom was thinned (down to ~2.5 nm), so that the electrodeposition current could flow through tunneling. A pulsed electrodeposition method was used to grow Ni and Ni₈₀Fe₂₀ nanowires. Different electrolytes were employed: a standard *Watts bath* (NiSO₄·6H₂O, NiCl₂·6H₂O, H₃BO₃) was used for Ni deposition; for Ni₈₀Fe₂₀ a solution with NiSO₄·7H₂O, FeSO₄·7H₂O, H₃BO₃, sacarine and sodium-lauryl sulfate was used. Transport and magnetotransport characterization, as a function of temperature (Fig. 1), will be shown and compared to magnetization measurements.

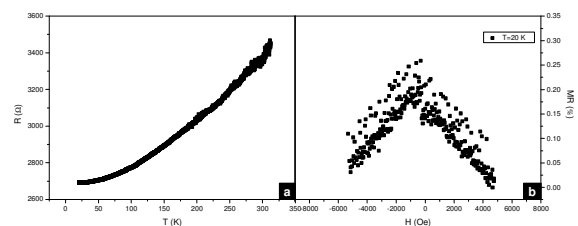


Fig. 2: Ni₈₀Fe₂₀ nanowires (a) R(T) curve; (b) magnetoresistance for different temperatures with magnetic field perpendicular to the nanowires axis.

P-73

ON THE ELECTROCHROMISM IN THE NON-CRYSTALLINE NIOBIUM PENTOXIDE ANODIC FILMS

L. Skatkov¹ & V. Gomozyov²
1 PCB "Argo", 4/23 Shaul ha-Melekh Str., Israel

2 National Technical University, 21 Frunze Str., Ukraine

Until present time electrochromism has been observed and studied only in Nb₂O₅ polycrystalline anodic films, which, unlike non-crystalline ones, demonstrate pronounced electrochromic properties [1].

This differing (from electrochromic effect viewpoint) properties of niobium pentoxide non-crystalline and polycrystalline anodic films makes us turn our attention to the surface morphology of oxide layers, since the volumetric properties of non-crystalline films are known to be favorable for electrochromism. The comparison of niobium pentoxide non-crystalline and polycrystalline layers reveal multipores surface in polycrystalline oxides, and highly unbroken surface in non-crystalline ones. In present communication the technique for generation of electrochromic effect (ECE) in non-crystalline Nb₂O₅ anodic films is proposed.

It should be emphasized that despite the fact that the metal-semiconductor phase transition with absorption jump – including ECE scenario, relates to polycrystalline Nb₂O₅ films, it is rather probable that in obtained non-crystalline niobium pentoxide films, the ECE mechanism is also similar to above described model. We would notice that the absence of distant order in the non-crystalline structure, generated during anodic layer growth, does not result in the suppression of such phase transition as we have considered above, in anodic oxide films.

[1] L. Skatkov, Abstr. Int. Meeting on Electrochromism IME-4 (Uppsala, Sweden, 2000). – P.74.

P-74

STRUCTURAL AND MAGNETIC CHARACTERIZATION OF FE/FE₃O₄ MIXED NANOPOWDERS

O. Crisan¹, J.M. Greneche², I. Skorvanek³, R. Nicula⁴

¹National Institute for Materials Physics, P.O. Box MG-7, 077125 Bucharest-Magurele, Romania;

²LPEC UMR CNRS 6087 Université du Maine, 72085 Le Mans cedex 9, France;

³Institute of Experimental Physics, Slovak Academy of Sciences, 040-01 Kosice;

⁴Institute of Physics, Rostock University, A. Bebel Str. 55, 18055 Rostock, Germany;

Nanostructured powders obtained by ball milling of a mixture of Fe and Fe₃O₄ at room temperature, were proven to undergo an incomplete redox reaction with formation of FeO in the synthesis process. This reaction is favoured via the high energy developed during the milling in the alloying process. Concurrent effects of milling such as grain refinement down to the nanometre scale lead at the end of the milling processes to a mixed multiphase nanopowder, with Fe and Fe oxide grains inter-dispersed. Such ferromagnetic – antiferromagnetic composites are extensively studied due to their exchange bias properties,

with a large impact in technological applications. We show in the present contribution that in the mixed Fe / Fe₃O₄ nanopowders, obtained with different relative metal / oxide proportions, the chemical reaction that leads to the formation of FeO during milling process is dependent upon the initial powders relative proportion. Moreover, with increasing temperature the system undergo an inverse phase transformation towards the initial Fe and Fe₃O₄ phases. Depending upon initial metal / oxide relative proportion, this transformation is incomplete leading to a multiphase metal / oxide microstructure with occurrence of Fe, FeO and Fe₃O₄ phases. This transformation was investigated via an energy dispersive in-situ X-ray diffraction experiment using the synchrotron radiation at DESY, Hasylab, Hamburg. The structural and magnetic characterization of the nanopowders mixture are studied using powder X-ray diffraction, Mossbauer spectrometry and magnetic measurements. The magnetic behaviour strongly depend upon initial weight ratio of the two mixed powders. The intrinsic mechanisms leading to the occurrence of exchange bias effects are discussed and related to the samples microstructural features.

P-75

FINITE VOLUME MODELLING OF THE NON-ISOTHERMAL FLOW OF A NON-NEWTONIAN FLUID IN A RUBBER'S EXTRUSION DIE

J. J. del Coz Díaz^a, P. J. García Nieto^b, J. Ordieres Meré^c and A. Bello García^a

^aDepartment of Construction, University of Oviedo, Viesques Departmental Building N°7 – 33208 Gijón (Spain)

^bDepartment of Applied Mathematics, Faculty of Sciences, C/ Calvo Sotelo, 33007 Oviedo (Spain)

^cDepartment of Mechanical Engineering, C/ Luis de Ulloa, 20 – 26004 Logroño (Spain)

Non-isothermal flow of a non-Newtonian fluid is the most complex and important problem in the rubber's extrusion process. In this way, the aim of this work is to describe the computer modelling of the laminar flow through a nozzle by the finite volume method (FVM). The basis of the general mathematical treatment of flow processes are the balance equations for mass, momentum and energy. The flow can be fully described only when the velocity vector and the thermodynamic data as pressure, density and temperature are known at any time and at any point of the flow. To determine these quantities the conservation equations are combined with the constitutive (material) equations which describe the correlations between parameters relating to motion and kinetics on the one hand and between the individual thermodynamic parameters on the other hand. Extrusion heads for the fabrication of rubber profiles are up to now designed on the basis of empirical knowledge of the non-linear inelastic flow behaviour involving the heat transfer. The liquid rubber exhibits a shear rate and temperature dependent viscosity, with 'shear thinning', that is, decreasing viscosity with increasing shear rate and temperature. We have taken the Power-Law model

in order to simulate this rubber's extrusion process. The mathematical model has the form $\mu(T) = K(T)I_2^{\{n(T)-1\}/2}$, where T, μ, I_2, n and K are termed the temperature, dynamic viscosity, the second invariant of the rate of deformation tensor, the power law index and the consistency, respectively. These last two parameters were obtained at different temperatures from experimental tests and used in the computational simulation. Finally we have modeled the extrusion process with different inlet pressures, for a type of nozzle, in order to calculate the outlet velocity and temperature distribution of the rubber and conclusions are exposed.

P-76

EVIDENCE OF INTRINSIC FERROMAGNETIC BEHAVIOUR OF THIOL CAPPED AU NANOPARTICLES BASED ON μ SR RESULTS

E. Goikolea, J.S. Garitaonandia, M. Insausti, J. Lago, I. Gil de Muro, J. Salado, J. Bermejo, D. S. Schmool
Zientzia eta Teknologia Fakultatea, Euskal Herriko Unibertsitatea (UPV/EHU), 644 P.K., 48080 Bilbao (Spain)

The study of Au nanoparticles (NPs) has increased noticeably owing to the new properties that emerge when decreasing particle size and modifying the surrounding media. Size diminution changes dramatically the electronic structure, and this, affects noticeably to the physical properties (size effect). The size reduction also increases the surface to volume relation (surface effect), and as a result of both effects, all atoms from a NP undergo electron redistribution. Moreover, the electronic configuration can also be altered by capping NPs with different organic ligands. In fact, recently published results show that certain Au NPs capped with various organic ligands present magnetic properties even at room temperature, in contrast to the diamagnetism found in bulk Au [1].

Up to now, the magnetic behaviour of this type of samples has been confirmed by means of "classical" magnetic measurements and, more recently, by Mössbauer spectroscopy and XMCD measurements [2]. In this sense, here we report μ SR results obtained in ISIS (EMU spectrometer), which are another experimental evidence of the intrinsic magnetic behaviour of dodecanethiol capped Au NPs. NPs have been measured at low (8 K) and room temperature varying the field (longitudinal and transversal) in the range of 0 - 700 G. Results show that NPs have very strong internal fields and the interactions are mainly hyperfine rather than dipolar. The spectra obtained when a field was applied show weak spontaneous oscillations indicating the presence of coherent internal fields within the particle. Besides, it has also been observed a fast temperature and applied field dependent exponential relaxation.

[1] P. Crespo; R. Litrán, T. C. Rojas, M. Multigner, J. M. de la Fuente, J. C. Sánchez-López, M. A. García, A. Hernando, S. Penedés, A. Fernández, *Phys. Rev. Lett.* **93** (2004) 087204.

[2] J. S. Garitaonandia, M. Insausti, E. Goikolea, M. Suzuki, J. D. Cashion, N. Kawamura, H. Ohsawa, I. Gil de Muro, K. Suzuki, F. Plazaola, T. Rojo, *Nano Lett. In press* (2008).

P-77

ELECTRON TRANSPORT IN HITPERM ALLOYS

K. Pękała
Faculty of Physics, Warsaw University of Technology, Koszykowa 75, 00-662 Warsaw, Poland

Paper reports electron transport investigation of the Hitperm alloys. Electrical resistivity and thermoelectric power (TEP) of Fe-Co-X-B-Cu (X = Nb-Zr, Zr, Hf-Zr, Hf) alloys were measured between 20 and 1100 K using the four probe and the differential methods, respectively. The resistivity of investigated alloys is rather low - between 100 - 140 $\mu\Omega\text{cm}$, with exception for alloys with X = Nb-Zr, which resistivity is about 180 $\mu\Omega\text{cm}$. In the later case the electron localisation model must be considered for the temperature dependence of resistivity. In all samples the effect of electron scattering on magnetic structure is observed.

A pronounced effect of magnetic scattering on temperature variation of TEP is also observed. This contribution is reflected by the nonlinear variation of TEP and the strong negative value as compared to non magnetic amorphous alloys. The structural and magnetic components of TEP are separated. The magnetic component is interpreted in terms of Kasuya and Herzer models. The value of magnetic component is correlated with magnetic properties these alloys. The crystallization processes are evidenced by electrical resistivity and TEP variation. An influence of nanocrystalline grain sizes on TEP behavior is discussed

P-78

MAGNETOTHERMOPOWER IN MAGNETIC NANOCOMPOSITES "AMORPHOUS FERROMAGNET $\text{Co}_{45}\text{Fe}_{45}\text{Zr}_{10}$ -AMORPHOUS DIELECTRIC Al_2O_n "

A. Granovsky¹, Yu. Kalinin², V. Belousov², and A. Sitnikov²
¹*Moscow State Univ., Faculty of Physics, Moscow, 119991, Russia*
²*Voronezh Technical State University, Voronezh, 394026, Russia*

The concentration and temperature dependences of the resistivity, thermopower and magnetothermopower of composites containing of amorphous nanoparticles $\text{Co}_{45}\text{Fe}_{45}\text{Zr}_{10}$ embedded in the Al_2O_n dielectric matrix are investigated. Below the percolation threshold, i.e., in the tunnelling conduction region, the absolute values of the thermopower of the composites under investigation are less than those above the percolation threshold. It is revealed that, in the tunnelling conduction region, the slope of the temperature dependences of the thermopower changes at a temperature of ~ 205 K. This can indicate that the

thermopower is sensitive to a change in the mechanism of conduction from the Mott law to a power relation that corresponds to the model of inelastic resonant tunneling through a chain of localized states in the dielectric matrix. Magnetothermopower is negative for nanocomposites fabricated with introduction of oxygen in the course of sputtering, but it is positive if nanocomposites are obtained in the atmosphere of both oxygen and argon. It was found that magnetothermopower of nanocomposites $\text{Co}_{45}\text{Fe}_{45}\text{Zr}_{10}\text{-Al}_2\text{O}_n$ is strongly asymmetric with respect of magnetic field reversal. It is shown that the developed theory of the tunnelling magnetothermopower is consistent with the obtained data.

P-79

THERMAL AND MAGNETIC BEHAVIOR OF COBALT-BASED ALLOYS

A. Rosales-Rivera, M. Gomez-Hermida, P. Pineda-Gomez
Laboratorio de Magnetismo y Materiales Avanzados, Facultad de Ciencias Exactas y Naturales, Universidad Nacional de Colombia, A.A. 127, Manizales, Colombia

A systematic study of the thermal and magnetic behavior of the amorphous $\text{Co}_{80-x}\text{Fe}_x\text{B}_{10}\text{Si}_{10}$ alloy ribbons is presented. The experiments were performed on samples of Co_{80} -

$\text{Fe}_x\text{B}_{10}\text{Si}_{10}$ with $x = 6, 8$ and 10 , prepared by the melt spinning technique. The thermal behavior was studied using differential scanning calorimetric (DSC) and thermogravimetric analysis (TGA). Six samples of appropriate weight of each of the ribbons were used for thermal analysis. The DSC and TGA runs were performed at various heat rates, $r = 2, 5, 7, 10, 15$ and 20°C , in nitrogen flow. The structure of the as-cast ribbons was analysed by XRD monochromatized $\text{Cu K}\alpha$ radiation, $\lambda = 1.5406\text{\AA}$, in a Rigaku diffractometer. The field (H) dependence of the magnetization, M, of the samples was measured, from -1 to 1 KOe at room temperature, with a vibrating sample magnetometer. The XRD patterns indicate that the as-cast ribbons are amorphous at room temperature. The crystallization kinetics was studied using the Avrami model [1]: $\ln(r/T_{\text{pcr}}) = (E_a/nRT_{\text{pcr}}) + \text{constant}$, where T_{pcr} is the primary crystallization temperature, E_a is the activation energy, n is the Avrami exponent and R is the ideal gas constant. A value of E_a has been determined for the different samples and it decreases as x increases changing from 3.44 to 3.28 eV. The TGA results confirm the development of the primary and secondary crystallization process of the nanocrystalline phase in $\text{Co}_{80-x}\text{Fe}_x\text{B}_{10}\text{Si}_{10}$ alloy ribbons observed in the DSC experiments. The M vs. H curves exhibit soft magnetic behavior.

LIST OF PARTICIPANTS

Last name	First name	Institution	Country	E-mail
Alvarez	Guillermo	Universidade Nacional Autónoma do México	México	memodin@yahoo.com
Amaral	Filipe	Universidade de Aveiro, Departamento de Física	Portugal	filipe.amaral@estgoh.ipc.pt
Amaral	João	Universidade de Aveiro, Departamento de Física	Portugal	jamaral@ua.pt
Apolinário	Arlete	Universidade de Porto, Departamento de Física	Portugal	arlette@portugalmail.pt
Araujo	João Pedro	Universidade de Porto, Departamento de Física	Portugal	jearaujo@fc.up.pt
Barandiarán	José Manuel	Universidad del País Vasco	Spain	manub@we.lc.ehu.es
Barbosa	José Gusman	Universidade do Minho, Departamento de Física	Portugal	jbarbosa@fisica.uminho.pt
Battezzati	Livio	Università di Torino	Italy	livio.battezzati@unito.it
Bednarcik	Jozef	Deutsches Elektronen-Synchrotron (HASYLAB)	Germany	jozef.bednarcik@desy.de
Betancourt	Israel	Universidade Nacional Autónoma do México	Mexico	israelb@correo.unam.mx
Blanco Rodrigues	Jesus Angel	University of Oviedo	Spain	jabr@uniovi.es
Blázquez Gámez	Javier S.	University of Seville	Spain	jsebas@us.es
Bonastre	Jordi	Universitat de Girona	Spain	jordi.bonastre@udg.es
Bossuyt	Sven	Vrije Universiteit Brussel	Belgium	sven.bossuyt@vub.ac.be
Braga	Maria Helena	Universidade do Porto, Faculdade de Engenharia	Portugal	mbraga@fe.up.pt
Bruna	Pere	Universitat Politècnica de Catalunya	Spain	pbruna@fa.upc.edu
Buján-Núñez	M ^a del Carmen	Universidade de Santiago de Compostela	Spain	qfmcnb@usc.es
Cerdeira Garcia	Maria Ángeles	Universidad de Oviedo	Spain	ance@uniovi.es
Chiriac	Horia	National Institute of Research and Development for Technical Physics	Romania	hchiriac@phys-iasi.ro
Choi	Duk-Yong	Australian National University	Australia	dyc111@rsphysse.anu.edu.au
Conde-Gallardo	Agustin	CINVESTAV del IPN	México	aconde@fis.cinvestav.mx
Costa	Benilde Oliveira	Universidade de Coimbra, Departamento de Física	Portugal	benilde@ci.uc.pt
Cowlam	Neil	University of Sheffield, Department of Physics and Astronomy	U.K.	n.cowlam@sheffield.ac.uk
Crisan	Ovidiu	National Institute for Materials Physics	Romania	ocrisan@yahoo.com
Cristiglio	Viviana	Institute Laue-Langevin	France	cristiglio@ill.fr
Cuello	Gabriel	Institute Laue-Langevin	France	cuello@ill.eu
Davies	Hywel	University of Sheffield, Department Engineering Materials	U.K.	h.a.davies@shef.ac.uk
Domènech Ferrer	Roger	Universitat Autònoma de Barcelona	Spain	roger@vega.uab.es

Ebrahimi	Sayyed	University of Tehran	Iran	saseyyed@ut.ac.ir
Elbaile	Laura	Universidad de Oviedo	Spain	elbaile@uniovi.es
Epifani	Mauro	Istituto per la Microelettronica ed i Microsistemi	Italia	mauro.epifani@le.imm.cnr.it
Escoda	Maria Lluisa	Universitat de Girona	Spain	lluisa.escoda@udg.edu
Espinosa de los Monteros Royo	Ana	Instituto de Ciencia de Materiales de Madrid	Spain	anaespinosa@icmm.csic.es
Facchini	Laura	Universitat Politècnica de Catalunya, Departamento de Física Aplicada	Spain	laufacchini@hotmail.com
Farle	Michael	University of Duisburg-Essen	Germany	michael.farle@uni-due.de
Favieres Ruiz	Cristina	Public University of Navarre	Spain	favieresc@unavarra.es
Fernández Garcia	Maria Paz	University of Oviedo, Department of Physics	Spain	fernandezpaz.uo@uniovo.es
Fernández Marzo	Florencio	University of the Basque Country, Chemical Engineering and Environment Department	Spain	iapfemaf@sp.ehu.es
Figueroa	Ignacio A.	University of Sheffield, Department of Engineering Materials	U.K.	i.a.figueroa@sheffield.ac.uk
Flohrer	Sybille	Vacuumschmelze GmbH & Co. KG	Germany	Sybille.Flohrer@vacuumschmelze.com
Ganetsos	Theodore	Technological Education Institute of Lamia, Department of Electronics	Greece	ganetsos@teilam.gr
García Díaz	José Ángel	Universidad de Oviedo, Departamento de Física	Spain	joseagd@uniovi.es
Garitaonandia	J.Saiz	Universidad del País Vasco	Spain	garita@we.lc.ehu.es
Ghanaatshoar	Majid	Shahid Beheshti University	Iran	m-ghanaat@cc.sbu.ac.ir
Glezer Markovich	Alexander	Institute for Physical Metallurgy Minsk	Russia	glezer@imph.msk.ru
Goikolea	Eider	Universidad del País Vasco	Spain	
González Fernández	Jésus Maria	Instituto de Magnetismo Aplicado	Spain	jmglez@estafeta.icmm.csic.es
Gorria	Pedro	Universidad de Oviedo, Departamento de Física	Spain	pgorria@uniovi.es
Granovsky	Alexander B.	Lomonosov Moscow State University	Russia	granov@magn.ru
Greneche	Jean Marc	Université de Le Mans	France	greneche@univ-lemans.fr
Gutierrez	Jon	Universidad del País Vasco	Spain	jon@we.lc.ehu.es
Hamidi Sangdehi	Seyedeh Mehri	Shahid Beheshti Universiti	Iran	M_Hamidi@sbu.ac.ir
Heiberg-Andersen	Henning	Institute for Energy Technology	Norway	henning.heibergandersen@gmail.com
Heinrich	Bret	Simon Fraser University	Canada	bheinric@sfu.ca
Hennet	Louis	Centre de Recherche sur les Matériaux à Haute Température	France	hennet@cnsr-orleans.fr
Herzer	Giselher	Vacuumschmelze GmbH & CO KG	Germany	Giselher.Herzer@vacuumschmelze.com
Hono	Kazuhiro	NIMS, University of Tsukuba	Japan	hono.kazuhiro@nims.go.jp
Insausti	Maite	Universidad del País Vasco	Spain	qipinpem@ehu.es

Kao	Ming-Cheng	Hsiuping Institute of Technology	Taiwan	kmc@mail.hit.edu.tw
Kozina	Olga	Saratov Division of Institute Radio-Engineering and Electronics RAS	Russia	KozinaON@info.sgu.ru
Kveder	Marina _Ilakovac	Ruder Boskovic Institute	Croatia	kveder@rb.hr
Lancok	Adriana	Institute of Inorganic Chemistry As Cr, v.v.i.	Czech Republic	ada@iic.cas.cz
Latuch	Jerzy	Warsaw University of Technology, Faculty of Materials Science and Engineering	Poland	jlat@inmat.pw.edu.pl
Leitão	Diana Cristina Silva	Universidade do Porto, Departamento de Física	Portugal	dleitao@fc.up.pt
Leydier	Marlène	CNRS-CRMHT	France	marlene.leydier@cnrs-orleans.fr
Lin	Chien-Han	Hsiuping Institute of Technology	Taiwan	jhlin@mail.hit.edu.tw
Liz-Marzan	Luis	Universidad de Vigo	Spain	Imarzan@uvigo.es
Lopes	Armandina Lima	Universidade do Porto, Departamento de Física	Portugal	Armandina.Lima.Lopes@cern.ch
Madurga	Vicente	Public University of Navarre	Spain	vmadurga@unavarra.es
Markovich	Vladimir	Ben-Gurion University of the Negev	Israel	markoviv@bgu.ac.il
Martínez-García	José Carlos	Universidad de Oviedo	Spain	jcmg@uniovi.es
Mata-Zamora	Esther	Centro de Ciencias Aplicadas y Desarrollo Tecnológico, UNAM	Mexico	memzamora@yahoo.com.mx
Mateo	Cintia	Universidade de Santiago de Compostela	Spain	qfcintia@usc.es
Miglierini	Marcel	Slovak Academy of Sciences, Bratislava	Slovakia	bruno@elf.stuba.sk
Mira Pérez	Jorge	Universidade de Santiago de Compostela	Spain	fajmirap@usc.es
Mogilyanski	Dmitry	Ben-Gurion University	Israel	mogily@bgu.ac.il
Mokhovikov	Alexander	Irkutsk State University	Russia	zubr@api.isu.ru
Montiel Sanchez	Maria Herlinda	Universidade Nacional Autónoma do México	México	herlinda_m@yahoo.com
Mora Aznar	María Teresa Clavaguera	Universitat Autònoma de Barcelona	Spain	mtmora@vega.uab.es
Moreira	José Manuel	Universidade de Porto, Departamento de Física	Portugal	jmmoreira@fc.up.pt
Ngai	Kia L.	Naval Research Laboratoty	USA	ngai@estd.nrl.navy.mil
Oleszak	Dariusz	Faculty of Materials Science and Engineering, Warsaw University of Technology	Poland	daol@inmat.pw.edu.pl
Oliveira	Joana Cacilda	Universidade do Porto, Faculdade de Engenharia	Portugal	jespain@fe.up.pt
Ordieres-Meré	Joaquin	University of La Rioja	Spain	jbmere@gmail.com
Ortega Ponce	Daniel	Universitat del Río San Pedro	Spain	daniel.ortega@uca.es
Ou	C.R.	Hsiuping Institute of Technology	Taiwan	crou@mail.hit.edu.tw
Pekala	Krystyna	Warsaw University of Technology	Poland	pekala@mech.pw.edu.pl
Pekala	Marek	Warsaw University of Technology	Poland	pekala@chem.uw.edu.pl
Pereira	André	Universidade do Porto, Departamento de Física	Portugal	ampereira@fc.up.pt

Pereira	Lino	Universidade do Porto, Departamento de Física	Portugal	c0302007@alunos.fc.up.pt
Pereira	Luiz	Universidade de Aveiro, Departamento de Física	Portugal	luiz@ua.pt
Pozdnyakova	Irina	CNRS-CRMHT , Orleans	France	pozdnaya@cnrs-orleans.fr
Prida Pidal	Victor De La	Universidad de Oviedo	Spain	vmpp@uniovi.es
Proença	Mariana	Universidade do Porto, Departamento de Física	Portugal	mippro@gmail.com
Ramos Sánchez	J. Guadalupe	Centro de Investigación y Estudios Avanzados del IPN	Mexico	gramos@investav.mx
Rivas Ardisana	Montserrat	Universidad de Oviedo, Departamento de Física	Spain	rivas@uniovi.es
Rodríguez Pierna	Angel	Universidad del País Vasco	Spain	iapropia@sp.ehu.es
Rodríguez Viejo	Javier	Universitat Autònoma de Barcelona	Spain	javirod@vega.uab.es
Romanova	Oxana	Kirensky Institute of Physics	Russia	rob@iph.krasn.ru
Rosales-Rivera	Andres	Universidad Nacional de Colombia	Colombia	arosalesr@unal.edu.co
Rozenberg	Evgeny	Department of Physics BGU of the Negev	Israel	evgenyr@bgu.ac.il
Rubinger	Carla Patricia Lacerda	Universidade de Aveiro, Departamento de Física	Portugal	carla@fis.ua.pt
Sagredo	Vicente	Universidad de Los Andes, Departamento de Física	Venezuela	sagredo@ula.ve
Salado	Javier	Universidad del País Vasco	Spain	javier.salado@ehu.es
Salmon	Philip S.	University of Bath	U.K.	P.S.Salmon@bath.ac.uk
Sánchez	Maria Luisa	Universidad de Oviedo, Departamento de Física	Spain	mlsr@uniovi.es
Sánchez Fernandez	Tatiana	Universidad de Oviedo, Departamento de Física	Spain	sancheztatiana.uo@uniovi.es
Sarkarati	Saeed	Shahid Beheshti Universiti	Iran	saeedsarkarati@gmail.com
Schmool	David	Universidade do Porto, Departamento de Física	Portugal	dschmool@fc.up.pt
Serantes	David	Universidade de Santiago de Compostela, Departamento de Física	Spain	davidsa@usc.es
Shalygina	Elena	Faculty of Physics, Moscow State University	Russia	shal@magn.ru
Silva	Ana Sofia Vieira	Universidade do Porto, Departamento de Física	Portugal	c0722004@alunos.fc.up.pt
Silva	Hugo	Universidade do Porto, Departamento de Física	Portugal	hsilva@ualg.pt
Skatkov	Leonid	PCB "Argo" Israel	Israel	sf_1skatkov@bezeqint.net
Skipper	Neal	University College London	U.K.	n.skipper@ucl.ac.uk
Skorvánek	Ivan	Slovak Academy of Sciences	Slovakia	skorvi@saske.sk
Sniadeck	Zbigniew	Polish Academy of Sciences	Poland	sniadecki@ifmpan.poznan.pl
Sousa	Célia	Universidade do Porto, Departamento de Física	Portugal	celiasousa@fc.up.pt
Sousa	João Bessa	Universidade do Porto, Departamento de Física	Portugal	jbsousa@fc.up.pt
Sousa	Nuno	Universidade do Porto, Departamento de Física	Portugal	nunodsousa@gmail.com
Suñol	Joan Josef	Universitat de Girona	Spain	joanjosep.sunyol@udg.es

Suzuki	Kiyonori	Monash University	Australia	kiyonori.suzuki@eng.monash.edu.au
Tadjiev	Damir	Sheffield University, Engineering Materials	UK	D.Tadjiev@sheffield.ac.uk
Tehranchi	Mohammad Mehdi	Shahid Beheshti University	Iran	teranchi@cc.sbu.ac.ir
Teixeira	José Miguel	Universidade do Porto, Departamento de Física	Portugal	jnteixeira@fc.up.pt
Torrens Serra	Joan	Universitat Autònoma de Barcelona	Spain	joan@vega.uab.es
Valente	Manuel Almeida	Universidade de Aveiro, Departamento de Física	Portugal	mav@ua.pt
Valenzuela	Raul	Instituto de Investigaciones en Materiales, UNAM	Mexico	monjaras@servidor.unam.mx
Varga	Rastislav	University of Kosice	Slovakia	rastislav.varga@upjs.sk
Vazquez	Manuel	Instituto de Ciencia de Materiales, CSIC	Spain	mvazquez@icmm.csic.es
Ventura	João Oliveira	Universidade do Porto, Departamento de Física	Portugal	joventur@fc.up.pt
Vinai	Franco	INRIM- National Institute of Metrological Research	Italy	f.vinai@inrim.it
Wang	Rongping	Australian National University	Australia	rongping.wang@anu.edu.au
Watts	Bernard	IMEM-CNR	Italy	watts@imem.cnr.it
Yelon	Arthur	Polytechnique Montréal	Canada	arthur.yelon@polymtl.ca
Yelsukov	Eugene	Physical-Technical Institute UrB RAS	Russia	yelsukov@fnms.fti.udm.ru
Zhu	Jie	Northwest A&F University our Argonne National Laboratory	USA	medfbi@gmail.com